



UNIVERSIDADE FEDERAL DE PERNAMBUCO

CENTRO DE TECNOLOGIA E GEOCIÊNCIAS

DEPARTAMENTO DE OCEANOGRAFIA

PROGRAMA DE PÓS GRADUAÇÃO EM OCEANOGRAFIA

CAMILA BRASIL LOURO DA SILVEIRA

**DIVERSIDADE DE HABITATS, CONECTIVIDADE E IMPACTOS HUMANOS EM
RECIFES COSTEIROS: uma análise integrada para o Planejamento Espacial Marinho**

Recife

2019

CAMILA BRASIL LOURO DA SILVEIRA

**DIVERSIDADE DE HABITATS, CONECTIVIDADE E IMPACTOS HUMANOS EM
RECIFES COSTEIROS: uma análise integrada para o Planejamento Espacial Marinho**

Tese apresentada ao Programa de Pós-graduação em Oceanografia, Universidade Federal de Pernambuco, como requisito parcial para obtenção do título de Doutor em Oceanografia

Área de concentração: Oceanografia
Biológica

Orientadora: Prof^a. Dr^a. Beatrice Padovani Ferreira

Coorientador: Prof. Dr. Gil Marcelo Reuss Strenzel

Recife

2019

Catálogo na fonte
Bibliotecário Gabriel Luz, CRB-4 / 2222

S587d Silveira, Camila Brasil Louro da.
Diversidade de habitats, conectividade e impactos humanos em recifes costeiros: uma análise integrada para o planejamento espacial marinho / Camila Brasil Louro da Silveira – Recife, 2019.
124 f.

Orientadora: Profa. Dra. Beatrice Padovani Ferreira.
Coorientador: Prof. Dr. Gil Marcelo Reuss Strenzel.
Tese (Doutorado) – Universidade Federal de Pernambuco. CTG. Programa de Pós-Graduação em Oceanografia, 2019.
Inclui referências.

1. Oceanografia. 2. Imagens de satélite. 3. Recifes de coral. 4. MaxEnt.. 5. Plataforma continental. I. Silveira, Camila Brasil Louro da (Orientadora). II. Reuss Strenzel, Gil Marcelo (Coorientador). III. Título.

UFPE

551.46 CDD (22. ed.)

BCTG / 2020-13

CAMILA BRASIL LOURO DA SILVEIRA

**DIVERSIDADE DE HABITATS, CONECTIVIDADE E IMPACTOS HUMANOS EM
RECIFES COSTEIROS: uma análise integrada para o Planejamento Espacial Marinho**

Tese apresentada ao Programa de Pós-graduação em Oceanografia, Universidade Federal de Pernambuco, como requisito parcial para obtenção do título de Doutor em Oceanografia

Aprovada em: 27/09/2019.

BANCA EXAMINADORA

Prof^ª. Dr^ª. Beatrice Padovani Ferreira (Orientadora)

Universidade Federal de Pernambuco

Prof^ª. Dr^ª. Tereza Cristina Medeiros de Araújo (Examinadora Interna)

Universidade Federal de Pernambuco

Prof^ª. Dr^ª. Helenice Vital (Examinadora Externa)

Universidade Federal do Rio Grande do Norte

Prof. Dr. George Olavo Mattos e Silva (Examinador Externo)

Universidade Estadual de Feira de Santana

Prof. Dr. Thierry Frédou (Examinador Externo)

Universidade Federal Rural de Pernambuco

AGRADECIMENTOS

Chegando o final desta longa etapa, é também o momento de agradecer às pessoas que foram indispensáveis por todo este percurso.

Gostaria de deixar registrado meu agradecimento à minha querida orientadora Prof^a. Beatrice Padovani Ferreira. As palavras são poucas para agradecer a confiança (e principalmente a paciência) em mim depositada durante estes anos e a admiração que sinto pela senhora!

Ao meu coorientador, Gil Strenzel, muito obrigada por me ensinar tanto e por abrir minha mente para o sensoriamento remoto.

Ao professor Mauro Maida, obrigada por todo o acesso e ajuda em todas as fases do desenvolvimento desta Tese.

A CAPES, Projeto Recifes Costeiros, Fundação Toyota do Brasil e Fundação SOS Mata Atlântica, e aos projetos PELD-TAMs, Ciências do Mar I e II, que proporcionaram auxílios financeiros, logísticos e de campo, tão necessários para o desenvolvimento desta Tese.

Aos professores do Programa de Pós-Graduação de Oceanografia da UFPE pelos tantos ensinamentos e por me fazer mergulhar ainda mais nos conhecimentos oceanográficos.

Aos voluntários e equipe do CEPENE e ICMBio, e à equipe Reef Check Brasil que me ajudaram infinitamente em todos os trabalhos de campo.

À minha mãe, meu pai, meu padrasto e minha madrasta, que mesmo de longe estão sempre apoiando minhas decisões com muito carinho e amor.

Ao meu irmão, o Dudu, amigo mais antigo! E às minhas irmãs de coração Nuna, Lai e Aninha.

À minha família, vós e vós (no Céu e na Terra), tios e tias, primos e primas, vocês me encheram de carinho longe de casa!

Ao meu marido, Ju, você sabe que sem você isso não seria possível. Obrigada pelo acalento mental e paz de espírito que você e Hu me trouxeram.

Aos meus amigos (Ana Lídia, Daniel, Isabela, Laura....) e LECOR: vocês foram maravilhosos!

RESUMO

O mapeamento da geobiodiversidade é um importante passo no processo de identificação de áreas prioritárias para o manejo e conservação. O sensoriamento remoto (mais especificamente, imagens de satélite) tem sido considerado uma metodologia segura para investigar habitats bentônicos, se calibrado com dados de campo confiáveis. No entanto, a aplicação destas ferramentas para áreas recifais no Atlântico Sul ainda é insuficiente, principalmente em regiões como o Nordeste brasileiro, que acumula limitações financeiras e topográficas para a utilização do sensoriamento remoto no meio marinho (e.g. baixa qualidade ou ausência de dados *in situ* para calibração, relevo marinho complexo, heterogeneidade de substratos). O complexo recifal de Tamandaré, na APA Costa dos Corais, abriga um mosaico de habitats interconectados, que inclui recifes de coral, gramíneas e manguezais. Em todo o mundo, esses ambientes costeiros sofrem impactos crônicos como poluição, sedimentação e erosão, e uso humano, que podem levar a perda ou transformação do ecossistema. Apesar de sua importância socioeconômica e ecológica, há uma escassez de mapeamento batimétrico e de cobertura dos recifes de Tamandaré e plataforma adjacente. Neste estudo, aplicamos uma abordagem de relativo baixo custo, com técnicas de sensoriamento remoto em diferentes resoluções para mapear os habitats bentônicos da zona costeira e identificar paleocanais e recifes mesofóticos na plataforma continental. Uma cena Worldview-03 (2 metros/pixel) foi utilizada no mapeamento dos habitats do ecossistema recifal, usando classificação supervisionada com o método *Vector Machine Classifier* e aproximadamente 1500 pontos de verdade de campo (acurácia média = 79%). Esta mesma cena foi utilizada para obter um modelo batimétrico da área e camadas derivativas adicionais (e.g. diversidade de habitats/área, rugosidade). Foi possível identificar áreas de elevada complexidade de habitats, como a atual ZPVM (conhecida como “área fechada”) de Tamandaré (máximo de 14 habitats/0.01km²). Utilizamos também o software MaxEnt para verificar a influência de dezoito variáveis ambientais na distribuição do coral *Millepora alcicornis*. O modelo resultante (AUC>0.98) revelou fatores ecológicos e topográficos atuantes na distribuição da espécie na região. Mapas de uso (turismo e pesca) mostraram também que além das variáveis ambientais, impactos antrópicos podem definir a presença ou ausência de grandes colônias de *Millepora alcicornis* nos recifes de Tamandaré, mesmo em uma APA. Adicionalmente, após extensivo processamento, imagens Landsat-8 OLI (30 metros/pixel) foram usadas para detectar feições de fundo na plataforma continental entre Alagoas e Pernambuco. Foi possível visualizar a paisagem marinha em uma área total de 9700 km², em regiões de profundidade

média de 45 metros. Detectamos 14 paleocanais nas imagens, 9 dos quais ainda não mapeados por métodos tradicionais. Estes canais são conhecidos como áreas de pesca importantes, com ocorrência de agregações reprodutivas de peixes. Os resultados alcançados evidenciam a complexidade topográfica e ecológica da zona costeira de Tamandaré e plataforma adjacente. Ademais, geram subsídios para o planejamento espacial marinho da APA Costa dos Corais, uma vez que fornecem um mapeamento detalhado da área e a descrição de metodologias e ferramentas avançadas para a obtenção de dados futuros.

Palavras-chave: Imagens de satélite. Recifes de coral. MaxEnt. Plataforma continental.

ABSTRACT

Mapping geobiodiversity is an important step towards identification of priority areas for conservation and management. Satellite imagery have been considered a trustworthy way of investigating benthic habitats when calibrated with reliable field data. Still, important tropical reefs around the world are faced with an array of limitations that challenge its application, like budgetary restrictions, topographical heterogeneity, turbidity and confounding signals. The coral reef complex of Tamandaré (Costa dos Corais MPA-Brazil), embrace a mosaic of interconnected habitats (mangroves, coral reefs, seagrass beds). Following a worldwide trend, these habitats are under chronic impacts such as sedimentation, erosion and human use that may lead to habitat loss. Despite the social and ecological importance, there is a lack of bathymetric and habitat maps in the area. We applied a budget-friendly, multi-resolution approach to map benthic habitats in the coastal zone and identify and mesophotic features on the platform. A high-resolution Worldview-03 scene was used in the habitat mapping of the reefs, using Vector Machine Classifier with an overall accuracy of 79%. The same image was used to derive the bathymetry of the area, and derivative layers (e.g. diversity of habitats/area, slope, bathymetric position index). We identified areas of increased biodiversity, like the no-take zone located in our study area (maximum of 14 habitats/0.01 km²). Eighteen environmental layers were used in MaxEnt (AUC>0.98) to make predictive models of *Millepora alcicornis* distribution. Results revealed ecological and topographical factors limiting the species distribution in the area. Tourism and fishing maps showed that not only environmental factors, but human use define the presence/absence of coral colonies in the area, even within an MPA. After extensive processing, a Landsat-8 OLI scene was used to detect bottom features on the continental platform. We were able to visualize the seascape in an area of 9700 km², with an average depth of 45 meters. We detected fifteen paleochannels, nine of them still unmapped by traditional means. These valleys are known as fishing grounds and can harbour fish spawning aggregations. Our results highlight the complexity of Tamandaré coastal zone and platform. The products and techniques used in this research generate subsidies for the marine special planning and future studies in Costa dos Corais MPA and areas that may face similar limitations.

Keywords: Satellite imagery. Coral reef. Habitat mapping. MaxEnt. Continental shelf.

SUMÁRIO

1	INTRODUÇÃO	9
2	MULTI RESOLUTION SATELLITE-DERIVED BATHYMETRY IN SHALLOW CORAL REEFS: IMPROVING LINEAR ALGORITHMS WITH GEOGRAPHICAL ANALYSIS	14
3	CORAL REEF MAPPING USING SATELLITE IMAGERY: A CONTRIBUTION FOR SEASCAPE MANAGEMENT	51
4	PUSHING SATELLITE IMAGERY TO NEW DEPTHS: SEASCAPE FEATURE MAPPING IN A TROPICAL SHELF	96
5	CONCLUSÃO	120
	REFERÊNCIAS	122

1 INTRODUÇÃO

Os recifes de coral são ambientes de extrema complexidade ecológica e geomorfológica (Bellwood *et al.* 2004; Pittman e Brown, 2011). São ecossistemas marinhos distribuídos em todo o mundo em regiões tropicais, nas plataformas continentais ou em ilhas oceânicas. Estes ambientes são considerados *hotspots* de biodiversidade (Roberts, 2002), transformando áreas naturalmente oligotróficas em ricos sistemas bióticos capazes de sustentar diversas formas de vida. Além disso, áreas recifais são locais de extrema importância econômica (Pascal *et al.*, 2016; Spalding *et al.*, 2017). São, em geral, locais de intensa atividade turística, fonte de recursos pesqueiros e lazer, e atuam como barreira física da ação erosiva de ondas na zona costeira. Atualmente, estima-se que bens e serviços provenientes de áreas recifais fornecem o meio de subsistência de 500 milhões de pessoas, sendo a base da economia de diversos locais diversas comunidades (Burke *et al.*, 2011, Wilkinson e Salvat 2012).

Apesar de sua inegável importância para a manutenção da vida marinha e do modo de vida de milhões de pessoas, recifes de coral estão sendo degradados em todo o mundo. A fragmentação destes ambientes é de especial preocupação em regiões costeiras. Ocupação desordenada, turismo excessivo, sobrepesca e poluição são considerados os principais causadores da modificação de habitats costeiros, entre os quais, o ambiente recifal (Braga e Gherardi, 2001; Bruckner, 2002; Ferreira e Maida, 2006). Ademais, a ligação entre fenômenos de larga escala como as mudanças climáticas, e o branqueamento e mortalidade de corais já é evidente. As transformações nunca foram tão extensas: 75% dos recifes de corais são considerados ameaçados (Burke *et al.*, 2011; Schlüter *et al.*, 2019). Os impactos são tamanhos e tão amplos que esta nova condição dos recifes é conhecida como “a crise dos recifes de corais” (Hodgson e Liebler, 2002; Bellwood *et al.*, 2004; Bak *et al.*, 2005).

A zona costeira brasileira é significativamente extensa, ocupando mais de três milhões de km² e quase 7500 km de extensão (MMA, 2002). Além de recifes de corais, abrigam uma variedade de habitats bentônicos e *geohabitats*, como recifes algálicos, areníticos, manguezais, prados de fanerógramas, bancos de algas, recifes mesofóticos, vales de plataforma, cânions submarinos e paleocanais. No Brasil os recifes se estendem desde o Rio Grande do Norte até o sul da Bahia, e sua distribuição tem sido dividida em seis principais regiões: 1) Ilhas e bancos oceânicos da cadeia de Fernando de Noronha; 2) Touros-Natal; 3) Pirangi-Maceió; 4) Baía de Todos os Santos-Camamu; 5) Porto Seguro-Cabrália e 6) Itacolomis e Abrolhos (Amaral & Jablonski, 2005). Adicionalmente aos impactos comuns a

zonas costeiras em todo o mundo, a costa brasileira sofre forte influência de impactos iniciados com o desmatamento da Mata Atlântica para os ciclos sucro-alcooleiros que se sucederam desde o descobrimento até os dias atuais. Ademais, a ocupação humana nesta área representa adensamentos comparáveis as zonas mais populosas do mundo (Lacerda *et al.*, 2002; Marques *et al.*, 2004).

Neste contexto de conflitos de uso, impactos e riqueza ecológica, insere-se a Área de Proteção Ambiental Costa dos Corais (APACC). Esta APA ocupa territórios de dois estados, Pernambuco e Alagoas, e é a maior Unidade de Conservação marinha do Brasil, abrangendo uma área total de aproximadamente 4135 km². A APACC é a primeira no país a incluir recifes costeiros, reconhecendo a importância ecológica, ambiental e econômica desses ecossistemas (Ferreira & Maida, 2006; ICMBio, 2012). Nos recifes costeiros da APACC os principais problemas atuantes que afetam diretamente a Unidade Marinha são: o turismo desordenado, descarga de efluentes da agricultura e urbanos, destruição de manguezais e outros ecossistemas costeiros (dunas, pradarias de fanerógamas), carreamento de sedimentos e agrotóxicos, pesca predatória e o aumento do fluxo de embarcações de pequeno a grande porte (ICMBio, 2012). Apesar de esforços de ordenamento, através de elaboração de plano de manejo e estabelecimento e conselhos consultivos (*e.g.* Plano de Manejo APA Costa dos Corais), tentativas de zoneamento do uso esbarram com falta de dados que permitam escolhas informadas sobre a representatividade dos tipos de recife e suas coberturas, e acabam sendo efetuadas com base somente em consenso local.

O estabelecimento de Áreas de Proteção Marinhas utilizando critérios baseados na visão do ecossistema como um todo tem sido amplamente descrito como uma das ferramentas mais efetivas na redução de perda e fragmentação de habitats marinhos (Agardy *et al.*, 2011). É importante também salientar que a eficácia prática destas áreas depende do quão ecologicamente apropriada a delimitação é, e do quão efetivo é seu manejo (Jameson *et al.*, 2002; Adam *et al.*, 2015).

Atualmente, o zoneamento da APACC é baseado em um sistema que visa a integração de interesses ecológicos e socioeconômicos, submetendo a zona costeira a um mosaico de áreas que foram estabelecidas a partir de decisões da sociedade, pesquisadores e poder público (ICMBio, 2012). Desta forma, locais que necessitam de ações de manejo distintas são organizados em zonas, que são: Zona de Uso Sustentável (ZUS), Zona de Praia (ZP), Zona de Conservação (ZC), Zona Exclusiva de Pesca (ZEP), Zona de Visitação (ZV), Zona de Preservação da Vida Marinha (ZPVM) e Zona de Transição (ZT).

Nos mais de quatro mil quilômetros quadrados da APACC, é possível encontrar um número de feições biogeográficas de pequena e média escala, principalmente inerentes aos recifes de corais, ou associadas à hidrodinâmica e condições ambientais. A biogeografia regional e local (McCook *et al.*, 2009; Hamilton *et al.*, 2010); e o conceito de conectividade ecológica (Roberts, 2002; Almany *et al.*, 2009; Gaines *et al.*, 2010); são tidos como dois dos principais critérios a serem considerados no desenvolvimento de áreas de proteção marinhas eficazes e representativas. Programar estes critérios a uma APA só é possível através da identificação, delimitação e do estudo dos diferentes tipos de habitats inseridos na área, e do entendimento da conectividade entre estas zonas biogeográficas.

Tendo em vista a extensão da área estudada, a necessidade de informações de maior escala se faz urgente. Medidas *in situ* são, por vezes, incapazes de se traduzir instantaneamente em escalas regionais e globais (Kerr e Ostrovsky, 2003), para isso, é necessário o uso de ferramentas como fotografia aérea e imagens de satélite, capazes de cobrir grandes áreas com diferentes resoluções (Philipson e Lindell, 2003). Desde 1975, quando foi realizada uma análise de imagens de satélite da Grande Barreira de Corais (Smith *et al.*, 1975), grande esforço tem sido feito a fim de incorporar imagens de satélite a estudos de ambientes coralíneos. O sensoriamento remoto (SR) consiste em imagens digitais como produto da medição da radiação eletromagnética emitida e absorvida pelo substrato em questão (Green *et al.*, 2000). A diferença dessas radiações reflete diferentes tipos de substrato, tornando possível o uso dessa ferramenta no mapeamento e distinção de locais em uma mesma área. Dessa forma, o SR pode ser utilizado para o zoneamento de habitats em um ecossistema recifal uma vez que diferentes substratos são traduzidos em diferentes tons na imagem resultante.

Assim, imagens de satélite possibilitam a aquisição de dados em larga escala e o reconhecimento das principais feições geográficas e biológicas do ecossistema recifal, além de ambientes em torno do recife (*e.g.* Andréfouët *et al.*, 2003; Eugenio *et al.*, 2017; Raitsos *et al.*, 2017). Atualmente, tendo em mãos uma imagem de boa qualidade (*i.e.* alta resolução, provenientes de sensores como IKONOS, *Quickbird*, *WorldView-2*, *WorldView-3*) é possível realizar uma gama de tratamentos para fins distintos. A interpolação de dados físicos, batimétricos, biológicos, ambientais e geomorfológicos provê uma visualização do ecossistema e suas interações como um todo, e a partir disso, importantes decisões de manejo podem ser tomadas de maneira estratégica (Hedley *et al.*, 2016; Selgrath *et al.*, 2016).

A utilização de imagens de satélite para o mapeamento do ambiente físico e ecológico é considerada uma metodologia de excelente custo benefício (Mumby *et al.*, 1999; Benfield *et al.*, 2007). Cenas com até 10 metros de resolução espacial podem ser obtidas sem custo e cenas com até 0.5 m de resolução têm um baixo custo de aquisição, se comparadas a outras metodologias (*e.g.* *Light Detection and Range* – LIDAR, pesquisas *in situ* com ecossondas e sonares). No entanto, apesar de todos os benefícios supracitados, o uso e aplicação destas ferramentas para áreas recifais no Atlântico Sul ainda são escassos. Esta situação é particularmente notável em regiões como o Nordeste brasileiro, que por sua vez, acumula limitações financeiras e topográficas para a utilização de técnicas de mapeamento no meio marinho (*e.g.* baixa qualidade ou ausência de dados *in situ* para calibração, relevo marinho complexo, heterogeneidade de substratos). O sensoriamento remoto por meio de imagens de satélite pode também auxiliar na detecção de feições de plataforma carbonática, apesar de não ser uma técnica comumente utilizada em áreas de profundidades maiores que 30 metros (Liceaga-Correa e Euan-Avila, 2002; Gao, 2009).

Ao considerar o monitoramento de áreas biologicamente complexas como recifes de corais utilizando imagens de satélite, uma preocupação especial deve ser dada aos dados de campo, calibradores de quaisquer análises derivadas das imagens. A partir da integração de dados remotos com estudos *in situ*, é possível um melhor entendimento das causas que envolvem perda de tecido coralíneo, diminuição na biomassa de peixes e perdas de diversidade em geral. Possibilita-se dessa forma, a interferência de forma preventiva e/ou mitigadora com melhor chance de sucesso para evitar maiores perdas de biodiversidade no meio marinho.

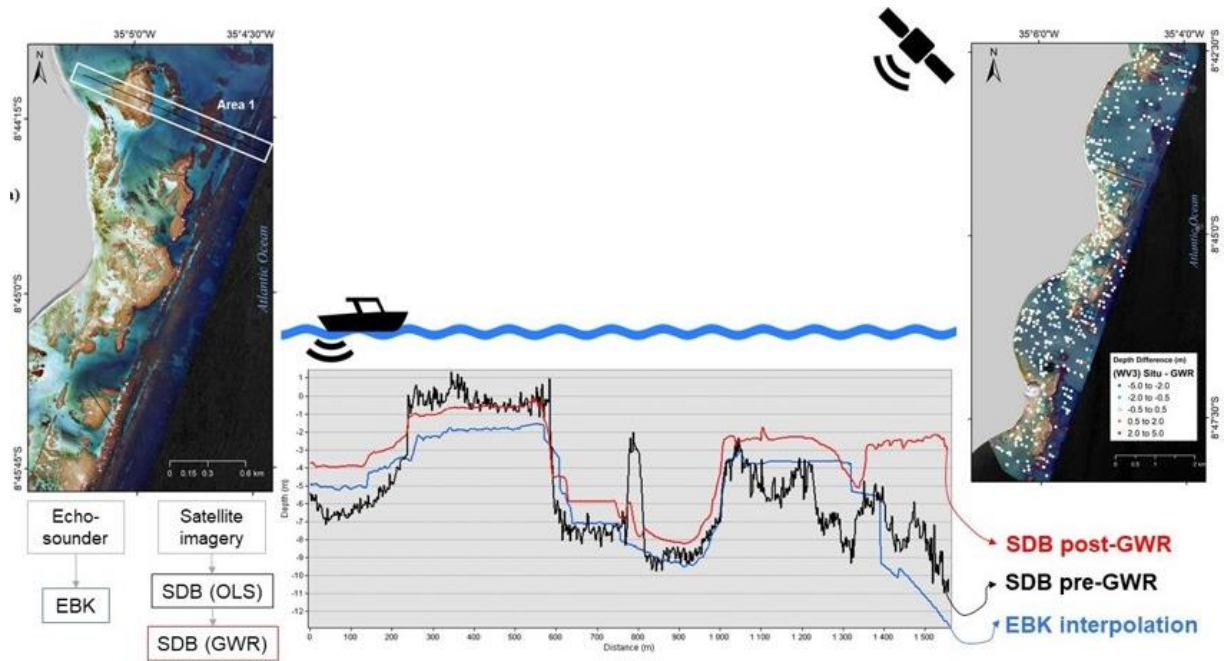
Esta Tese foi elaborada considerando as principais dificuldades envolvidas no mapeamento de habitats bentônicos e de plataforma rasa. Teve, portanto, como objetivo geral, contribuir para o avanço do conhecimento dos recifes e do mapeamento da geobiodiversidade através de ferramentas orbitais acessíveis, subsidiando assim o Planejamento Espacial Marinho e implementação de medidas de manejo. Diferentes ferramentas foram aplicadas no mapeamento batimétrico e ecológico a área de estudo, uma região de reconhecida importância por sua diversidade, protegida por quatro unidades de conservação (incluindo uma zona de uso restrito) que enfrentam inúmeros desafios frente ao acelerado desenvolvimento.

Assim, este estudo foi dividido em três capítulos, organizados em artigos científicos. No primeiro e no segundo capítulos, a abordagem é focada na zona costeira de Tamandaré, constituída por um mosaico de habitats onde predomina o ecossistema recifal. Os recifes

costeiros de Tamandaré estão em uma região rasa, extremamente complexa topograficamente e que confere desafios para a batimetria *in situ*. Desta forma, no primeiro capítulo é apresentado um mapa batimétrico obtido integrando dados coletados em campo por ecossonda (*single-beam*) e imagens de satélite de alta e média resolução. O segundo capítulo integra as métricas topográficas (derivadas a partir da batimetria construída anteriormente) com métricas ecológicas (obtidas *in situ* e remotamente) para modelar a distribuição de grandes colônias de coral nos recifes da área. A modelagem preditiva é feita de forma que permita analisar a influência de cada variável, e como estas atuam em conjunto para limitar ou possibilitar a ocorrência da espécie no ambiente recifal de Tamandaré. Além disso, a integração com o mapeamento de uso permite uma visão integrada da área, com camadas ecológicas, topográficas e seres humanos atuando de forma conjunta em uma área de proteção ambiental. O terceiro capítulo apresenta uma visão da plataforma continental a partir de imagens processadas, obtidas gratuitamente. Este capítulo representa uma nova oportunidade no uso de sensoriamento remoto por satélite em áreas de plataforma como a do Nordeste brasileiro, ao verificar feições biologicamente importantes em áreas a mais de 40m de profundidade.

Em suma, este estudo almejou contemplar toda a paisagem marinha da região, unindo um mapeamento detalhando e de fina resolução da zona costeira com uma visão em larga escala da plataforma continental.

2 MULTIREOLUTION SATELLITE-DERIVED BATHYMETRY IN SHALLOW CORAL REEFS: improving linear algorithms with geographical analysis



2.1 Abstract

Bathymetric maps are one of the first steps for most hydrological and ecological studies of the seascape, as depth is a determinant factor in the distribution of organisms, patterns of wave exposure and coastal circulation. The coral reefs of Tamandaré-Brazil, located at Costa dos Corais Marine Protected Area (MPA), encompass a mosaic of interconnected habitats of complex geomorphology, including coral reefs, algal and seagrass beds. These coastal habitats are subjected to chronic impacts such as sedimentation, reef erosion and increasing human use leading to habitat loss. Despite their social and ecological importance and conservation measures in place, there is a lack of bathymetric and habitat maps of this coast. Indeed, in situ surveys are not always feasible in shallow coral reef areas. The present study offers a detailed bathymetric mapping of the area using multiresolution satellite imagery. One Landsat-8 (December 2016) and one WorldView-03 (February 2017) imagery were used to derive medium (30m) and high-resolution (2m) bathymetry of the study area. Single-beam echo sounder surveys were performed to obtain field data to calibrate the depth retrieving algorithms: Linear Model, Band-Ratio Model, Principal Component Analyses of the transformed bands, and Geographically Weighted Regressions (GWR). For both resolution datasets, results showed that the algorithms' Root Mean Squares were significantly improved by the GWR technique ($RMS > 0.9$), due to its adaptability to the bottom heterogeneity found in complex areas such as coral reefs. Specific geomorphological reef zones were recognizable in the resulting bathymetric maps, such as intra-reef lagoon, reef crest, fore-reef, and reef flat. This research concluded that affordable methods such as single-beam data coupled with satellite imagery through GWR can provide the required inputs for mapping shallow areas with complex relief. Such results may be further used to habitat mapping, necessary to inform the multiple-use zonation foreseen in MPA management plans.

Keywords: Landsat. WorldView. High-resolution. Remote sensing. Satellite imagery. Tropical. Coastal reef. Heterogeneous. Geographically-weighted regression. Single-beam

2.2 Introduction

The influence of underwater relief on the biodiversity in the coastal zone and coral reef ecosystems is well documented and described globally (Ledlie *et al.*, 2007; Wilson *et al.*, 2007; Mumby and Steneck, 2008; Graham, 2014; Gonzalez-Rivero *et al.*, 2017). The three-dimensional nature of these habitats enables the coexistence of a wide variety of ecological niches and thus increases biodiversity (Hoegh-Guldberg *et al.*, 2007; Fabricius *et al.*, 2011). The maintenance of the inherent relief complexity of coral reefs is a key process in protecting and monitoring the ecological, social and economic functions performed by these ecosystems.

All over the world, coral reef health has been weakened by local (*e.g.* population growth, oil spill, pollution) and global impacts (*e.g.* climate change, overfishing) (Halpern *et al.*, 2008; Hughes *et al.*, 2003). Coastal coral reefs can be adversely impacted, suffering with direct impacts to its structure by activities like trampling (Barker and Roberts, 2004; Rinkevich, 1995), river discharge (McCulloch *et al.*, 2003) pollution, coastal erosion (Syvitski *et al.*, 2005) and tourism-related damage (Davenport and Davenport, 2006). These impacts are known to cause flattening of the relief (*i.e.* three-dimensionality loss) and subsequent declines in coral and fish biodiversity (Alvarez-Filip *et al.*, 2009; Graham, 2014). Therefore, relief variations must be inferred and monitored closely in various spatial scales to avoid further negative impacts on reef biodiversity and services (Bozec *et al.*, 2015; Darling *et al.*, 2017; Kuffner and Toth, 2016).

One of the first and most crucial steps in recognizing morphology and the diversity of marine environments is the study of local bathymetry (Eugenio *et al.*, 2015; Purkis, 2018), as bathymetric data allow the observation of the complexity of the bottom relief. Field bathymetry of the coastal zone is usually constrained by environmental and technical conditions that prevent its applicability to complex and shallow areas such as tropical coral reefs (Gao, 2009; Kanno *et al.*, 2011). The structural complexity, defined as the heterogeneity of natural elements and topographic irregularities (Taniguchi and Tokeshi, 2004), is one of the main characteristics of tropical coral reefs, but is also the main constraint for surveying these environments (Su *et al.*, 2008).

Due to the difficulties regarding in situ bathymetric surveys in coral reefs, techniques that obtain or derive depth data remotely have been developed and improved since the first applications of remote sensing in tropical waters (*e.g.* Chauvaud *et al.*, 1998; Mumby *et al.*, 1997, 1998). More recent advances in remote sensing have allowed the development of fine resolution bathymetric data (*i.e.*, pixel less than 10 m) (Collin *et al.*, 2017; Eugenio *et al.*,

2015; Hamylton *et al.*, 2015). However, state-of-the-art LIDAR and high-resolution satellite imagery technology are still not feasible due to budgetary constraints in several areas, (Kuenzer *et al.*, 2015; Pickrill and Todd, 2003). So, even when considering the variety of options available for obtaining bathymetry, some highly important areas (both biologically and economically) still lack quality regional-scale bathymetric data. Examples of this are abundant in Brazil, a country of continental size that harbours the only coral reef formations in the South Atlantic (Leao *et al.*, 2003).

The Brazilian coastal zone, particularly in the Northeast region, has several of the constraints faced in bathymetric mapping, which include low-quality pre-existing field data, high, complex relief in shallow waters and heterogenous substrata. The coral reefs of Tamandaré - Pernambuco, are located close to the coast (less than 1 km) and thus experience impacts intensified by recent developments (Ferreira and Maida, 2006; ICMBio, 2012). The area is of great biological and socio-economic importance and part of the Costa dos Corais, a Marine Protected Area (MPA) that spreads over 120 km of coastline (ICMBio, 2012). Multiple-use zonation, aiming to reconcile conservation and human activities, is one of the main strategies of a Federal Government's Management Plan for this MPA (ICMBio, 2012). In this region, the ecological and economic importance of the area contrasts with the lack of representative bathymetric data on a regional scale.

The main objective of this study is to aid in the process of deriving bathymetry in coastal shallow coral reefs environments. Considering the challenges involved in coral reef relief research, different depth deriving algorithms were tested in a multi resolution analysis. Four different approaches and methodologies were applied to derive bathymetry for medium and high-resolution satellite imagery. The second goal of this study was to produce a bathymetric map of the seascape in the study area that can be used a base map for future research, and as a tool to assist decision making, follow up monitoring and management strategies in the coral reef area.

2.3 Methods

This section describes the study area, the bathymetric field survey and the steps required to derive bathymetry from Landsat-8 and WorldView-3 satellite imagery.

2.3.1 Study Area

This research was conducted at the reef complex on the coast of Tamandaré, in the state of Pernambuco, Brazil, located in Costa dos Corais MPA (Figure 1). The study area is

composed by two main bays: Carneiros Bay (North) and Tamandaré Bay (South), which are bounded by two rivers: Formoso and Mamucabas, respectively. These rivers' discharge account for increased turbidity in the area, especially during winter and autumn (April – September) (Macedo, 2009).

The study area is a shallow platform area where the reef formations are arranged in a particular pattern of three parallel lines along the coast (Maida and Ferreira, 1997). The topography of the area is complex, with high reliefs and emerged reef flats in low tide. The reefs of Tamandaré harbour rich fauna compared to other reefs of the Northeast Brazil (Ferreira and Maida, 2006; Leao *et al.*, 2003) and have been morphologically described since Laborel (1969). Within Costa dos Corais MPA, these environments are inserted in areas with different degrees of protection, among them: no-take zones, exclusive fishing zones and conservation zones (ICMBio, 2012). Since 2017, Tamandaré' seascape is also a site listed in the Long Term Ecological Research (LTER) network. In spite of scientific efforts and ecological and social importance of the marine environment in the region, the coastal zone of Tamandaré still lacks bathymetric information that can be properly applied in research and local demands.

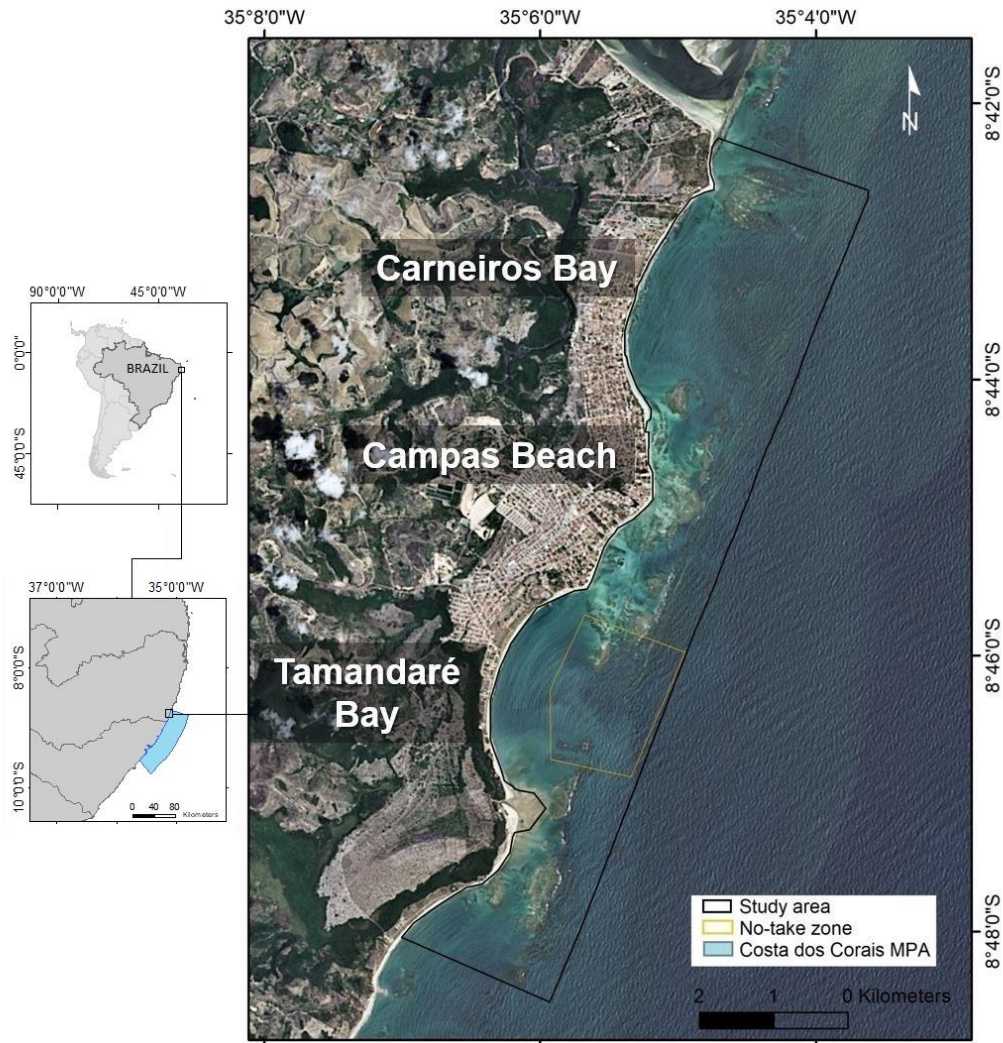


Figure 1 Study area at Tamandaré (PE, Brazil) reef complex, located within the limits of Costa dos Corais Marine Protected Area (MPA). Coordinates of WGS84 / UTM zone 25S. Brazil's and South America's polygons source: IBGE (2017)

2.3.2 *In situ* Bathymetric Survey

The bathymetric surveys were conducted during January and February 2017, using a single beam echo sounder (SonarMite BT-TM System ®). The survey followed a pre-set path, based on shore-perpendicular transects of an average length of 2 km and arranged 25-100 meters apart from each other. The survey tracks totalled 200 km, corresponding to a 22.5 km² area. All surveys were conducted on the high tide time to allow maximum water depth.

Resulting bathymetric data were processed using ERDAS IMAGINE® and ArcGIS® softwares. Duplicated points were identified, deleted and a correction of transducer depth was carried out. Tidal height correction was performed based on tide charts provided by the Brazilian Hydrographic Authority (DHN, 2017) for the closest harbour, Suape - Imbituba vertical datum – reference level RN5-DHN (estimated error = 0.1 m). The tide regime in the

region is classified as strongly mesotidal and astronomical, with an average of 12.42 hours, meaning two high tides and two low tides per lunar day (Gomes and da Silva, 2014; Hayes, 1979). As these tidal tables only display the time and height of the high and low tides, the data were merged and interpolated using spline method to fit the bathymetric data to a tide value of 0.0 m, and to the tide height of the remote sensing data.

The short time-lapse (*i.e.* less than two months) between the bathymetric surveys and both satellite images used in this study reduced the chance of significant variations on the bottom relief. To ensure comparability between the data sets, the bathymetric data were plotted in GIS software and converted to a grid matching the resolution of the satellite images. In the case of more than one depth point per cell, the value of the grid cell was calculated using the mean depth value.

Empirical Bayesian Kriging (EBK) is considered a robust method of data interpolation (Danielson *et al.*, 2016; Krivoruchko, 2012; Pilz and Spöck, 2008). Its approach is based on the calculation of multiple semivariograms, thus decreasing the error introduced by the estimation of a single semivariogram (*i.e.* one best fit model) for all unknown regions (Krivoruchko, 2012). It has been widely used for interpolating bathymetric data, especially considering its possibility to produce accurate predictions for moderate non-stationary input data (*e.g.* Araújo and Amaral, 2016; Bennecke and Metaxas, 2017; Mulcan *et al.*, 2015; Zang *et al.*, 2014). EBK was chosen as interpolation method to convert the bathymetric point data into a digital elevation model (DEM) that could be compared with the satellite derived bathymetry (SDB).

2.3.3 Satellite-Derived Bathymetry

This section details the approach used to derive the medium and high-resolution bathymetric data from satellite imagery. First, the acquisition and pre-processing of remote sensing data are described, followed by the calculation and application of the chosen algorithms.

2.3.3.1 Satellite-imagery data

The Landsat-8 OLI (L8) scene was downloaded from USGS database (<http://earthexplorer.usgs.com>) and WorldView-3 (WV3) scene was acquired through DigitalGlobe. Both images were taken during the dry season (summer) when sea water transparency is higher, and the sea surface is less rough due to low wind friction. The scenes were selected based on visual criteria such as low cloud cover, sun glint and turbidity. Table 1

displays the details of each scene.

Table 1. Details and coverage of Landsat-8 (L8) and WorldView-3 (WV3) images used in this study. Scene, map projection, datum, coverage, sun azimuth and elevation, acquisition time and date and resolution were described in each dataset's metadata file. Tide at acquisition (m) was calculated based on tide charts provided by Brazilian Hydrographic Authority (DHN).

Satellite sensor	Landsat-8 OLI	WorldView-3
Scene	LC82140662016346LGN00	104001002788CE00
Map projection	UTM	UTM
Datum	WGS84; Ellipsoid: WGS84	WGS84; Ellipsoid: WGS84
Coverage	X: -9.73430 to -7.63743 Y: -36.57156 to -34.50052	X: -8.80934577 to -8.68585772 Y: -35.11410824 to -35.06263346
Sun azimuth	122.66	94.20
Sun elevation	60.80	65.70
Date acquired	11/12/2016	23/02/2017
Scene center time	12:29:45	12:55:08
Resolution (m/px)	30	2
Tide at acquisition	2.5 m above spring tide	1.1 m above spring tide

2.3.3.2 Pre-processing of satellite data

The pre-processing steps of L8 data were atmospheric and radiometric correction, land masking and sun glint removal. A similar procedure was applied to the WV3 scene, with the exception of sun glint removal, which was not necessary due to the practical absence of glint in the scene.

2.3.3.2.1 Atmospheric correction

Atmospheric correction was carried out to minimize atmospheric effects and thus, improve the recovery of surface reflectance (Richter and Schläpfer, 2002) of L8 and WV3 imagery. ATCOR module in ERDAS IMAGINE® software was applied to produce atmospherically and radiometrically corrected datasets, using specific parameters for the area and for each sensor as inputs.

2.3.3.2.2 Land masking

After converting digital number values to surface reflectance, a land mask was built to remove unwanted land areas from the image. The Near Infrared (NIR) band was used to allow better visualization of the water/land boundaries. The land mask was then manually

vectorized to also include vessels and off-land constructions such as piers and harbours in the area, excluding these pixels from the following analysis.

2.3.3.2.2 Glint removal

The sun glint removal (*i.e.* de-glint) was carried out to remove the effects of the light reflection on sea surface. Hedley's method (Hedley *et al.*, 2005) was chosen to de-glint the L8 scene. This method was applied to each L8 visible band (coastal blue, blue, green and red), which were stacked to produce the final de-glinted scene.

The resulting images (atmospherically corrected, not influenced by land pixels and de-glinted) were used for the calculation of depth retrieval algorithms. The processing results for each dataset are presented in Figure 2.

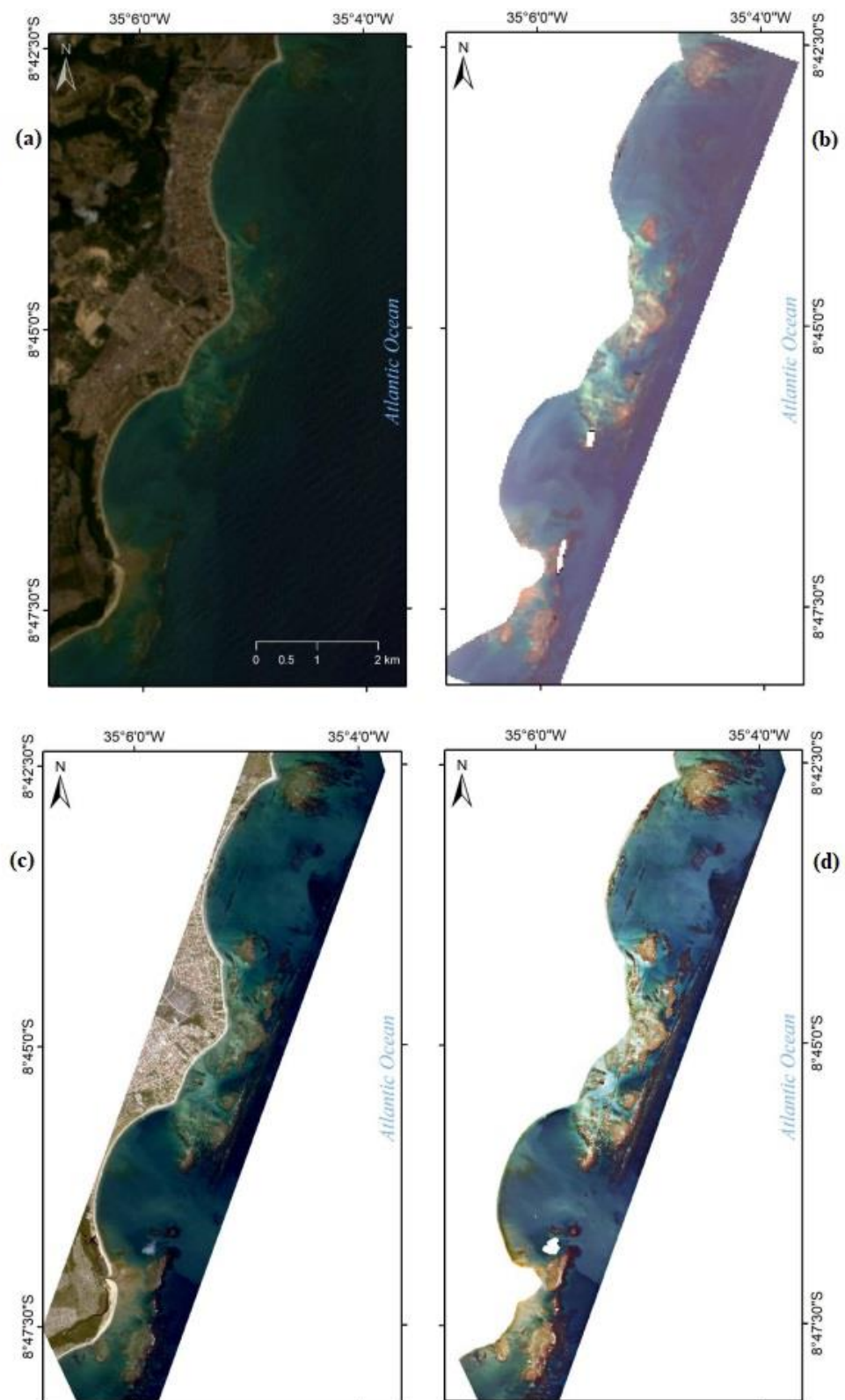


Figure 2 Before and after pre-processing of both datasets, all four presented RGB (red, green, blue) 4,3,1: (a) Original Landsat-8 image of Tamandaré coral reef complex; (b) Landsat-8 strip of the study area after atmospheric correction, land masking and sun glint removal; (c) Original WorldView-3 image; (d) WorldView-3 image of the study area after atmospheric correction and land masking

2.3.3.3 Depth retrieval from satellite imagery

The methodology for depth values retrieval from multispectral satellite imagery has been applied mainly using two approaches: the linear model (LM) (Lyzenga, 1985; Lyzenga *et al.*, 2006) and ratio bands model (RBM) (Stumpf *et al.*, 2003). The latter is theoretically better suited for areas with heterogeneous bottom, such as coral reefs (Stumpf *et al.*, 2003). For this work, adaptations of both algorithms were tested on L8 and WV3 visible bands. Also, Principal Component Analysis (PCA) (Gholamalifard *et al.*, 2013) was added to the procedure, to identify components that best relate with depth and to test the possibility of using such component to build the depth retrieval algorithm.

The application of these methods relied on raster calculations to obtain derived values for each pixel of the image. Initial procedures and calculations for the depth retrieval from L8 and WV3 followed the same methodology, shown in the workflow below (Figure 3).

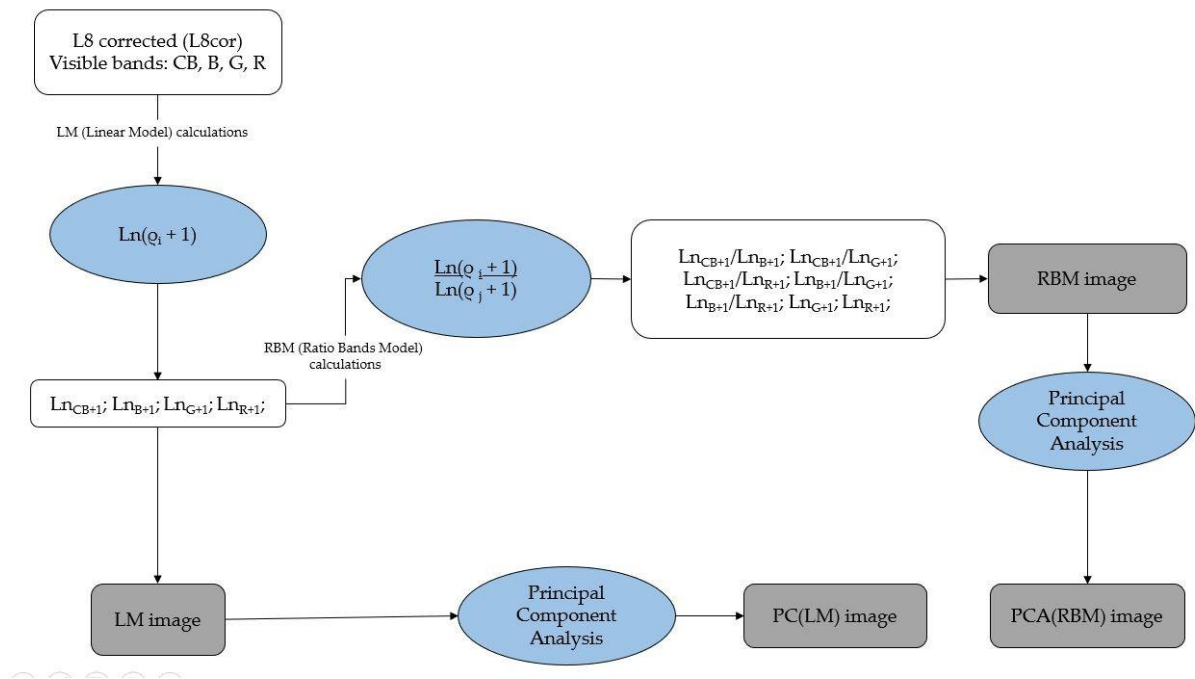


Figure 3 Workflow illustrating the inputs (white background), functions (blue) and outputs (gray) in the process of calculating the bands to be used in the depth retrieval algorithms. To produce the Linear Model (LM) variables, first, the natural logarithms plus one ($\ln p_i + 1$) of each visible band were calculated; resulting \ln bands were stacked to the raster “LM image”. The ratio of each \ln band against one another ($\ln p_i + 1 / \ln p_j + 1$) were the inputs to produce the “RBM image”. Principal Component Analyses (PCAs) were performed in each of these later images to produce the PCA(LM) and PCA(RMB) outputs

The following analyses were implemented in ArcMap 10 software using the Spatial Statistics Toolbox (Modelling Spatial Relationships Tool). Exploratory regressions were performed in each dataset, to verify which output’s band (and/or combination or bands) best

correlated with *in situ* depth values (*i.e.* higher Root-Mean-square). The original bathymetric data was gridded to match L8 (30 m) and WV3 (2 m) resolutions.

The results of exploratory regressions allowed the investigation of the best depth predictors (Table 2). These predictors were tested as possible explanatory variables in a prediction model using Ordinary Least Squares (OLS) regressions in a training dataset containing 80% of the field data, for each model. The resulting expressions were tested against the remaining 20% of field data (testing dataset). An error comparison between the depth predictions of the equations and the depth values obtained by single-beam echo sounder confirmed the Root Mean Squares (RMS) obtained in the OLS suggested equations.

Table 2 Results of Exploratory regressions using Ordinary Least Squares (OLS) for the medium resolution dataset - Landsat-8 (L8) and high-resolution dataset – WorldView-3 (WV3). All variables included in the models showed a p value < 0.01. A VIF of 7.5 was used to reduce multicollinearity issues.

Model	L8		WV3	
	RMS (VIF < 7.5)	Model	RMS (VIF < 7.5)	Model
LM	0.63	-Blue +Green	< 0.5	-
RBM	0.63	-Blue/Green	0.61	-blue/green -blue/yellow
PCA (LM)	0.71	+PC1 – PC2 -PC3 + PC4	0.64	+PC1 – PC2 -PC3 -PC4
PCA (RBM)	0.72	-PC1 +PC3 +PC4	0.65	-PC1 -PC2 +PC3 +PC4

For both datasets, corresponding grids were built, and the pixels' values of the best predictors were sampled. The pixels were used as input in the resulting equations to produce each satellite derived bathymetric map.

The correlations ($RMS < 0,8$) between depth and the predictors led to an error analysis. A Spatial Correlation Analysis was applied to the residuals, and its results indicated clustered distributions for both the L8 and WV3 datasets. Previous studies have confirmed the potential use of Geographically Weighted Regression (GWR) to decrease the errors inferred by applying one global model to a heterogeneous area (*e.g.* Monteys *et al.*, 2015; Su *et al.*, 2013; Vinayaraj *et al.*, 2016). This model addresses bottom type heterogeneity by adapting its parameters to geographical variations, identifying and applying optimal parameters for each area. Thus, GWR was applied to improve the models' outputs. GWR was applied to the algorithm which yielded the best results in the OLS regressions (Table 2). For both datasets, the algorithm with higher RMS was the Principal Component Analysis of the Ratio Bands Model, (PCA-RBM) as shown on Table 2.

2.4 Results

The current section presents the results of *in situ* surveys and the medium and high-resolution satellite-derived bathymetry. Additionally, the comparison between the resulting models and the testing dataset is demonstrated.

2.4.1 *In situ* Bathymetry

The single-beam depth data ranged from -17.4 meters to -0.20 meters. Tide correction was performed to the data to eliminate depth differences due to tide variations during field surveys' dates and times. Depth in the area reached approximately 1.7 m in the shallowest areas, exposed during low tides, and -16.0 m in the deepest channels, located mainly on the fore reef of the last reef line (Table 3).

Table 3 Post-processed depth values obtained by the single-beam echo-sounder during the field survey at Tamandaré reef complex.

Total depth records	Minimum (m)	Maximum (m)	Mean	St. deviation
209184	-15.90	1.72	-4.09	3.72

Bathymetric data acquired by the single-beam survey were plotted and interpolated using EBK to produce a DEM of the study area (Figure 4). EBK's cross-validation prediction error results were: Root-Mean-Square = 0.24; Root-Mean-Square-Standardized = 0.96; Mean Standardized Error = 0.0006; Average Standard Error = 0.34. This model was later resampled to allow comparison between the medium and high-resolution satellite derived bathymetry (30 and 2 m, respectively).

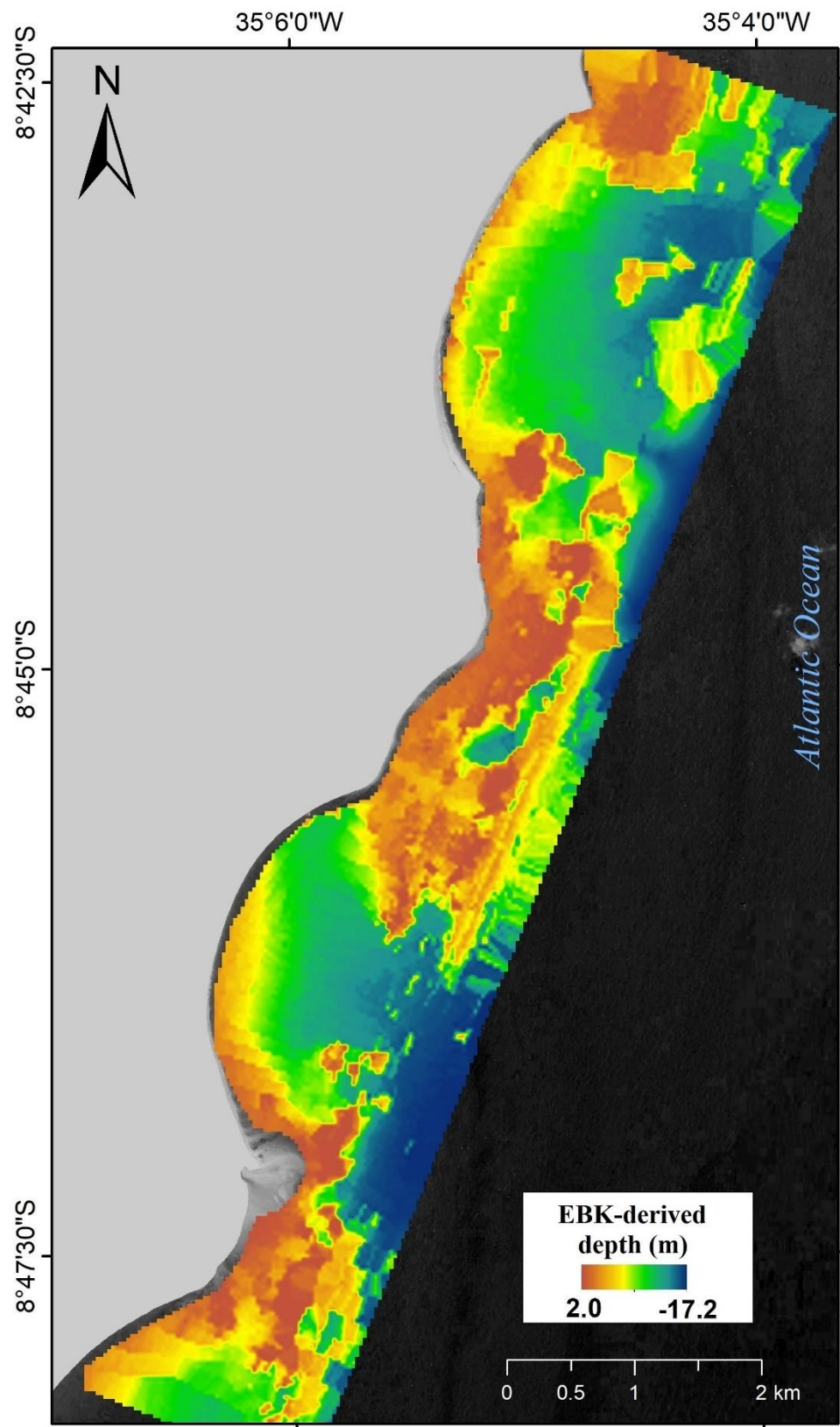


Figure 4 Digital elevation model of Tamandaré coral reef complex generated using the depth values retrieved by single beam echo-sounder. Empirical Bayesian Kriging (EBK) was the geostatistical method of interpolation

2.4.2 Satellite-Derived Bathymetry

To calibrate the satellite depth derivation algorithms, all available *in situ* data points were gridded to match the imagery datasets (Figure 5). Observing the field survey final path, several data gaps were noticed in the research area. Very shallow (or even emerged reef tops) and areas with high turbulence were bypassed or had their transect path divided in two, to be later accessed.

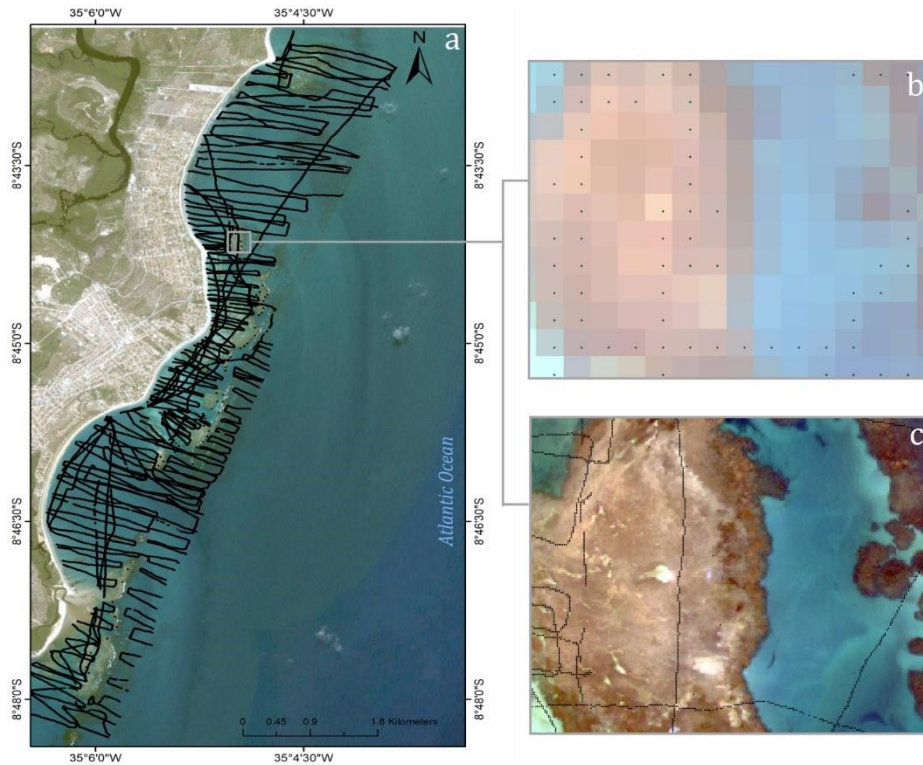


Figure 5 Field depth points distribution and grids used to calibrate the satellite depth derivation algorithms. (a) shows the post-processed field data points acquired by single beam echo-sounder (Google Earth image); (b) and (c) show a close-up of the data distribution for the Landsat-8 (spatial resolution = 30 m) and WorldView-3 (spatial resolution = 2 m) datasets, respectively

The satellite-derived data was calculated applying the best predictors as input bands of the OLS equations (Table 2). In addition, the best results were chosen from the previous analyses to predict the depths in the area using GWR (Table 4).

Table 4 Best results for the Ordinary Least Squares (OLS) and Geographically Weighted Regression (GWR) analysis carried out to test the correlation between the bands combinations and ground depth data by different models and for each satellite dataset – Landsat-8 (L8) and WorldView-3 (WV3) imagery.

	Best fit model	OLS RMS	GWR RMS
L8	PCA(RBM)	0.72	0.92
WV3	PCA(RBM)	0.65	0.95

2.4.2.1 Medium resolution satellite-derived bathymetry

The four bathymetric maps derived from OLS using Landsat-8 bands bear similar resemblance with each other (Figure 6). The maximum depth is variable dependent on the algorithm applied. LM algorithm and its derived PCA show deeper depth limits (Figures 6a and 6c) than RBM and its PCA (Figures 6b and 6d).

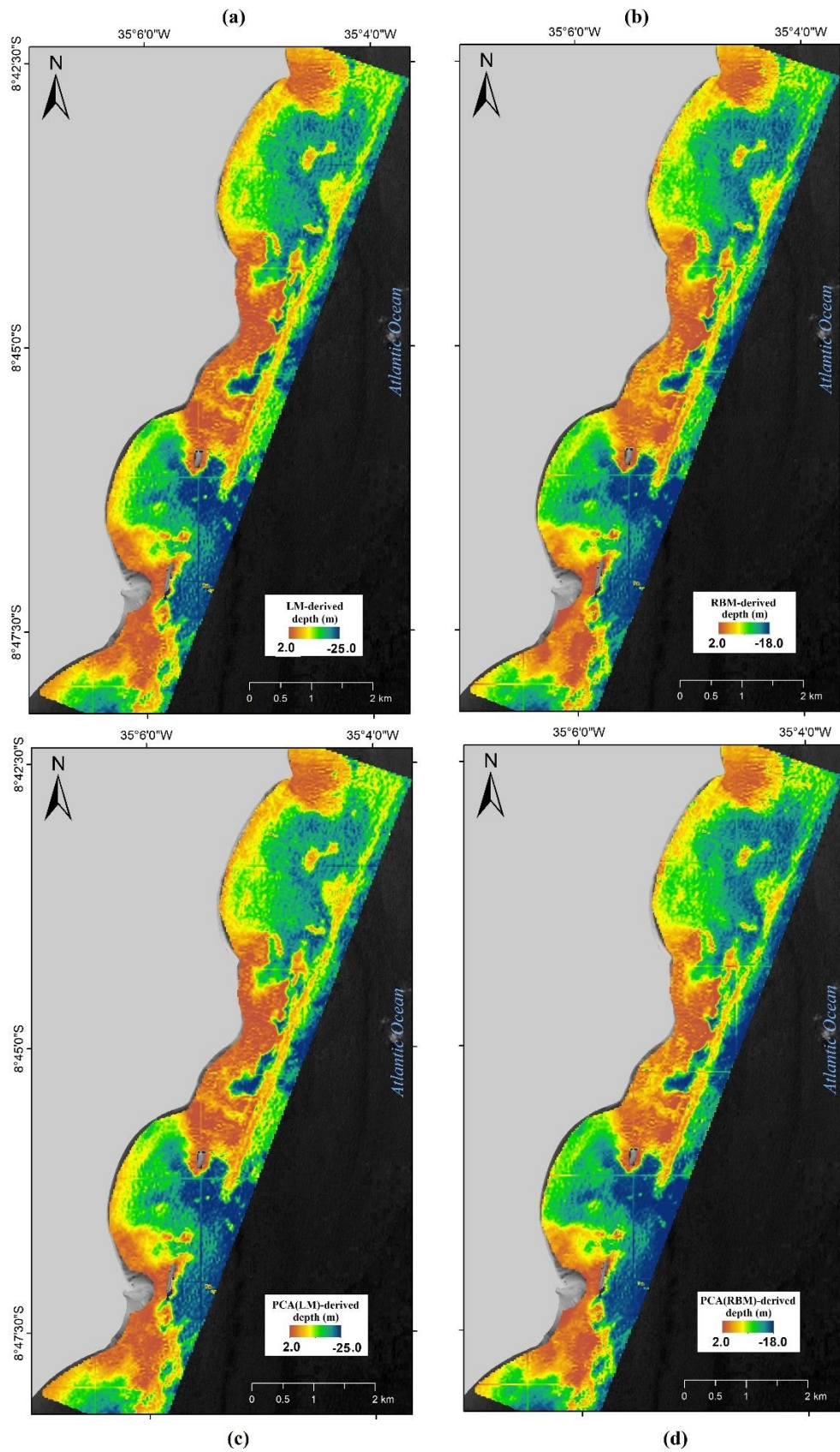


Figure 6 Medium resolution satellite (Landsat-8) depth derivation in Tamandaré Coral Reef Complex, using: (a) Linear Model (LM); (b) Ratio Band Model (RBM); (c) Principal component analysis of log-transformed bands (PCA[LM]); (d) Principal components analysis of the ratio bands model (PCA[RBM])

Applying a GWR to the best OLS results improved the RMS (from 0.72 to 0.92). The GWR-derived bathymetry successfully shows reef boundaries, subtle depth variations across different substrata and across sand channels (Figure 7). Of all the previous bathymetric maps, the GWR derivation shows the best fit to ground truth data.

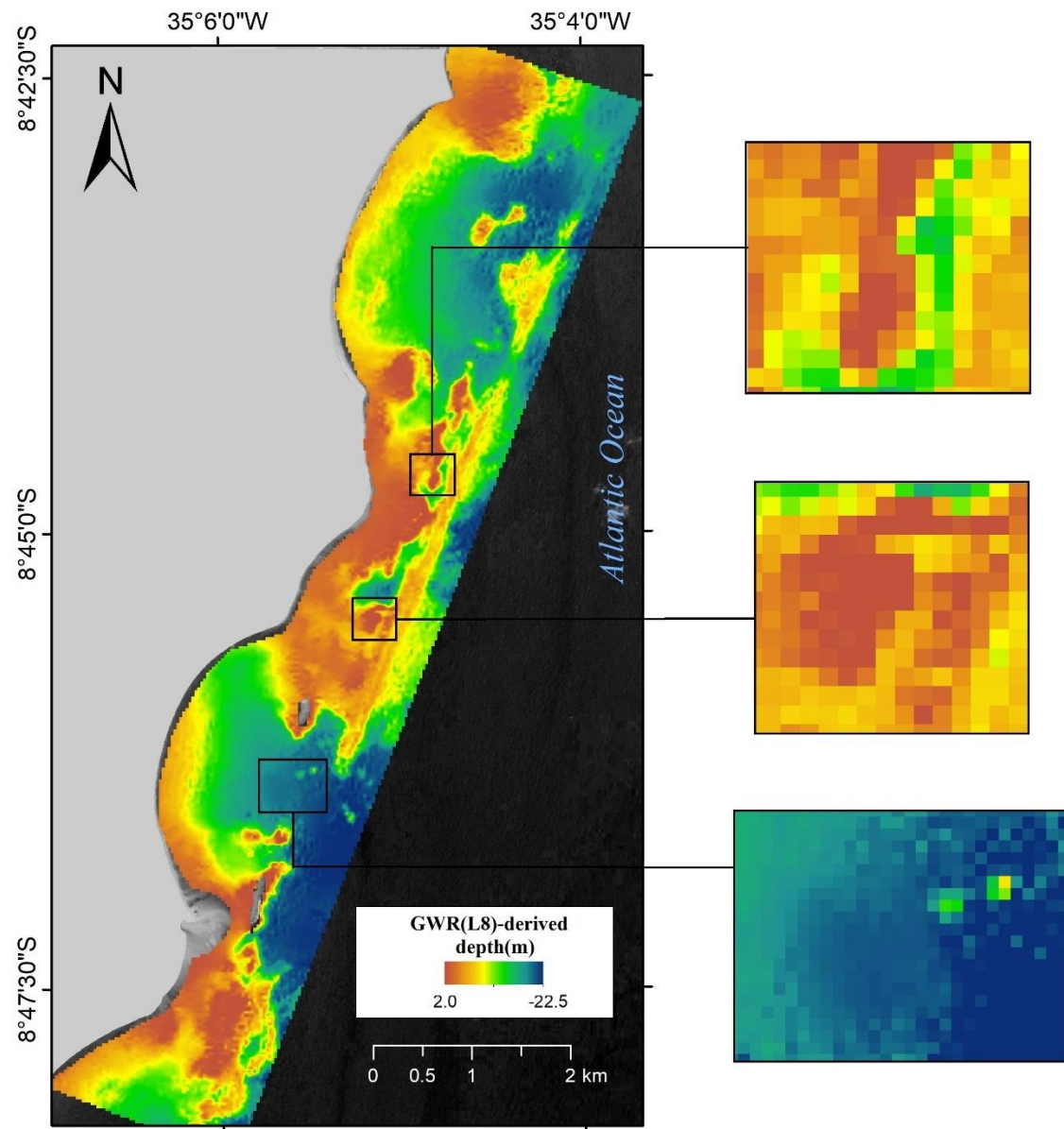


Figure 7 Medium resolution satellite (L8) depth derivation in Tamandaré Coral Reef Complex, using Geographically Weighted Regressions (GWR). Three images on the right show close-ups of different areas in the scene (reefs with deep and shallow borders, sand channels)

A raster difference operation (Figure 8) was applied to expose the differences between all three datasets (EBK, PCA-RBM and GWR) in a pixel-by-pixel basis. This operation allowed the visualization of which areas were responsible for the most variable results.

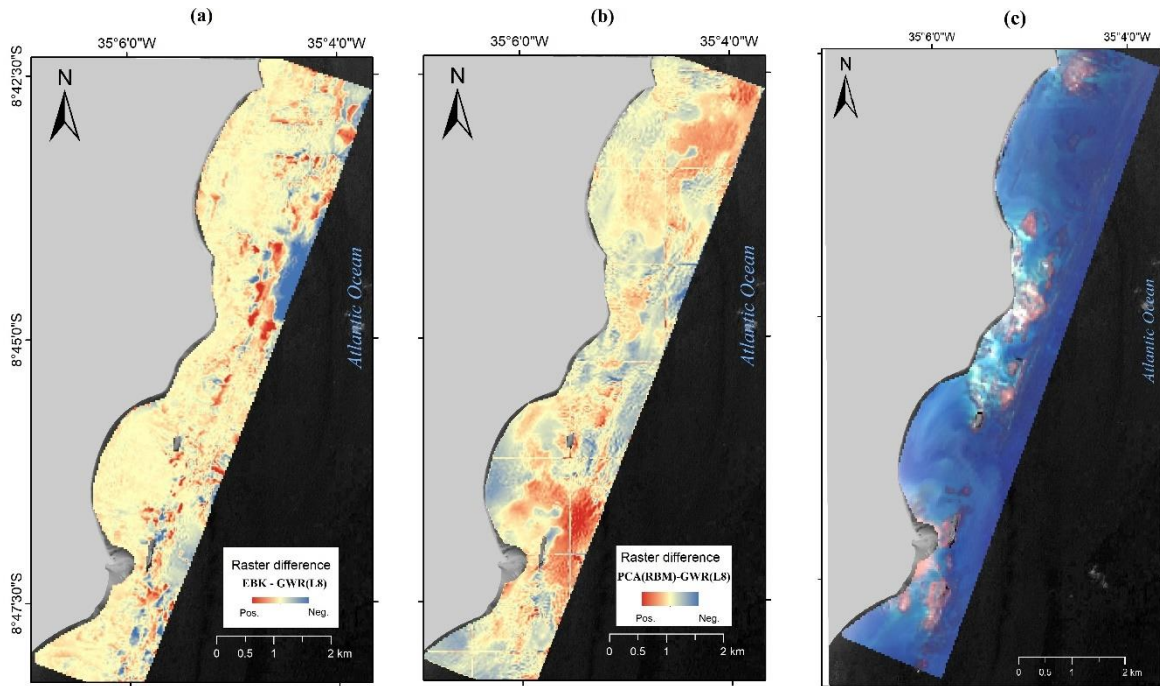


Figure 8 Results of raster operations for medium resolution bathymetry: (a) “Empirical Bayesian Kriging (EBK) minus Geographically Weighted Regression (GWR)” and (b) “PCA(RBM) minus GWR. Positive values (red) show areas where GWR depth values were lower (deeper) than EBK or PCA(RBM). Negative values (blue) show shallower estimations by GWR than the compared model. Neutral colours show high agreement areas. (c) Landsat-8 (L8) (RGB432)

The medium resolution satellite bathymetric derivation (L8-SDB) results are consistent with the regional depth and reef distribution. The three reef lines pattern is well defined, and large-scale relief are spotted throughout the scene (*e.g.* channels, depth variation between large reef formations, wide tide pools and lagoons). Most depth differences between the field bathymetry DEM and L8-SDB are in areas that represent a challenge for *in situ* data acquisition. Lower correlations between PCA(RBM) and GWR derived bathymetry infer a contribution of a lighter water colour in the shallowest estimations by PCA(RBM). The reefs present in the eastern borders of the image may indicate a depth overestimation by PCA(RBM), due to their darker visual representation.

2.4.2.2 High resolution satellite-derived bathymetry

The results of the high-resolution satellite derivation and comparisons with *in situ* interpolations follow the same scheme as the previous section. OLS results for the best WV3 depth predictors are shown in Figure 9. The linear model (LM) was not used to calculate a bathymetric map due to its low correlation with *in situ* values ($RMS < 0.5$).

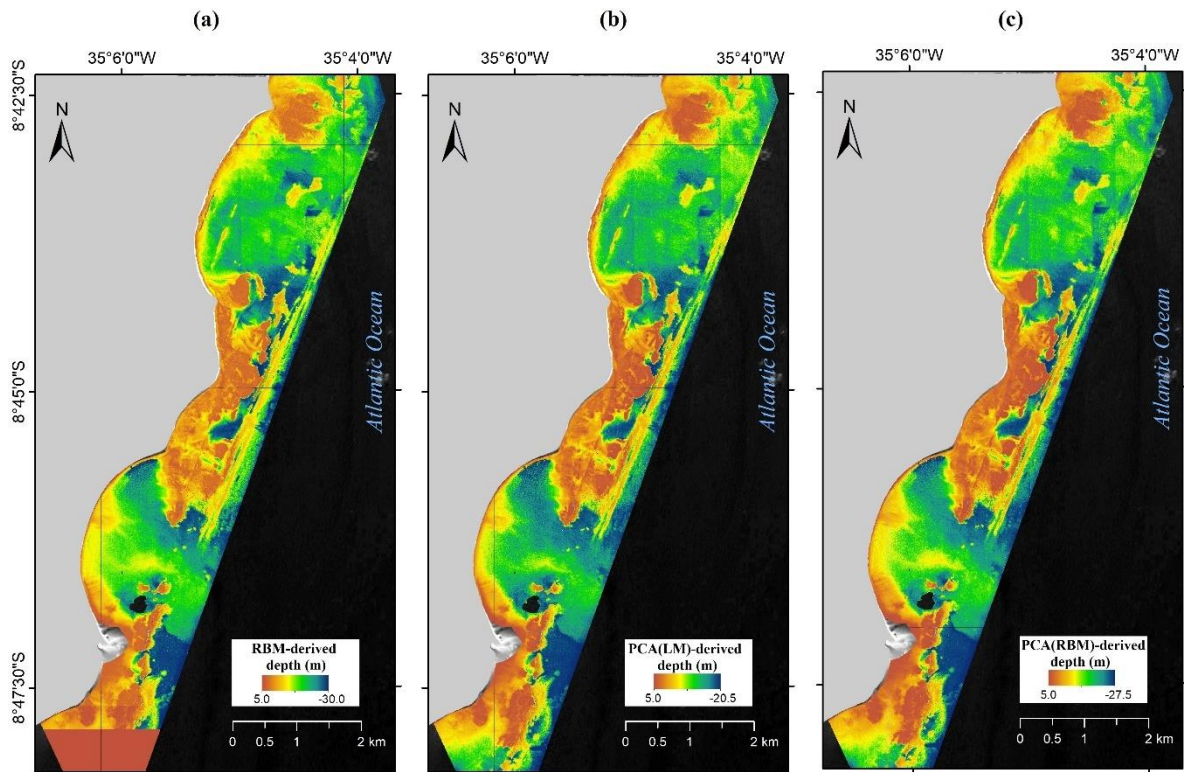


Figure 9 High resolution satellite (WorldView-3) depth derivation in Tamandaré Coral Reef Complex, using: (a) Ratio Band Model (RBM); (b) Principal component analysis of log-transformed bands (PCA[LM]); (c) Principal components analysis of the ratio bands model (PCA[RBM])

Analogous to the medium-resolution derivation, the bathymetric maps derived from OLS using Worldview-3 bands look similar to each other in general. The maximum depths are again, different, dependent on the method. RBM's values registered up to 30-meter deep areas, what may be identified as an exaggeration, considering *in situ* values and the other derivation results. The three maps show a great level of detail, with well-defined reefs, even in more complex areas, such as the reefs in the central zone of the image.

PCA(RBM) model was used as input to produce the GWR bathymetric model (Figure 10), improving the RMS of the algorithm from 0.65 to 0.95. The close-up images show specific structure variations, like small tide pools on reef flats and, distinct reef zoning and small-scale variations in deeper reefs. On the other hand, due to the high-resolution of the image and the arrangement of *in situ* data, the resulting image exhibited artefacts even after applying smoothing techniques. These “glitches” resemble narrow ridges, both parallel and orthogonal to the shoreline and are caused by the distance between data points from one transect to another, and to the number of neighbours used to derive the GWR model.

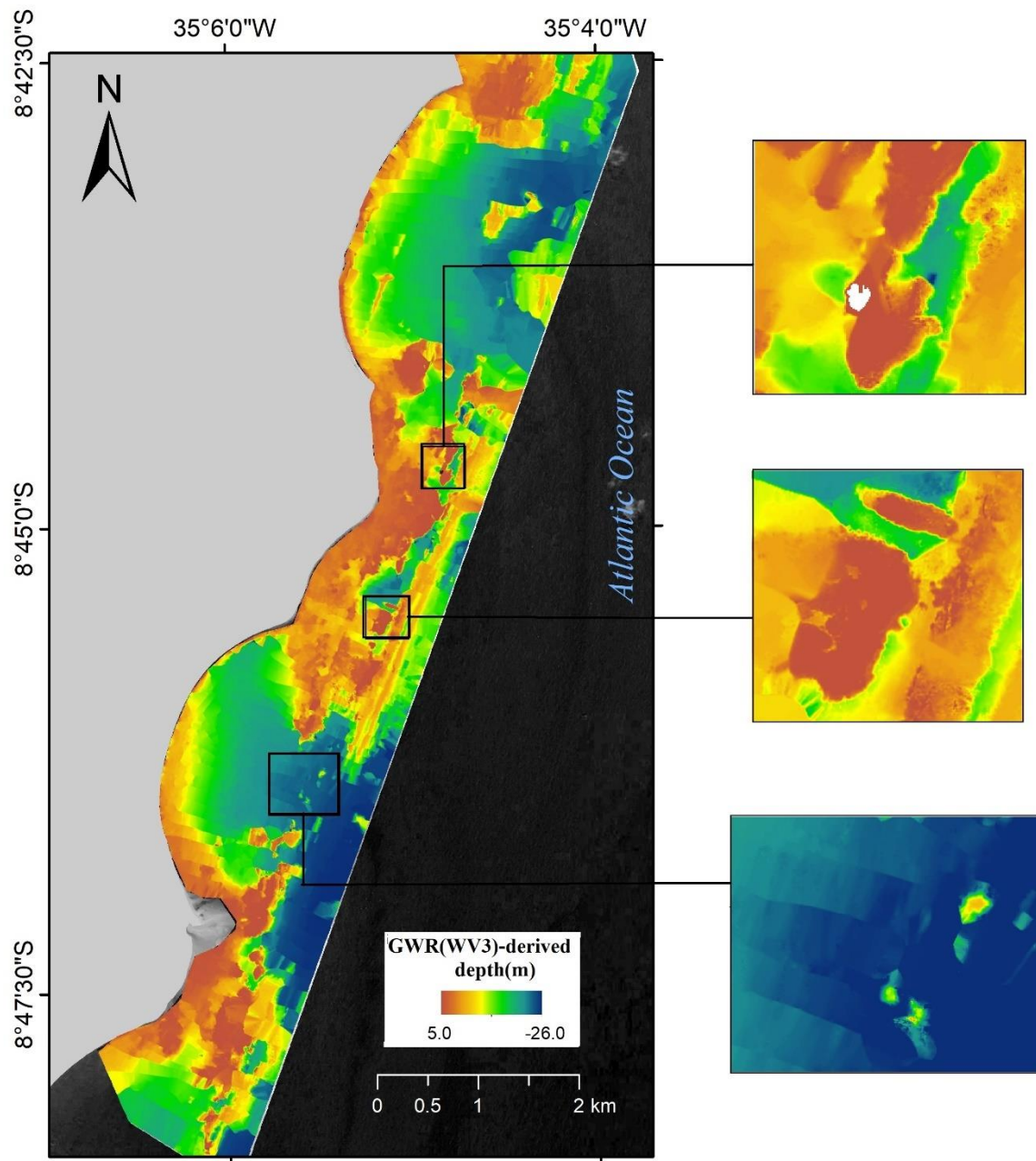


Figure 10 High-resolution satellite (WV3) depth derivation in Tamandaré Coral Reef Complex, using Geographically Weighted Regressions (GWR). Three images on the right show close-ups of different areas in the scene

GWR(WV3) results were compared against EBK interpolation of *in situ* values and against the best OLS predictor (PCA[RBM]) to identify further discrepancies between the three bathymetric datasets (Figure 11).

EBK's comparison with GWR(WV3) the majority of the area has a neutral colour, exhibiting similar values. The different values appear to be considerable extreme in colour (dark red and dark blue) but small in area. These are mostly in zones lacking *in situ* data, reflecting possible errors in the EBK interpolation. Comparing the PCA(RBM) results, it is

possible to notice that the differences are much more diffuse in area but in general, are represented by a neutral colour scheme. PCA(RBM) appear to be more influenced by the water colour than the GWR, showing shallower values in known deep areas (*e.g.* sand channels in the lower and upper bays visible in Figure 11c).

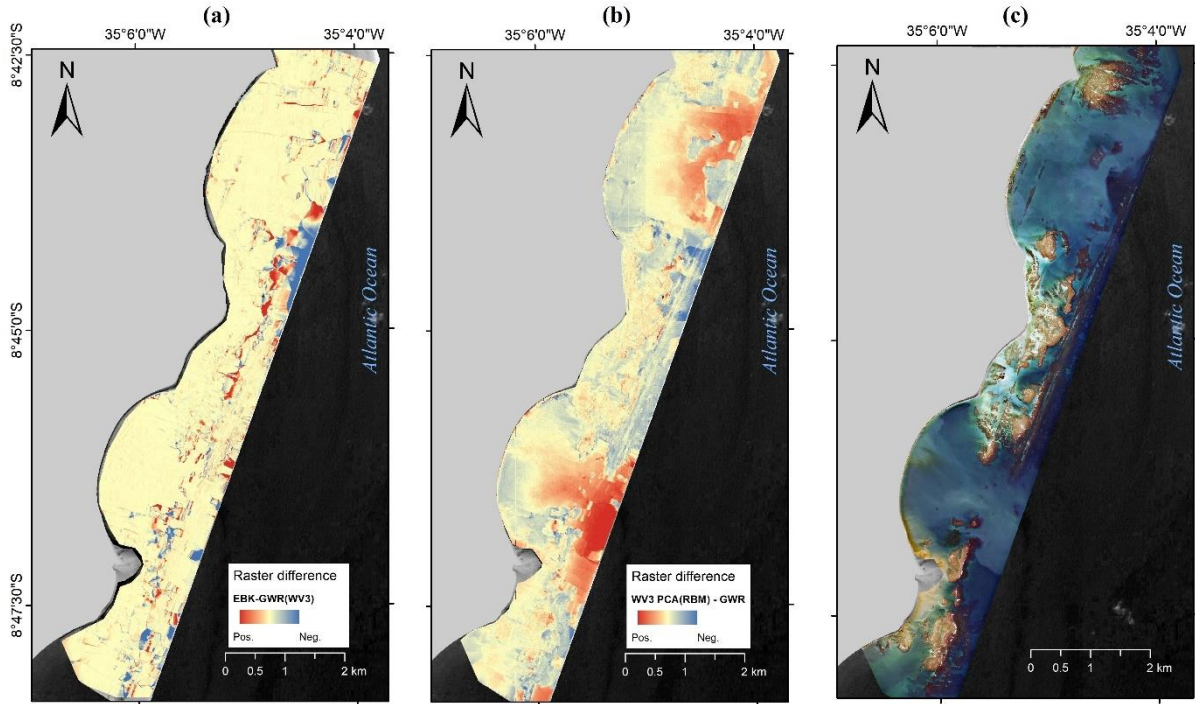


Figure 11 Result of raster operations for high-resolution bathymetry: (a) “EBK minus GWR”; and (b) “PCA(RBM) minus GWR. Positive values (red) show areas where GWR depth values were lower (deeper) than EBK or PCA(RBM). Negative values (blue) show shallower estimations by GWR than the compared model. Neutral colours show high agreement areas. (c) WV3 (RGB431) is provided for comparison purposes

2.4.2.3 Bathymetric models’ comparison with *in situ* testing dataset

Each model was tested against the testing dataset (*i.e.* 20% of the original *in situ* data) to analyse the differences between depth values derived by the bathymetric models and the values observed *in situ*. Figures 12 and 13 show the analyses’ results for the medium and high-resolution bathymetric models, respectively. The medium resolution model derived from EBK interpolation (Figure 12a) shows more depth differences than the high-resolution EBK derivation (Figures 13a), which can be due to resampling the depth data to match Landsat’s 30-meter resolution. For both datasets, OLS-derived models (Figures 12b, 13b) show the highest deviations from *in situ* values. The resulting depth differences confirm the water colour influence in these models observed in Figures 8 and 11. GWR-derived maps (Figures 12c, 13c) seem to account for these discrepancies, as the majority of depth difference values are within a 0.5-m range.

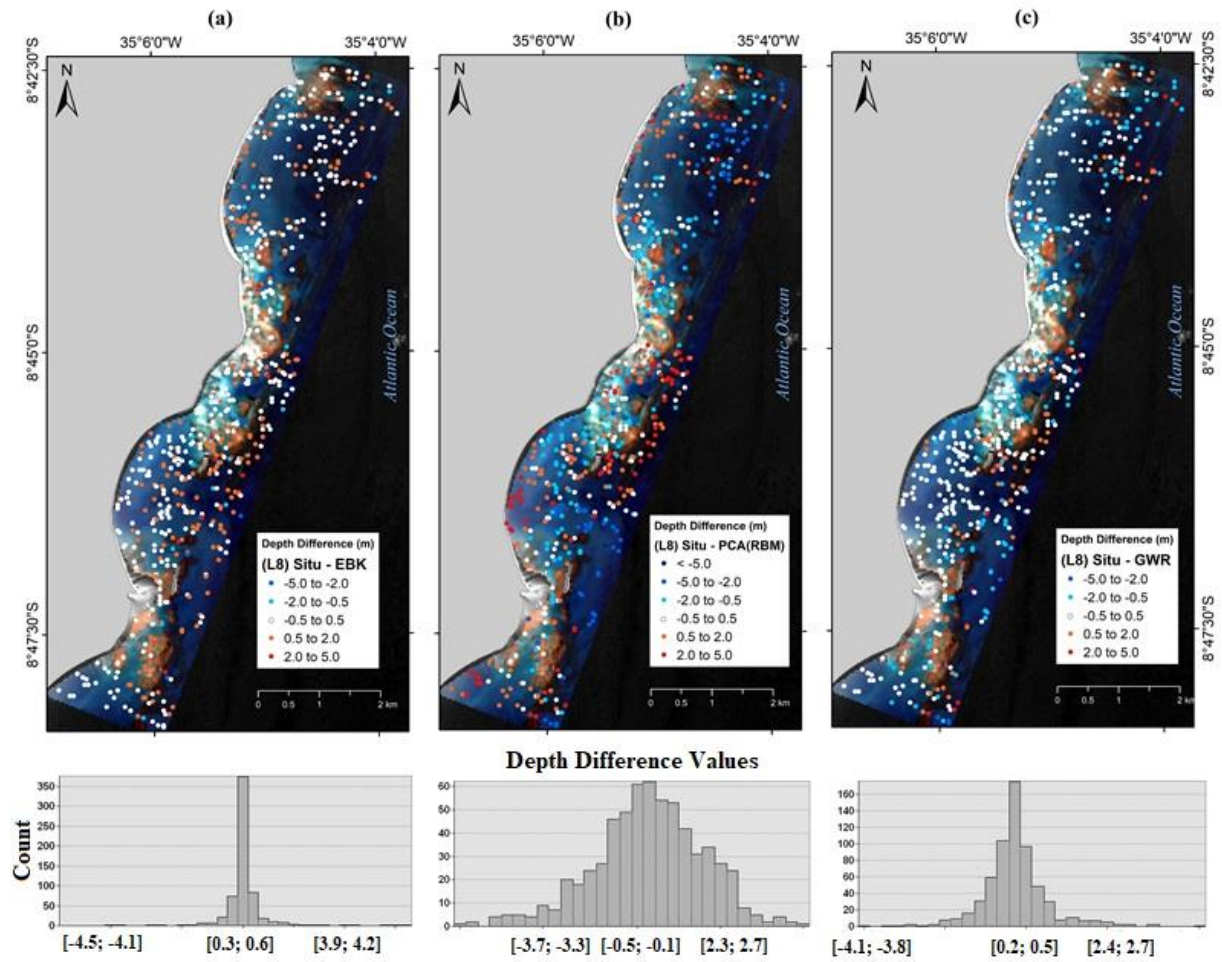


Figure 12 Medium resolution dataset's differences observed between in situ depth values and; a) EBK-derived depth; b) Principal Component Analysis of the Ratio-Band Model (PCA[RBM])-derived depth; c) Geographically Weighted Regression (GWR)-derived depth. Blue points show areas where the real (situ) depth were deeper than predicted by the models, red points show areas where the real depth were shallower than the predicted by the models and white points show high agreement between the datasets (i.e. depth difference < 0.5 m)

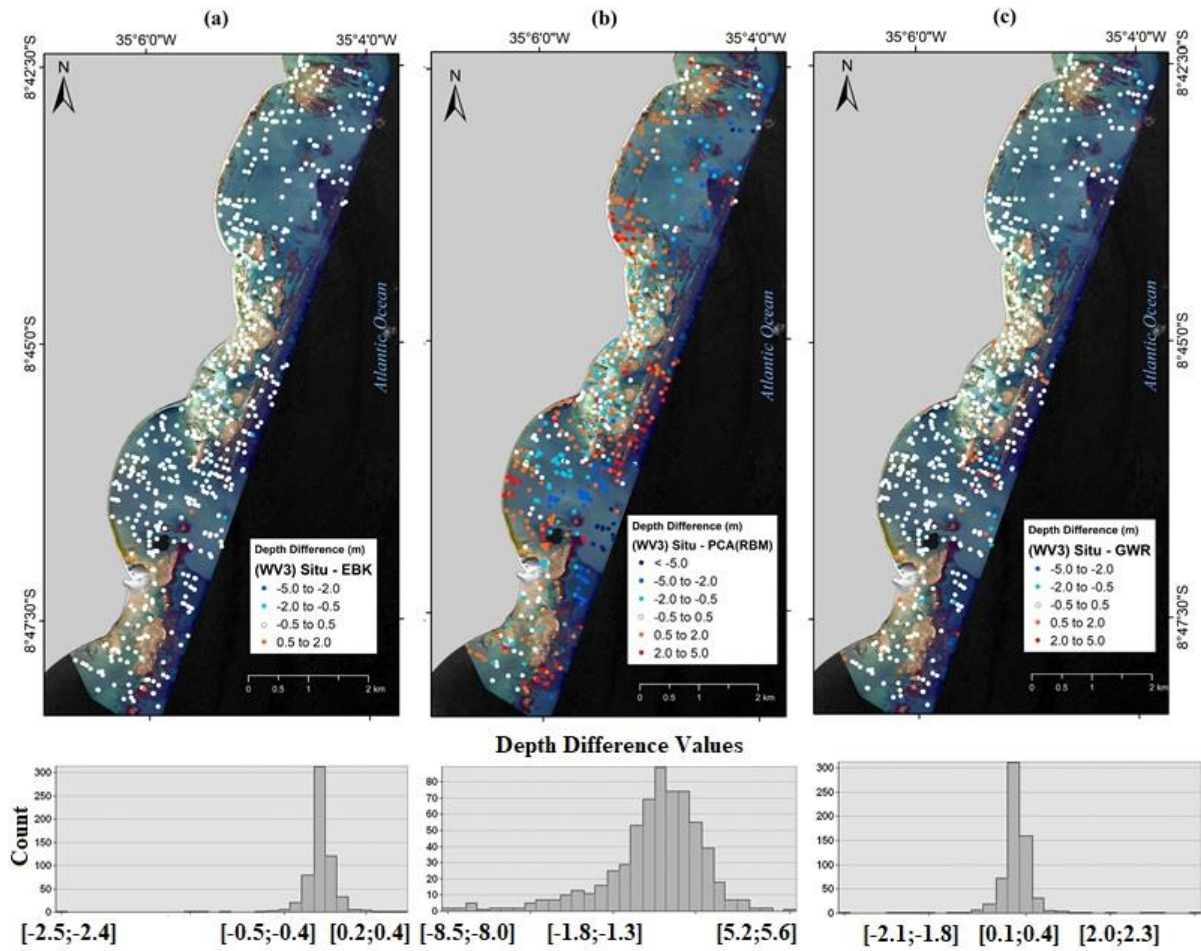


Figure 13 High resolution dataset's differences observed between in situ depth values and; a) EBK-derived depth; b) Principal Component Analysis of the Ratio-Band Model (PCA[RBM])-derived depth; c) Geographically Weighted Regression (GWR)-derived depth. Blue points show areas where the real (situ) depth were deeper than predicted by the models, red points show areas where the real depth were shallower than the predicted by the models and white points show high agreement between the datasets (i.e. depth difference < 0.5 m)

2.4 Discussion

Depth is one of the main controlling physical factors in the distribution of benthic and fish communities (Green *et al.*, 2005; Wilson *et al.*, 2007; Pittman *et al.*, 2009). The complexity of the relief in a coral reef environment needs to be analysed at different scales: it requires a scale small enough to perceive the details of the ecosystem, yet large enough to cover large areas that harbour the complexity intrinsic to coral reefs. Satellite imagery can be classified by spatial resolution, based on the size of each pixel: very high (< 1 m/pixel), high (1 – 10 m), moderate or medium (10 – 100 m) and low (> 100 m) (Hedley *et al.*, 2016). Deriving depth by remote sensing in coral reefs is generally accomplished by using moderate (*e.g.* Hedley *et al.*, 2018; Pacheco *et al.*, 2015; Vinarayaj *et al.*, 2016) or high-resolution datasets (*e.g.* Collin and Hench, 2012; Doxani *et al.* 2012; Manessa *et al.*, 2016; Monteys *et*

al., 2015). Considering the large area covered by each satellite image, remote sensing is considered a feasible option for mapping and monitoring coral reefs, as it can be implemented in fine resolution in a large spatial scale (Mumby *et al.*, 2004).

The first step to study the depth variations in the study area was a bathymetric survey, as field data is necessary to calibrate the algorithms used to derive bathymetry from satellite imagery. Several authors (*e.g.* Su *et al.*, 2014; Kabiri, 2017) have used depth data from local nautical charts to calibrate bathymetry from remote sensing, thus avoiding the onerous field survey. This was not possible in the area due to errors and sparse data associated with the outdated nautical chart for the Tamandaré coastal region.

The linear and ratio models (LM and RBM) are widely used to derive depth from satellite imagery (*e.g.* Gao 2009; Contreras-Silva *et al.*, 2012; Zoffoli *et al.*, 2014; Casal *et al.*, 2019). The ratio approach is an adaptation of the LM approach, and it was developed to minimize the effects of varying albedo in heterogeneous areas (Stumpf *et al.*, 2003). Therefore, in a coral reef region, with heterogeneous bottom substrate and complex relief, RBM is expected to show higher correlation with *in situ* values. Oppositely, in the present research, LM and RBM showed similar correlation (Figure 6 a, b) for the medium-resolution bathymetry (LM-L8 RMS and RBM-L8 RMS = 0.63). This contrasts to what was observed in previous studies (*e.g.* Stumpf *et al.*, 2003) but agrees with some others (Lyons *et al.*, 2011; Pacheco *et al.*, 2015), that considered the LM an acceptable method for deriving bathymetry in shallow waters. For the high-resolution dataset (Figure 10 a, b), this result was quite different, since LM could not be used to derive bathymetry due to its extremely low RMS. This result by itself can attest to the differences in using multiple satellite sensors, even when applied to the same study area, tuned with the same ground data and following the same corrections' protocol. The ratio of the blue and green bands, consistently used in remote sensing bathymetric derivation (*e.g.* Daniell, 2008; Jagalimgam *et al.*, 2015; Stumpf *et al.*, 2003), was also the best fit for the RBM using Landsat-8 and WorldView-3 pixel values.

The Principal Component Analyses of LM and RBM (Figures 6 c, d and 10 c, d) yielded the best results for linear regression for both satellite images (for L8, PCA-LM RMS = 0.71, PCA-RBM RMS = 0.72; and for WV3, PCA-LM RMS = 0.64, PCA-RBM = 0.65). The range of values found in the present study is generally considered reasonably good results and have been used to derive bathymetry and topographic metrics from satellite image (*e.g.* Gholamalifard *et al.*, 2013; Knudby *et al.*, 2010), so both these coefficients can already be considered good depth predictors (RMS > 0.65). This result can be applied to estimate the

depth of other areas in the same scene, which, when considering the total size of the original Landsat 8 scene for example (185 x 180 km), can be very promising for future studies.

Even though the PCA(LM) and PCA(RBM) were the best OLS discriminators of depth, they were still influenced by spatial effects. This error yielded the need of a geographically adaptative model, which effectively improved the results. Other studies corroborate this approach (*e.g.* Monteys *et al.*, 2015; Vinarayaj *et al.*, 2016), showing better performances of geographically adaptative models over one “global” model for the whole scene. This GWR applied to obtain the best results is locally specific, and although it may properly predict missing data in the study area, its applicability in other parts of the scene is limited.

Regarding the differences between EBK interpolation of *in situ* values and the SDBs the majority of the surface areas show good similarity. As previously stated, deeper areas, most reef tops and high turbidity zones do not show high accuracy due to gaps in the survey transects. SDB could predict the depth values of these areas, inferring that the error relies on the interpolation and not on the bathymetry derived by L8 or WV3. In fact, the depth range in the study area was almost ideal, as the coastal blue and blue bands (present in both sensors) have their maximum penetration in 30 meters in perfectly transparent water and about 15-20 m in normal conditions (Gao, 2009; Liceaga-Correa and Euan-Avila, 2002).

Both scenes selected for this study were taken during summer (December 2016 and February 2017 for L8 and WV3 respectively), to minimize the chance of high sediment influx from the two main rivers in the area. Even so, it is possible to see a sediment plume across the region in both images. Reduced accuracy in depth derivation by satellite imagery due to sedimentation was observed in previous works (*e.g.* Green *et al.*, 2000; Monteys *et al.*, 2015). This appears to be an issue in this research only in the OLS derivations but was mitigated by the GWR. In summary, the medium resolution bathymetric map derived from GWR (Figure 8) improves the results of EBK interpolation (removes artefacts from the resulting raster and corrects the errors due to missing data) and of the OLS derivation (GWR was less influenced by water colour that overestimates depths in coral reef tops and underestimates in high-sediment areas). For the reasons mentioned, it was considered the best medium resolution bathymetry for the area, and thus, the resulting bathymetric map is recommended for use in future studies and demands.

GWR high-resolution derivation is highly important as it offers a spatial resolution detailed enough to allow ecological studies (Eugenio *et al.*, 2015; Purkis, 2018). The results (Figure 12) show a much more detailed vision of the area, with structures and patterns that

could not be observed in the medium resolution bathymetry. The high definition mapping of the complex coral reef area is a substantial improvement especially for the derivation of bathymetry-dependant metrics such as rugosity that can be used to infer complexity areas and as a tool in management decision.

The main morphological features described for the reefs in the area (Maida and Ferreira, 1997), with the three reef lines parallel to the coast, could be observed in the SDBs generated by the algorithms. The differences in results of the medium-resolution bathymetry, the high-resolution bathymetry, and the algorithms used to generate them can be noticeable when profiles of a large area (Figure 14) and a small area (Figure 15) are analysed. These profiles were generated following the same path made during the field survey.

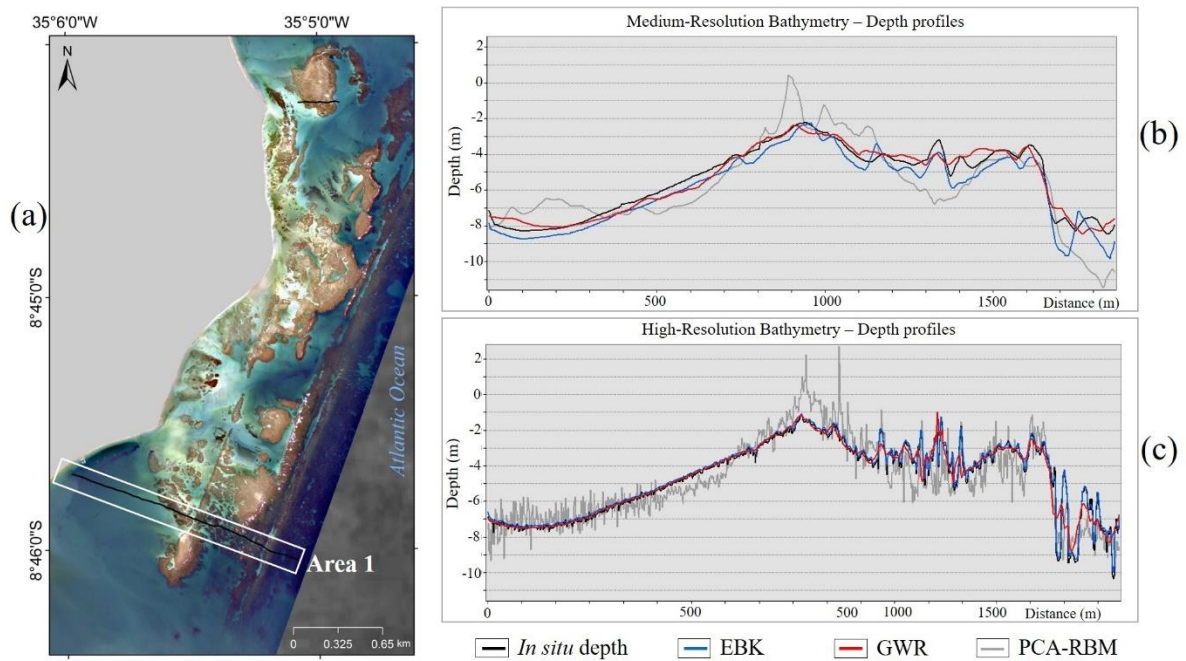


Figure 14 Depth profiles of “Area 1” (>1500m) in Tamandaré coral reef complex on single-beam survey transects using the different depth derivative algorithms. The profiles on the right show *in situ* depth values (black), Empirical Bayesian Kriging (EBK) interpolation (blue), Principal Component Analysis of the Ratio Bands Model (PCA[RBM]) (grey) and Geographically Weighted Regression (GWR) (red). (a) location of “Area 1”, considered a large area for the scope of this research, WorldView-3 RGB 431 is displayed for visualization purposes. (b) Medium-resolution bathymetric profiles; (c) High-resolution bathymetric profiles

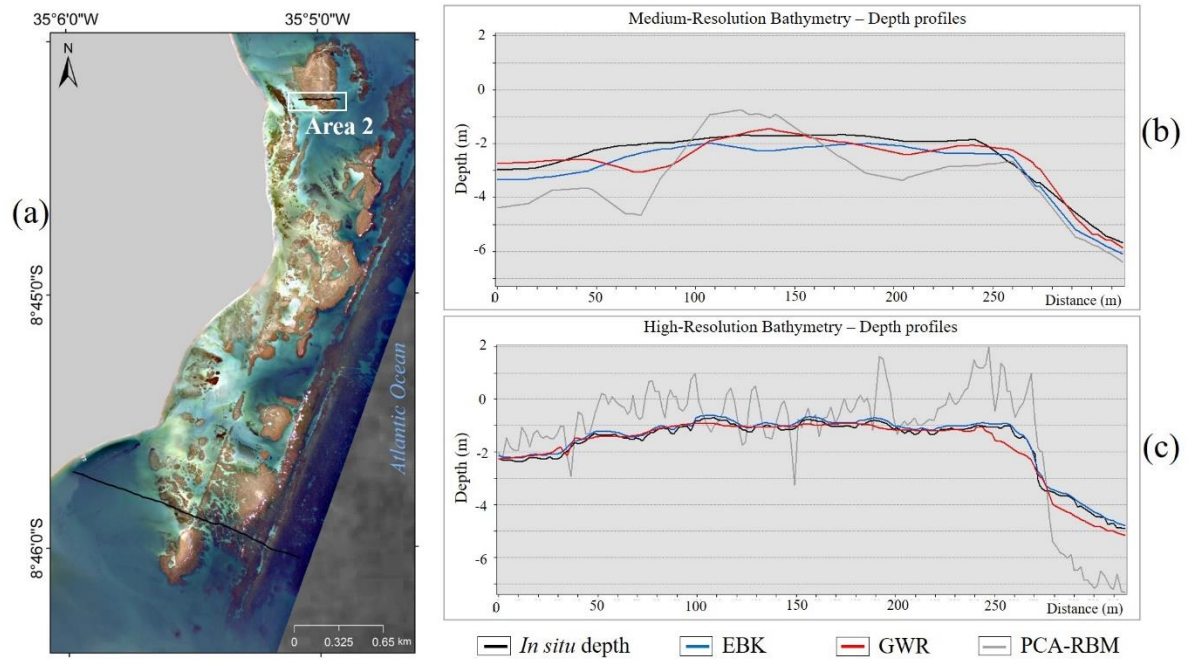


Figure 15 Depth profiles of “Area 2” (< 500 m) in Tamandaré coral reef complex on single-beam survey transects using the different depth derivative algorithms. The profiles on the right show *in situ* depth values (black), Empirical Bayesian Kriging (EBK) interpolation (blue), Principal Component Analysis of the Ratio Bands Model (PCA[RBM]) (grey) and Geographically Weighted Regression (GWR) (red). (a) location of “Area 2”, considered a small area for the scope of this study, WorldView-3 RGB 431 is displayed for visualization purposes. (b) Medium-resolution bathymetric profiles; (c) High-resolution bathymetric profiles

The profiles of the medium-resolution bathymetry (Figure 14b) across a large area show the agreement between the algorithms and depth values obtained by single-beam survey. Analysing closely, GWR and EBK were able to perceive an increase of depth at the beginning of the profile (first 150m). This lagoon is very close to the shore and can reach more than 8 m of depth in the first 50 m. This area should be monitored closely, as it can be a hazard to beach users. On the other hand, this particular relief's configuration (depth and proximity to the coast) has made this area historically known as an ideal harbour location (Branner, 1904; Oliveira, 1864). PCA-RM is not able to detect this lagoon in the first 200 m of the profile, probably influenced by water colour and high sedimentation in the area. It is possible to visualise a gradual decrease of depth until the profile reaches the second reef line (circa 1000 m). The algorithms show the complex relief associated with the spur-and-groove and fragmentation in the region between the second and third reef lines. Satellite imagery of the region (*e.g.* Figures 2 and 14a) allow the observation of the third reef life throughout the region. These reefs, as described by Maida and Ferreira (1997) form a barrier line and can be exposed during low tides. In this profile, the third line is first detected at 1600 m, followed by a lagoon and the remaining reef formation. Due to high rugosity and increased wave action, field survey of these features was challenging and sometimes, not possible. In areas with

missing field data, EBK interpolation registered a sudden increase of depth (Figure 4), missing the outer reef line. On the other hand, SDB profiles were able to register this feature, evidencing better suitability to map such regions.

The high-resolution bathymetry of Area 1 (Figure 14c) show similar geomorphologic features in the area. The narrow lagoon (1700 m) separating the shallower portion of the third reef line from its deeper fore reef and intra-reef lagoons can be seen in the profiles and were registered by all three algorithms. Even though it is a large area, the level of detail brought by the GWR derived from WV3 is remarkable: small topographic variations can be seen throughout the profile, successfully showing the complex relief of the reefs and sand channels.

The small scale profiles (Figure 15) confirm the robustness of the high-resolution GWR for detailed studies. While in the medium-resolution bathymetry it is only possible to observe the presence of a reef (Figure 15b), distinct geomorphological zoning and specific structures are efficiently observed in the high-resolution GWR profile (Figure 15c). The vertical zonation of the Tamandaré reefs, first described more than four decades ago (*i.e.* Laborel, 1969 and later, by Maida and Ferreira, 1997), were registered in detail by the GWR(WV3) bathymetry. In the first 40 meters of the profile, it is possible to observe the lagoon and the beginning of the reef with a step-like formation associated with the back-reef slope. Two small intra-reef lagoons (or tide-pools) can be visualized (circa 120 and 180 m), as well as small indentations across the reef flat. The reef crest appears (240-250 m from the beginning of the profile) followed by an upper fore-reef slope and the fore-reef wall. The possibility of detecting these specific zoning and small-scale relief support the application of GWR(WV3) on a local and detailed scale in coral reefs.

Discrepancies between the previous description of the area (*i.e.* Maida and Ferreira, 1997) and the resulting GWRs depth derivations (Figures 8 and 12) indicate that some changes may have occurred in the area in the last 20 years. The reefs in front of Campas beach were formerly depicted as being separated from the shore by a shallow lagoon occupied by a seagrass bed (Maida and Ferreira, 1997). This area now appears to be almost attached to the coastline, with little bathymetric variations and very shallow depths. This suggests that in the two decades between the studies, the lagoon has been filled up by sediments and as a consequence of this sedimentation, a decrease in seagrass cover may have occurred. The fact that the shallow area also functions as an anchoring area for the local marinas during summer could have added to destabilization of the bottom, causing a loop between seagrass loss causing, and caused by, increased sediment suspension.

The tendency to siltation was also observed by Strenzel (2004) when comparing the coastal bathymetry of Tamandare bay in 1961 and 2001. Since then, anthropogenic pressures in the coastal zone of Tamandaré have gradually increased (IBGE, 2017) and may have contributed to coastal erosion and sediment accumulation on the lagoon and on top of the reefs. These reefs' proximity to the coast add other sources of direct impacts (*e.g.* human trampling, which cause physical destruction of the structure) (Santos *et al.*, 2015; Sarmiento and Santos, 2012). These observations suggest loss of structural habitat complexity and therefore, loss of biodiversity. They also confirm the urge for more studies targeting the benthic morphology in the area at both regional and fine scales.

Considering the well-established role of the bathymetry in the coral reef environment, any significant bathymetric change in the reef area must be addressed as soon as possible to avoid destructive impacts (Mumby *et al.*, 2004). The application of a multiresolution approach is recommended, specifically, Landsat-8 for a broad-scale analysis and WorldView-03 for fine-scale studies. Monitoring the area in a temporal scale also becomes possible: once the base map is generated, it is possible to detect changes in the area using multitemporal analysis, as already exemplified in this study. GWRs in GIS environment can be used to predict the change in the dependent variable (depth) by altering the explanatory variables (pixel values). This provides a range of testing scenarios and diagnostics for past/future spatial changes that are highly important for management and monitoring strategies (Dunn and Halpin, 2009; Hedley *et al.*, 2016; Mumby *et al.*, 2004). In addition, the remotely sensed bathymetry derived in this study can be used to derive terrain complexity parameters in a broad (*i.e.* 10-100 m) (*e.g.* Duan *et al.*, 2016; Hedley *et al.*, 2018) and fine scales (*i.e.* 1-10 m) (*e.g.* Collin *et al.*, 2013; Ferrari *et al.*, 2018) matter. These metrics can then be applied in coral reef health evaluations and as a tool in MPA design.

2.5 Conclusions

This study suggests that deriving depth by remote sensing and more precisely, satellite imagery, is a feasible alternative for a shallow, high relief coastal coral reefs, like the study area, since other methods are unavailable and/or cost-ineffective.

An EBK interpolation of *in situ* values was not enough to depict the bottom relief of this coastal coral reef area, as shallower regions and areas with increased wave action were not accessed during the field survey. On the other hand, the *in situ* data points that were properly acquired were highly valuable to calibrate the SDB models.

Considering SDB models derived from linear regressions, PCA(RBM) was the best depth predictor using both Landsat-8 and WorldView-03 images. Although such models could be used for the bathymetric mapping of Tamandaré coastal zone, applying GWR is recommended, as it substantially improved the results.

Medium resolution SDB using GWR is recommended for mapping large areas and structures. L8's low cost, high temporal resolution, repeatability and coverage allow further monitoring and broader scale studies to be done in the area and areas alike. WV3 derived bathymetry using GWR showed capability of mapping the sea floor in the level of detail required by a range of ecological studies. Thus, this bathymetric model may be used as input in fine resolution terrain modelling and may contribute to the habitat mapping of the region. In fact, this research is the first step in the high-resolution monitoring of the area and contributes in present and future ecological and management programs.

2.6 Acknowledgments

The authors thank the Center for Research and Conservation of Marine Biodiversity of the Northeast (CEPENE) of the Chico Mendes Brazilian Institute of Biodiversity (ICMBIO) and Projeto Recifes Costeiros, Fundação Toyota do Brasil, Fundação SOS Mata Atlântica for supporting the field work. The authors are grateful to all volunteers, specially Gaspar A.L.B, Lippi, D., and Coxey, M., for their great help with the field work and helpful insights. This research is a contribution of the Long-Term Ecological Research Program (PELD-CNPq 441632/2016-5 ILTER-Brazil -Tamandaré site 18), and Ciências do Mar II, AUXPE 1979/2014. This study was financed in part by the Coordenação de Aperfeiçoamento de Pessoal de Nivel Superior – Brasil (CAPES) – Finance Code 001.

References

- Alvarez-Filip, L.; Dulvy, N.K.; Gill, J.A.; Côté, I.M., and Watkinson, A.R., 2009. Flattening of Caribbean Coral Reefs: Region-Wide Declines in Architectural Complexity. *Proceedings of the Royal Society of London B: Biological Sciences*, 276(1669) 3019-3025. doi:10.1098/rspb.2009.0339.
- Araújo, P. and Amaral, R., 2016. Mapping of coral reefs in the continental shelf of Brazilian Northeast through remote sensing. *Journal of Integrated Coastal Zone Management*, 16(1), 5-20. dx.doi.org/10.5894/rgci616
- Barker, N.H.L. and Roberts, C.M., 2004. Scuba diver behaviour and the management of diving impacts on coral reefs. *Biological Conservation*, 120(4), 481–89. doi:10.1016/j.biocon.2004.03.021.

- Bennecke, S. and Metaxa, A., 2017. Is substrate composition a suitable predictor for deep-water coral occurrence on fine scales? *Deep Sea Research Part I: Oceanographic Research Papers*, 124, 55-65. doi:10.1016/j.dsr.2017.04.011
- Bozec, Y.M.; Alvarez-Filip, L., and Mumby, P.J., 2015. The Dynamics of Architectural Complexity on Coral Reefs under Climate Change. *Global Change Biology*, 21(1), 223-35. doi:10.1111/gcb.12698.
- Branner, J.C., 1904. The stone reefs of Brazil, their geological and geographical relations with a chapter on the coral reefs. *Bulletin of the Museum of Comparative Zoology at Harvard College*, 54, 1-285
- Casal, G.; Monteys, X.; Hedley, J.; Harris, P.; Cahalane, C., and McCarthy, T., 2019. Assessment of empirical algorithms for bathymetry extraction using Sentinel-2 data. *International Journal of Remote Sensing*, 40(8), 2855-2879. doi:10.1080/01431161.2018.1533660.
- Chauvaud, S.; Bouchon, C., and Maniere, R., 1998. Remote sensing techniques adapted to high resolution mapping of tropical coastal marine ecosystems (coral reefs, seagrass beds and mangrove). *International Journal of Remote Sensing*, 19(18), 3625-3639. doi:10.1080/014311698213858.
- Collin, A. and Hensch, J.L., 2012. Towards Deeper Measurements of Tropical Reefscape Structure Using the WorldView-2 Spaceborne Sensor. *Remote Sensing*, 4(5), 1425-1447. doi:10.3390/rs4051425.
- Collin, A.; Etienne, S., and Planes, S., 2013. High-energy events, boulder deposits and the use of very high resolution remote sensing in coral reef environments. *Proceedings from the International Coastal Symposium (ICS) 2013. Journal of Coastal Research*, Special Issue No. 65, pp. 690-695. doi:10.2112/si65-117.1
- Contreras-Silva, A.I.; López-Caloca, A.A.; Tapia-Silva, F.O., and Cerdeira-Estrada, S., 2012. Satellite Remote Sensing of Coral Reef Habitats Mapping in Shallow Waters at Banco Chinchorro Reefs, México: A Classification Approach. In: Escalante-Ramirez, B. (ed.), *Remote Sensing – Applications*. IntechOpen, pp. 528-551. doi:10.5772/36210
- Daniell, J.J., 2008. Development of a Bathymetric Grid for the Gulf of Papua and Adjacent Areas: A Note Describing Its Development. *Journal of Geophysical Research: Earth Surface*, 113(F1). doi:10.1029/2006JF000673.
- Danielson, J.J.; Poppenga, S.K.; Brock, J.C.; Evans, G.A.; Tyler, D.J.; Gesch, D.B.; Thatcher, C.A., and Barras, J.A., 2016. Topobathymetric Elevation Model Development using a New Methodology: Coastal National Elevation Database. *Advances in Topobathymetric Mapping, Models, and Applications. Journal of Coastal Research*, Special Issue No. 76, pp. 75-89. doi:10.2112/SI76-008
- Darling, E.S.; Graham, N.A.J.; Januchowski-Hartley, F.A.; Nash, K.L.; Pratchett, M.S., and Wilson, S.K., 2017. Relationships between Structural Complexity, Coral Traits, and Reef Fish Assemblages. *Coral Reefs*, 36(2), 561-75. doi:10.1007/s00338-017-1539-z.
- Davenport, J. and Davenport, J.L., 2006. The Impact of Tourism and Personal Leisure Transport on Coastal Environments: A Review. *Estuarine, Coastal and Shelf Science*, 67(1-2), 280-292. doi:10.1016/j.ecss.2005.11.026.

- DHN. Diretoria de Hidrografia e Navegação, 2017. *Tábua das Marés para o Porto de Suape (Estado de Pernambuco)*. <http://www.dhn.mar.mil.br>. Accessed: Jul,2017
- Doxani, G.; Papadopoulou, M.; Lafazani, P.; Pikridas, C., and Tsakiri-Strati, M., 2012. Shallow-Water Bathymetry Over Variable Bottom Types Using Multispectral Worldview-2 Image. *International Archiver of the Photogrammetry, Remote Sensing and Spatial Information Sciences*, 39(8), 159-164. doi:10.5194/isprsarchives-XXXIX-B8-159-2012
- Duan, Y.; Liu, Y.; Li, M.; Zhou, M., and Yang, Y., 2016. Survey of reefs based on Landsat 8 operational land imager (OLI) images in the Nansha Islands, South China Sea. *Acta Oceanologica Sinica*, 35(10), 11-19. doi:10.1007/s13131-016-0898-6
- Dunn, D.C. and Halphin, P.N., 2009. Rugosity-based regional modelling of hard-bottom habitat. *Marine Ecology Progress Series*, 377, 1-11. doi:10.3354/meps07839
- Eugenio, F.; Marcello, J., and Martin, J., 2015. High-Resolution Maps of Bathymetry and Benthic Habitats in Shallow-Water Environments Using Multispectral Remote Sensing Imagery. *IEEE Transactions on Geoscience and Remote Sensing*, 53(7): 3539-3549. doi:10.1109/TGRS.2014.2377300.
- Fabricius, K.E.; Langdon, C.; Uthicke, S.; Humphrey, C.; Noonan, S.; De'ath, G.; Okazaki, R.; Muehllehner, N.; Glas, M.S., and Lough, J.M., 2011. Losers and Winners in Coral Reefs Acclimatized to Elevated Carbon Dioxide Concentrations. *Nature Climate Change*, 1(3), 165–69. doi:10.1038/nclimate1122.
- Ferrari, R.; Malcolm, H.A.; Byrne, M.; Friedman, A.; Williams, S.B.; Schultz, A.; Jordan, A., and Figueira, W.F., 2018. Habitat structural complexity metrics improve predictions of fish abundance and distribution. *Ecography*, 41(7), 1077-1091. doi:10.1111/ecog.02580.
- Ferreira, B.P. and Maida M., 2006. *Monitoramento dos recifes de coral do Brasil: situação atual e perspectivas*. Brasília: MMA (Environmental Ministry)/SBF.
- Gao, J., 2009. Bathymetric Mapping by Means of Remote Sensing: Methods, Accuracy and Limitations. *Progress in Physical Geography: Earth and Environment*, 33(1), 103-116. doi:10.1177/0309133309105657.
- Gholamalifard, M.; Kutser, T.; Esmaili-Sari, A.; Abkar, A., and Naimi, B., 2013. Remotely Sensed Empirical Modeling of Bathymetry in the Southeastern Caspian Sea. *Remote Sensing*, 5(6), 2746-2762. doi:10.3390/rs5062746.
- Gomes, G. and da Silva, A.C., 2014. Coastal Erosion Case at Candeias Beach (NE-Brazil). *Journal of Coastal Research*, 71(1), 30-40. doi:10.2112/SI71-004.1.
- González-Rivero, M.; Harborne, A.R.; Herrera-Reveles, A.; Bozec, Y.M.; Rogers, A.; Friedman, A.; Ganase, A., and Hoegh-Guldberg, O., 2017. Linking Fishes to Multiple Metrics of Coral Reef Structural Complexity Using Three-Dimensional Technology. *Scientific Reports*, 7(1). doi:10.1038/s41598-017-14272-5.
- Graham, N.A.J., 2014. Habitat Complexity: Coral Structural Loss Leads to Fisheries Declines. *Current Biology*, 24(9), R359–R361. doi:10.1016/j.cub.2014.03.069.
- Green, E.; Mumby, P.J.; Edwards, A.J., and Clark, C.D., 2000. *Remote Sensing Handbook for Tropical Coastal Management*. Paris: Unesco Publishing, 2000.
- Halpern, B.S.; Walbridge, S.; Selkoe, K.A.; Kappel, C.V.; Fiorenza, M.; D'Agrosa, C.; Bruno, J.F.; Casey, K.S.; Ebert, C.; Fox, H.E.; Fujita, R.; Heinemann, D.; Lenihan, H.S.;

Madin, E.M.P.; Perry, M.T.; Selig, E.R.; Spalding, M.; Steneck, R., and Watson, R., 2008. A Global Map of Human Impact on Marine Ecosystems. *Science*, 319(5865), 948-952. doi:10.1126/science.1149345.

Hamylton, S.; Hedley, J., and Beaman, R., 2015. Derivation of High-Resolution Bathymetry from Multispectral Satellite Imagery: A Comparison of Empirical and Optimisation Methods through Geographical Error Analysis. *Remote Sensing*, 7(12), 16257–16273. doi:10.3390/rs71215829.

Hayes, M.O., 1979. Barrier Island Morphology as a Function of Tidal and Wave Regime. In: Leatherman, S.P. (ed.), *Barrier Islands, from the Gulf of St. Lawrence to the Gulf of Mexico*. New York: Academic Press, pp. 1-27

Hoegh-Guldberg, O.; Mumby, P.J.; Hooten, A.J.; Steneck, R.S.; Greenfield, P.; Gomez, E.; Harvell C.D.; Sale, P.F.; Edwards, A.J.; Caldeira, K.; Knowlton, N.; Eakin, C.M.; Iglesias-Prieto, R.; Muthiga, N.; Bradbury, R.H.; Dubi, A., and Hatziolos, M.E., 2007. Coral Reefs Under Rapid Climate Change and Ocean Acidification. *Science*, 318(5857), 1737-1742. doi:10.1126/science.1152509.

Hughes, T.P., 2003. Climate Change, Human Impacts, and the Resilience of Coral Reefs. *Science*, 301(5635), 929-33. doi:10.1126/science.1085046.

Instituto Brasileiro de Geografia e Estatística - IBGE. *Brazil's cities panorama*. <https://cidades.ibge.gov.br/brasil/pe/tamandare/panorama>. Accessed Oct, 2017.

Instituto Chico Mendes de Conservação a Biodiversidade – ICMBio, 2012. *Plano de Manejo da APA Costa dos Corais. Tamandaré-PE*, 1, 74p. Available online: http://www.icmbio.gov.br/apacostadoscorais/images/stories/plano_de_manejo/PM_APACC_2013_JANEIRO.pdf.

Jagalingam, P.; Akshaya, B.J., and Hegde, A.V., 2015. Bathymetry Mapping Using Landsat 8 Satellite Imagery. *Procedia Engineering*, 116, 560-66. doi:10.1016/j.proeng.2015.08.326.

Hedley, J.D.; Harborne, A.R., and Mumby, P.J., 2005. Technical note: Simple and robust removal of sun glint for mapping shallow-water benthos. *International Journal of Remote Sensing*, 26(10), 2107-2112. doi:10.1080/01431160500034086.

Hedley, J.D.; Roelfsema, C.; Brando, V.; Giardino, C.; Kutser, T.; Phinn, S., and Koetz, B., 2018. Coral reef applications of Sentinel-2: Coverage, characteristics, bathymetry and benthic mapping with comparison to Landsat 8. *Remote Sensing of Environment*, 216, 598-614. doi:10.1016/j.rse.2018.07.014

Hedley, J.D.; Roelfsema, C.; Chollett, I.; Harborne, A.; Heron, S.; Weeks, S.; Skirving, W.; Strong, A.; Eakin, C.; Christensen, T.; Ticzon, V.; Bejarano, S., and Mumby, P.J., 2016. Remote Sensing of Coral Reefs for Monitoring and Management: A Review. *Remote Sensing*, 8(2), 118. doi:10.3390/rs8020118.

Kabiri, K., 2017. Accuracy Assessment of Near-Shore Bathymetry Information Retrieved from Landsat-8 Imagery. *Earth Science Informatics*, 10(2), 235-245. doi:10.1007/s12145-017-0293-7.

Kanno, A.; Koibuchi, Y., and Masahiko, I., 2011. Shallow Water Bathymetry from Multispectral Satellite Images: Extensions of Lyzenga's Method for Improving Accuracy. *Coastal Engineering Journal*, 53(4), 431-450. doi:10.1142/S0578563411002410.

Knudby, A.; LeDrew, E., and Brenning, A., 2010. Predictive Mapping of Reef Fish Species Richness, Diversity and Biomass in Zanzibar Using IKONOS Imagery and Machine-Learning Techniques. *Remote Sensing of Environment*, 114(6), 1230-1241. doi:10.1016/j.rse.2010.01.007.

Krivoruchko, K., 2012. Empirical bayesian kriging. Esri: Redlands, CA, USA. <https://www.esri.com/NEWS/ARCUSER/1012/files/ebk.pdf>. Accessed Jun, 2019.

Kuenzer, C.; Ottinger, M.; Wegmann, M.; Guo, H.; Wang, C.; Zhang, J.; Dech, S., and Wikelski, M., 2014. Earth observation satellite sensors for biodiversity monitoring: potentials and bottlenecks. *International Journal of Remote Sensing*, 35(18), 6599-6647. doi:10.1080/01431161.2014.964349.

Kuffner, I.B. and Lauren, T.T., 2016. A geological perspective on the degradation and conservation of western Atlantic coral reefs. *Conservation Biology*, 30(4), 706-715. doi:10.1111/cobi.12725.

Laborel, J., 1969. Madreporaires et hydrocoralliaires recifaux des cotes Bresiliennes. Systematique, ecologie repartition verticale et geographique. *Results Scientifique du Campagne de Calypso*, 9(25), 171-229.

Leao, Z.; Kikuchi, R., and Testa, V., 2003. Corals and coral reefs of Brazil. *Latin American Coral Reefs*, 9-52. doi:10.1016/B978-044451388-5/50003-5

Ledlie, M.H.; Graham, N.A.J.; Bythell, J.C.; Wilson, S.K.; Jennings, S.; Polunin, N.V.C., and Hardcastle, J., 2007. Phase Shifts and the Role of Herbivory in the Resilience of Coral Reefs. *Coral Reefs*, 26(3), 641-653. doi:10.1007/s00338-007-0230-1.

Liceaga-Correa, M.A. and Euan-Avila, J.I., 2002. Assessment of Coral Reef Bathymetric Mapping Using Visible Landsat Thematic Mapper Data. *International Journal of Remote Sensing*, 23(1), 3-14. doi:10.1080/01431160010008573.

Lyzenga, D.R.; Malinas, N.P., and Tanis, F.J., 2006. Multispectral bathymetry using a simple physically based algorithm. *IEEE Transactions on Geoscience and Remote Sensing*, 44(8), 2251-2259. doi:10.1109/TGRS.2006.872909

Lyzenga, D.R., 1985. Shallow-Water Bathymetry Using Combined Lidar and Passive Multispectral Scanner Data. *International Journal of Remote Sensing*, 6(1), 115-125. doi:10.1080/01431168508948428.

Lyons, M.; Phinn, S., and Roelfsema, C., 2011. Integrating Quickbird Multi-Spectral Satellite and Field Data: Mapping Bathymetry, Seagrass Cover, Seagrass Species and Change in Moreton Bay, Australia in 2004 and 2007. *Remote Sensing*, 3(1), 42-64. doi:10.3390/rs3010042.

Macedo, E.C., 2009. Um ensaio sobre a sedimentação e suas implicações ecológicas nos recifes costeiros da baía de Tamandaré/PE. Recife, Pernambuco: Universidade Federal de Pernambuco (Federal University of Pernambuco), Master's thesis, 144p.

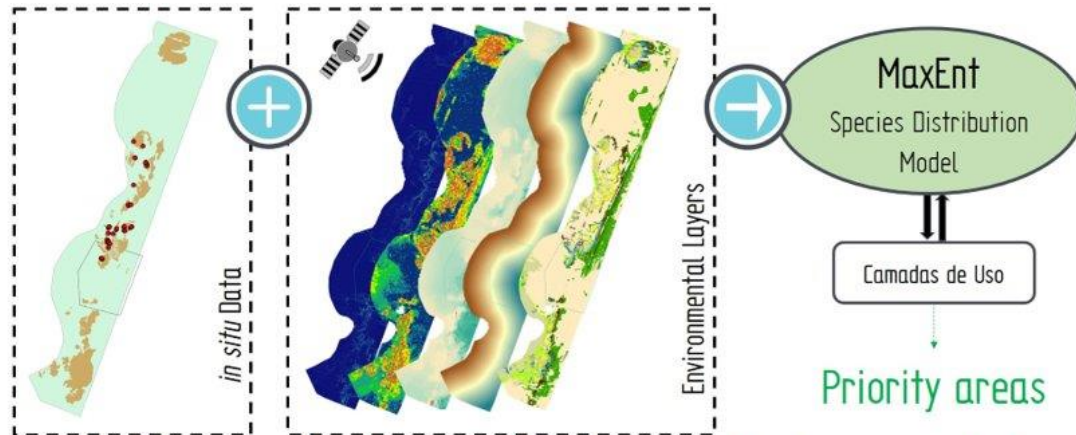
Maida, M. and Ferreira, B., 1997. Coral Reefs of Brazil: Overview and Field Guide. *Proceedings of the 8th International Coral Reef Symposium*, 1, 263-274.

Manessa, M.D.M.; Kanno, A.; Sekine, M.; Haidar, M.; Yamamoto, K.; Imai, T., and Higuchi, T., 2016. Satellite-Derived Bathymetry Using Random Forest Algorithm and Worldview-2

- Imagery. *Geoplanning Journal of Geomatics and Planning*, 3(2), 117-126. doi:10.14710/geoplanning.3.2.117-126.
- McCulloch, M.; Fallon, S.; Wyndham, T.; Hendy, E.; Lough, J., and Barnes, D., 2003. Coral Record of Increased Sediment Flux to the Inner Great Barrier Reef since European Settlement. *Nature*, 421(6924), 727-730. doi:10.1038/nature01361.
- Monteys, X.; Harris, P.; Caloca, S., and Cahalane, C., 2015. Spatial Prediction of Coastal Bathymetry Based on Multispectral Satellite Imagery and Multibeam Data. *Remote Sensing*, 7(10), 13782-13806. doi:10.3390/rs71013782.
- Mulcan, A.; Mitsova, D.; Hindle, T.; Hanson, H., and Coley, C., 2015. Marine Benthic Habitats and Seabed Suitability Mapping for Potential Ocean Current Energy Siting Offshore Southeast Florida. *Journal of Marine Science and Engineering*, 3(2), 276-298. doi:10.3390/jmse3020276.
- Mumby, P.J.; Clark, C.D.; Green, E.P., and Edwards, A.J., 1998. Benefits of water column correction and contextual editing for mapping coral reefs. *International Journal of Remote Sensing*, 19(1), 203–210. doi:10.1080/014311698216521.
- Mumby, P.J.; Green, E.P.; Edwards, A.J., and Clark, C.D., 1997. Coral Reef Habitat Mapping: How Much Detail Can Remote Sensing Provide? *Marine Biology*, 130(2), 193–202. doi:10.1007/s002270050238.
- Mumby, P.J. and Steneck, R.S., 2008. Coral Reef Management and Conservation in Light of Rapidly Evolving Ecological Paradigms. *Trends in Ecology & Evolution*, 23(10), 555-563. doi:10.1016/j.tree.2008.06.011.
- Mumby, P.J.; Skirving, W.; Strong, A.E.; Hardy, J.T.; LeDrew, E.F.; Hochberg, E.F.; Stumpf, R.P., and David, L.T., 2004. Remote Sensing of Coral Reefs and Their Physical Environment. *Marine Pollution Bulletin*, 48(3-4), 219-228. doi:10.1016/j.marpolbul.2003.10.031.
- Oliveira, M.A.V., 1864. Roteiro da Costa do Brasil do Rio Mossoró ao Rio de S. Francisco do Norte. *Typographia Perseverança*, Rio de Janeiro, Brazil.
- Pacheco, A.; Horta, J.; Loureiro C., and Ferreira, O., 2015. Retrieval of Nearshore Bathymetry from Landsat 8 Images: A Tool for Coastal Monitoring in Shallow Waters. *Remote Sensing of Environment*, 159, 102-116. doi:10.1016/j.rse.2014.12.004.
- Pickrill, R.A. and Todd, B.J., 2003. The multiple roles of acoustic mapping in integrated ocean management, Canadian Atlantic continental margin. *Ocean & Coastal Management*, 46(6), 601-614. doi:10.1016/S0964-5691(03)00037-1.
- Pilz, J. and Spöck, G., 2008. Why do we need and how should we implement Bayesian kriging methods. *Stochastic Environmental Research and Risk Assessment*, 22(5), 621-632. doi:10.1007/s00477-007-0165-7
- Pittman, S.J.; Costa, B.M., and Battista, T.M., 2009. Using Lidar Bathymetry and Boosted Regression Trees to Predict the Diversity and Abundance of Fish and Corals. *Journal of Coastal Research*, Special Issue No. 53, pp. 27-38. doi:10.2112/SI53-004.1.
- Purkis, S.J., 2018. Remote Sensing Tropical Coral Reefs: The View from Above. *Annual Review of Marine Science*, 10(1), 149-168. doi:10.1146/annurev-marine-121916-063249.

- Richter, R. and Schl pfer, D., 2002. Geo-atmospheric processing of airborne imaging spectrometry data. Part 2: Atmospheric/topographic correction. *International Journal of Remote Sensing*, 23(13), 2631-2649. doi:10.1080/01431160110115834.
- Rinkevich, B., 1995. Restoration Strategies for Coral Reefs Damaged by Recreational Activities: The Use of Sexual and Asexual Recruits. *Restoration Ecology*, 3(4), 241-251. doi:10.1111/j.1526-100X.1995.tb00091.x.
- Sarmiento, V.C. and Santos, P.J.P., 2012. Trampling on Coral Reefs: Tourism Effects on Harpacticoid Copepods. *Coral Reefs*, 31(1), 135-146. doi:10.1007/s00338-011-0827-2.
- Santos, G.S.; Burgos, D.C.; Lira, S.M.A., and Schwamborn, R., 2015. The Impact of Trampling on Reef Macrobenthos in Northeastern Brazil: How Effective Are Current Conservation Strategies? *Environmental Management*, 56(4), 847-858. doi:10.1007/s00267-015-0552-7.
- Strenzel, G.M.R., 2004. Caracterizaci n del paisaje sumergido costero para la gesti n de  reas marinas protegidas. Gran Canaria, Spain: Universidad de Las Palmas de Gran Canaria, Ph.D. Dissertation, 188p.
- Stumpf, R.P.; Holderied, K., and Sinclair, M., 2003. Determination of Water Depth with High-Resolution Satellite Imagery over Variable Bottom Types. *Limnology and Oceanography*, 48(1), 547-556. doi:10.4319/lo.2003.48.1_part_2.0547.
- Su, H.; Hongxing L., and Heyman, W.D., 2008. Automated Derivation of Bathymetric Information from Multi-Spectral Satellite Imagery Using a Non-Linear Inversion Model. *Marine Geodesy*, 31(4), 281-298. doi:10.1080/01490410802466652.
- Su, H.; Liu, H.; Wang, L.; Filippi, A.M.; Heyman, W.D., and Beck, R.A., 2013. Geographically adaptive inversion model for improving bathymetric retrieval from satellite multispectral imagery. *IEEE Transactions on Geoscience and Remote Sensing*, 52(1), 465-476. doi:10.1109/TGRS.2013.2241772.
- Syvitski, J.P.M., 2005. Impact of Humans on the Flux of Terrestrial Sediment to the Global Coastal Ocean. *Science*, 308(5720), 376-380. doi:10.1126/science.1109454.
- Taniguchi, H. and Tokeshi M., 2004. Effects of Habitat Complexity on Benthic Assemblages in a Variable Environment. *Freshwater Biology*, 49(9), 1164-1178. doi:10.1111/j.1365-2427.2004.01257.x.
- Vinayaraj, P.; Venkatesh, R., and Masumoto, S., 2016. Satellite-Derived Bathymetry using Adaptive Geographically Weighted Regression Model. *Marine Geodesy*, 39(6), 458-478. doi:10.1080/01490419.2016.1245227.
- Wilson, S.K.; Graham, N.A.J., and Polunin., N.V.C., 2007. Appraisal of Visual Assessments of Habitat Complexity and Benthic Composition on Coral Reefs. *Marine Biology*, 151(3), 1069-1076. doi:10.1007/s00227-006-0538-3.
- Zhang, L.; Li, N.; Jia, S.; Wang, T., and Dong, J., 2015. A method for DEM construction considering the features in intertidal zones. *Marine Geodesy*, 38(2), 163-175. doi:10.1080/01490419.2014.937883.
- Zoffoli, M.; Frouin, R., and Kampel, M., 2014. Water Column Correction for Coral Reef Studies by Remote Sensing. *Sensors*, 14(9), 16881-16931. doi:10.3390/s140916881.

3 CORAL REEF MAPPING USING SATELLITE IMAGERY: a contribution for seascape management



Where are the large colonies of *Millepora alcicornis*?
How and why are they distributed in the region?

3.1 Abstract

Mapping topographical and ecological relevant measures that can be interpreted as habitat complexity proxies is essential to assist strategic decisions that aim to conciliate use and conservation in coral reef ecosystems. Satellite-based remote sensing has been frequently used to derive environmental values in spatial scales large enough to depict entire ecosystems at once. Additionally, high-resolution datasets have recently become available and cost-effective, making these ideal tools to map coral reef areas, if calibrated with reliable field data. Our study region is situated on the Northeast Coast of Brazil and located within a Marine Protected Area (Costa dos Corais), subjected mostly to human-related impacts such as pollution, fishing, unorderly tourism and coastal sedimentation. The coral reefs of Tamandaré are in a shallow, topographically complex area which offers numerous challenges for *in situ* mapping. The geobiodiversity of the area was derived using high and medium resolution datasets (i.e. WorldView-03 and Landsat-8 OLI) and georeferenced photos and videos acquired *in situ*. We derived ecological (e.g. benthic cover, habitat diversity per area), topographical (e.g. bathymetry, rugosity) and local (e.g. distance to shore, turbidity) to analyse the distribution of a dominant coral species in the region, *Millepora alcicornis*. Habitat suitability for the occurrence of the species was calculated using MaxEnt (AUC > 0.98). We have also assessed the relevance and effectiveness of a no-take area in the region. The model identified topographical limiting factors to the settling and growth of coral colonies in the area, such as the distance to the shore and depth. Albeit, the most important variables were ecological, showing the importance of maintaining high biodiversity values in a coral reef ecosystem. Integrating the habitat suitability model with absence data and human use maps suggested the impact of fishing and tourism as potential inhibitors to coral growth. The results in this study reinforce the importance of a no-take zone and protective measures for the maintenance of local biodiversity. Furthermore, it offers a detailed mapping of the coral reef complex of Tamandaré, which may be applied in future research.

Keywords: Coral reef. *Millepora alcicornis*. MaxEnt. Remote Sensing. Benthic mapping.

3.2 Introduction

Coral reefs are considered hotspots of marine biodiversity and complex ecosystems, both ecologically and geomorphologically (Bellwood *et al.*, 2004; Pittman and Brown, 2011). Furthermore, these environments support socioeconomic activities and can be essential for the livelihood of millions of people (Wilkinson and Salvat, 2012; Burke *et al.*, 2017). For these reasons, they are usually considered as priority conservation areas (Pittman *et al.*, 2007; Magris *et al.*, 2016), in an effort to ensure the maintenance of coral reefs' ability to provide their usual goods and services.

Despite their importance, reefs around the world are in serious decline, and are faced with a wide range of impacts, varying from local (e.g. population growth, pollution, erosion, coastal sedimentation) (Bellwood *et al.*, 2004; Halpern *et al.*, 2008) to global threats (e.g. climate change, overfishing, El-Niño related bleaching and mortality) (Hughes *et al.*, 2007; Hughes *et al.*, 2017). These effects may be heightened in coastal reefs, where frequent direct human impacts related to activities occurring in the reef framework occur (Davenport and Davenport, 2006; Pittman *et al.*, 2011; Lai *et al.*, 2015).

The establishment of Marine Protected Areas (MPAs) using ecosystem-based approach have been constantly described as one of the most effective tools to reduce habitat loss (Agardy *et al.*, 2011) and harmful impacts in coral ecosystems. Nevertheless, the practical effectiveness of such areas relies heavily on how ecologically appropriate the chosen region is and how efficiently they are managed (Jameson *et al.*, 2002; Adam *et al.*, 2015). MPAs should, ideally, be specified based on representativeness of the habitat types in the area and prior knowledge of biologically (and/or economically) essential species and ecosystems (Bridge *et al.*, 2012).

Species Distribution Models (SDM) can provide useful insights on how the biodiversity is distributed across a region based on environmental conditions (Elith *et al.*, 2011). Thus, these models have been used as tools to help identifying and delineating areas of biological importance and complexity (e.g. Selig *et al.*, 2012; Bridge *et al.*, 2012) and facilitate the determination of MPAs. MaxEnt (Philips, Dudík and Schapire, 2017; version 3.4.1) is an SDM tool which produces straightforward, quantitative and spatially explicit information on the interactions of environmental variables and targeted species. By doing so, it derives an output map of "habitat suitability", which in practical terms, depicts how suitable a certain location is for the presence of a certain species. An initial step of modelling biodiversity distribution is implying and calculating environmental variables that may

influence the distribution of the species (Poulos *et al.*, 2015). The major challenge is usually the acquisition of these environmental data, particularly at spatial extents and resolutions that reflect ecologically meaningful habitat structure.

The influence of topography and underwater relief in coastal coral reef ecosystems is well documented (Ledlie *et al.*, 2007; Graham and Nash, 2014; González-Rivero *et al.*, 2017). Additionally, the maintenance of their inherent relief complexity a key process in protecting and monitoring the basic functions performed by these ecosystems. Satellite-based remote sensing has been used to map tropical coral reefs since the 70's, with the launching of the first Landsat satellite (Green *et al.*, 1996). Technological advancements on the last decade have enabled the acquisition of satellite data, in resolutions capable of mapping biological assemblages on coral reef areas and their topographical environment (Collin and Hench, 2012; Reshitnyk *et al.*, 2014). Furthermore, satellite imagery is a budget-friendly way of deriving important habitat variables such as bathymetry (*e.g.* Silveira *et al.*, 2019), terrain complexity (*e.g.* Lundblad *et al.*, 2006) and benthic cover (*e.g.* Andréfouët *et al.*, 2003; Eugenio *et al.*, 2011), making them frequently reliable allies in SDMs and conservation planning.

This study aims to integrate cost-effective and multi-resolution remote sensing techniques, species distribution models and human use layers to aid in the management of a tropical coastal reef in Northeast of Brazil. Located in the most extensive MPA in the country (Costa dos Corais), the coral reef complex of Tamandaré if of great biological socioeconomic importance and harbours many commercially important fisheries (Ferreira and Maida, 2006; ICMBio, 2012). The main reef framework in the region is located less than 1 km from the coastline, and the entire region experiences impacts intensified by recent developments, overfishing, pollution and disorderly tourism (Castro and Pires, 2001; Ferreira and Maida, 2006). The area includes the first and oldest no-take area in the MPA (Ferreira *et al.*, 2006a). Multiple-use zonation, aiming to reconcile conservation and human activities, is one of the main strategies of a Federal Government's Management Plan for this MPA (ICMBio, 2012). However, criteria for eligibility of those zones are often more practical than scientific, partially due to data limitations on ecological aspects. The present study aims to develop and test methods to aid in those choices, while evaluating the effectiveness of previous management measures in the region.

3.3 Methods

This research was conducted under a permit issued for the authors by the Brazilian Ministry of Environment (MMA – Ministério do Meio Ambiente and ICMBio – Instituto Chico Mendes de Biodiversidade).

3.3.1 Study Area

The study area is located in the South of Pernambuco State, Brazil (Figure 1). The city of Tamandaré is a region known for its biodiversity, associated with mangroves, estuaries and coral ecosystems present throughout the area (Ferreira *et al.*, 2006b). The city has two main rivers, Formoso and Mamucabas, which are the main sediment source for this coastal zone (Macedo, 2009), especially during winter months.

The reefs of Tamandaré resemble fringing reefs and are arranged in a particular pattern of three lines parallel to the coast (Maida and Ferreira, 1997). They harbour a rich fauna and flora compared to similar areas of the Brazilian Northeast region (Leao *et al.*, 2003; Ferreira and Maida, 2006). These environments are inserted in the Costa dos Corais Marine Protected Area (MPA), in zones with different degrees of protection, among them: no-take zones, exclusive fishing zones and conservation zones (ICMBio, 2012).

They are located in a shallow carbonate platform, where the clear water, proximity to the coast and biodiversity make this region a regional tourist spot (Ferreira *et al.*, 2006b; Silveira, 2018). The area harbours many commercially valuable fish species, and artisanal fishing is one of the most traditional activities and source of income in the area (Ferreira *et al.*, 2001; ICMBio, 2012). One of Costa dos Corais MPA's main goal is to reconcile the use of the ecosystem, specifically fishing, tourism, and its possible derivative impacts, with maintaining the region's ecological status. Propelled by this objective, 2.6 km² no-take zone (i.e. Marine Life Preservation Zone) was also implemented in Tamandaré, in which no human activity is allowed, with the exception of MPA monitoring and research purposes.

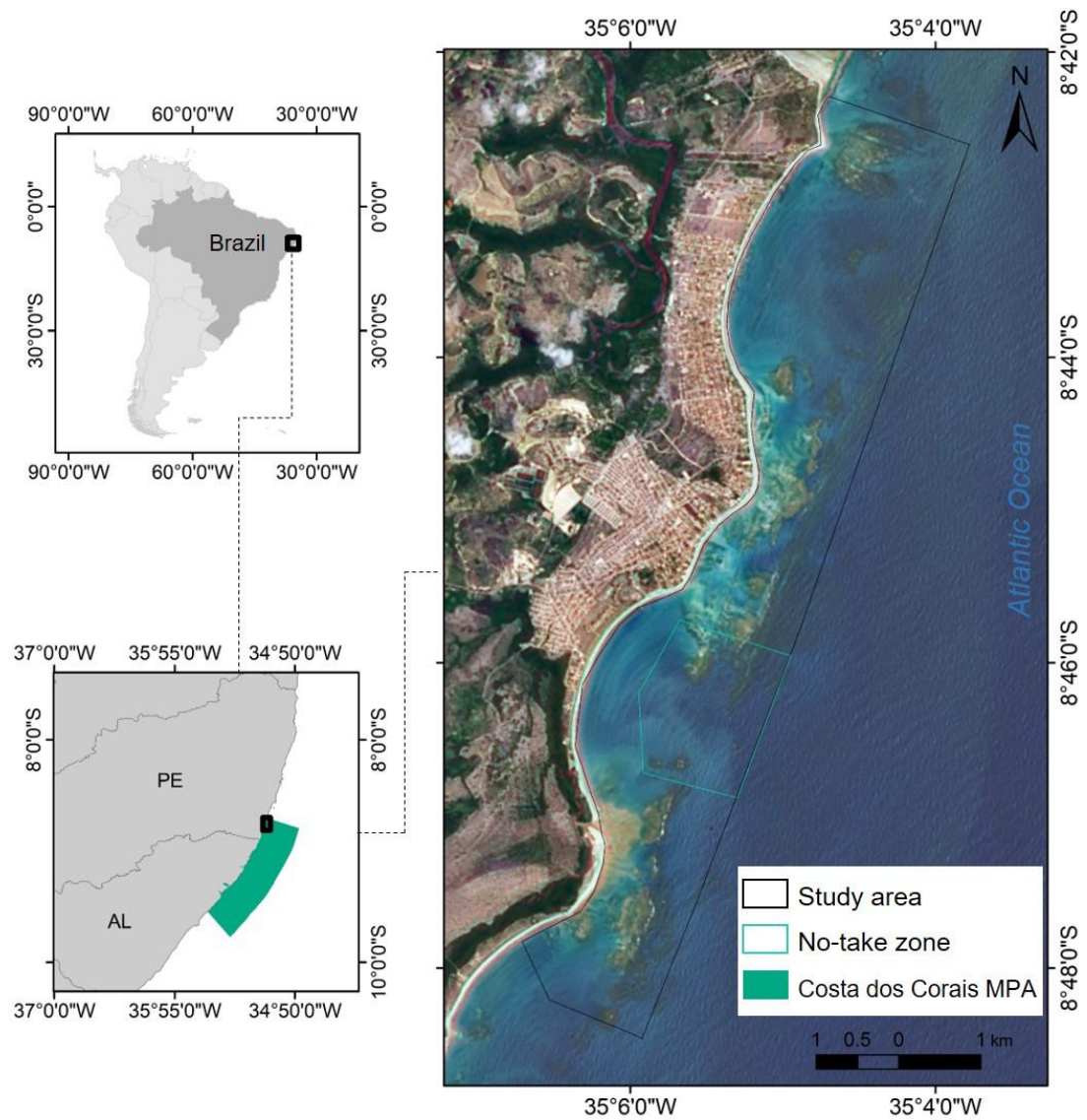


Figure 1 Study area at the coral reefs of Tamandaré (hollow black polygon) and the location of the no-take zone (hollow blue polygon). The area is located within the limits of Costa dos Corais MPA (green polygon). Satellite Image: Landsat8 RGB431

3.3.2 Modeling suitable habitats for *Millepora alcicornis*

We used MaxEnt software in this research to create predictive models of the location of large colonies of the hydrocoral *Millepora alcicornis*. This hydrocoral can be observed in Brazilian coral reefs mostly in its tree-like, branching morphotype and more rarely, in its encrusting form. Laborel (1969) described three main morphotypes (*i.e. cellulosa*, *digitata* and *fenestrata*), which are closely related to the level of turbidity and turbulence in the region. In Tamandaré coastal reefs, only observations of the branching form (*fenestrata*) have been registered.

This methodology has been widely used to produce species distribution models, and thus, analyse and predict suitable habitats for a range of terrestrial and marine species (*e.g.* Couce *et al.*, 2012; Freeman *et al.*, 2013; Bargain *et al.*, 2017). We chose this software due to its robustness and capacity of working well with presence-only data, even in small numbers (Philips and Dudík, 2008; Bridge *et al.*, 2012). MaxEnt identifies where a certain species is most likely to occur, based on how similar each pixel in the area is to the presence pixels. To do so, it relies on two sets of input data: first, known occurrences of the target species (or group of) and second, topographical, physical and/or biological data on their environment. The role of each environmental feature is also calculated and depicted by response curves, which provide important information on the plausibility of the resulting model (Merow *et al.*, 2013). To interpret and evaluate the results, MaxEnt provides a metric of model fit, “area under the receiver-operator curve” (AUC), which is a threshold measure of the model’s discriminatory ability (an AUC score < 0.5 means the resulting model is no better than a random prediction) (Merow *et al.*, 2013; Radosavljevic and Anderson, 2014).

We used default parameters to run the analysis (convergence threshold of 0.00005 and maximum iteration value of 500) and a “logistic” output type. Duplicated records were removed from the analysis, and 70% of occurrence data was used as training, and the remaining 30%, used as test data. It is imperative to remember that MaxEnt’s raw output relying on presence-only data, as is the case of this study, should not be interpreted as probability of occurrence, but rather as a relative measure of how suitable a location is for the occurrence of a certain species based on the input layers provided.

In this research, points where we found large colonies of the hydrocoral *Millepora alcornis* (diameter > 100 cm) were used as presence data. We applied a machine learning approach, which suggests including all reasonable predictors and letting the algorithm choose which are the most important ones (Merow *et al.*, 2013). The environmental variables chosen here are displayed on Figure 2 and have been applied in previous similar studies (*e.g.* Bridge *et al.*, 2012; Costa *et al.*, 2015). Additionally, other authors have showed the importance of using variables in varying window sizes (*e.g.* Etnoyer *et al.*, 2018). Therefore, our topographical and ecological data were derived in different scales, to consider a wider range of spatial resolution in which a predictor can impact the final model.

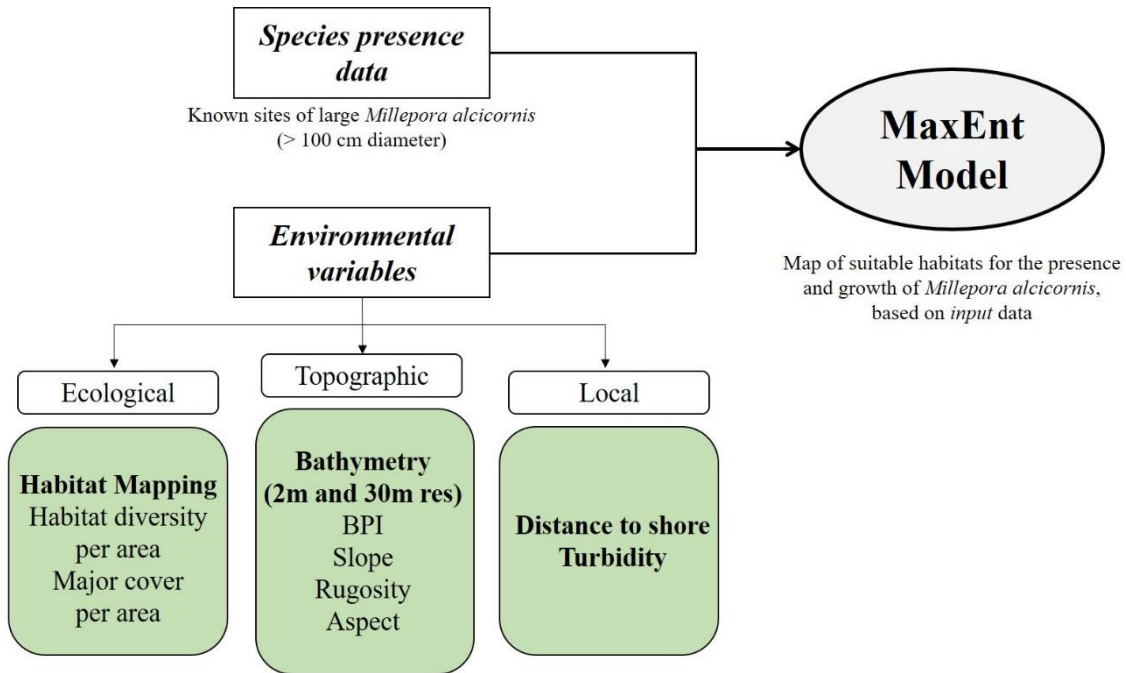


Figure 2 Histogram of the process to derive the predictive distribution model of *Millepora alcicornis* in MaxEnt.

3.3.2.1 Species presence data

Underwater mapping of hydrocoral *Millepora alcicornis* was conducted from February 2017 to May 2019, as part of a conjoined, ongoing effort to map the benthic habitats and monitor the coral reefs of the area (Ferreira *et al.*, 2018). *Millepora alcicornis* is considered an important reef builder and has a broad distribution throughout the reefs in the study area (Maida and Ferreira, 1997; Ferreira and Maida, 2006; Amaral *et al.*, 2008), with zoning patterns that respond to physical factors (Lewis, 2006). As habitat mapping was also an important layer and had to be developed during this research, we purposely surveyed areas of known occurrence of the species as well as areas of known absence, such as seagrass and macroalgae beds, sand and exposed reef tops.

Field survey was undertaken using photo and video transects and a diver-towed GPS (Garmin eTrex 20x) (Roelfsema and Phinn, 2010; Roelfsema *et al.*, 2015; Poulos *et al.*, 2016) recording location data at 5-second intervals. For the photo-transects, a 30x30cm quadrat was used, made using poly vinyl chloride (PVC) for the frame and handle. Video recordings were undertaken by a patiently swimming diver using a GoPro coupled on top of a one-meter handle. To enable the estimation of size of each coral colony, a measuring tape was attached to a PVC one-dimensional frame (Figure 3). The location of each coral colony was recorded by checking the time stamp of the specific photos and video frames containing the species and syncing it with a digital watch carefully synchronized with the towed GPS.

Specimens of *Millepora alcicornis* were also classified by size, following a minimum diameter rule of 100 cm. This was done to ensure the site was truly colonized by the species, since *Millepora alcicornis*' branches can be fragmented, dispersed, and start settlement and growing rapidly even under unexpected conditions (Rodríguez *et al.*, 2019; Wirtz and Zilberberg, 2019).

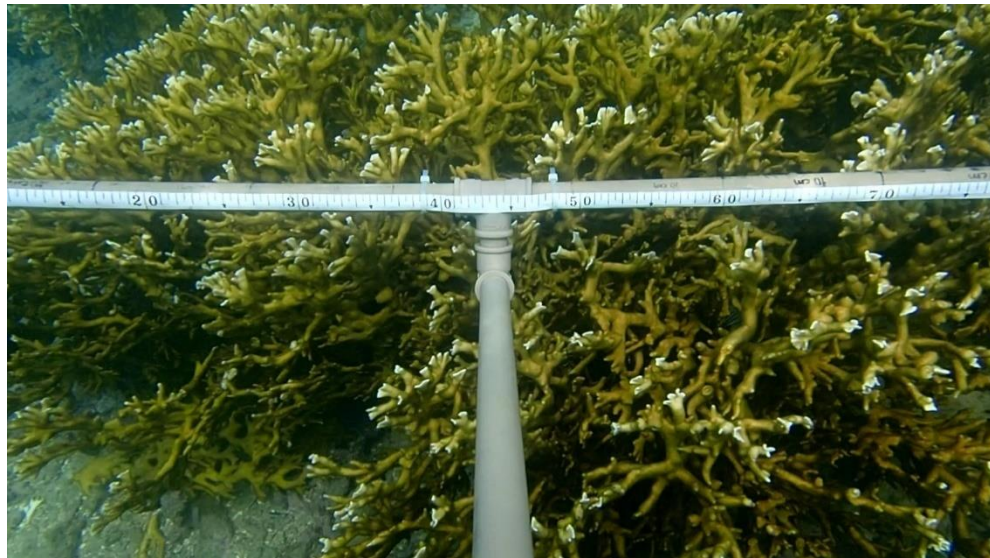


Figure 3 PVC apparatus (handle and frame with metric tape) used in the field study to obtain presence records and measurements of *Millepora alcicornis* colonies

3.3.2.2 Environmental layers

The environmental layers that were used as input in MaxEnt modelling were divided in three categories: ecological (biological), topographical and local.

3.3.2.2.1 Ecological

The ecological layers included the benthic habitat mapping of Tamandaré reefs and its derivatives in different scales (i.e. diversity of habitats and major cover per area). Biological features and benthic cover are known to greatly influence settlement, growth and distribution of corals (Dalleau *et al.*, 2010; McManus *et al.*, 2019), and thus were deemed essential in this study.

The habitat map was produced by supervised classification of a WorldView-03 scene, which provided excellent detail due to its spatial resolution (2 meters/pixel). The processing steps of the satellite imagery were radiometric and atmospheric correction, land and cloud masking and water column corrections (*e.g.* Green *et al.*, 2000; Andréfouet *et al.*, 2003; Deidda and Senna, 2012). Glint correction is a usual step in this process but was not necessary as the image showed negligible sun glint in the study area.

Field data collection was done in coordination with *Millepora alcicornis* colonies surveys, using georeferenced photo and videos (*e.g.* Roelfsema *et al.*, 2010, Roelfsema *et al.*, 2015). Approximately 7500 frames resulted from these campaigns, which were synchronized with GPS data and placed on the satellite scene. First, the main benthic cover was identified visually, following, whenever possible, the *Reef Check Brazil* substrate cover identification scheme (Ferreira *et al.*, 2018). Additionally, all coral colonies (of all species occurring in the area) were identified, counted and colonies with a diameter of more than 50 cm were singled out and measured. We selected the most representative points of each benthic cover identified to be used as training set in the supervised classification of WorldView-3 image (1500 points). A machine learning algorithm, Vector Machine Classifier (Spatial Analyst Toolbox in ArcMap 10.4), was used to classify the scene and map the 15 classes we identified in the region. To test the accuracy of the resulting habitat map, we selected 30 pixels per class (totalling 150 pixels) and analysed the suggested cover against points that were not used to train the algorithms, which resulted in an overall accuracy of 79%. 10 frames per class were also analysed in CPCe software (Kohler and Gill, 2006) using 15 points per photo, to quantify each cover's percentage.

Using this habitat map, we derived the habitat diversity and the major cover layers for three window sizes 30 x 30 m (900m²), 50 x 50 m (2500 m²) and 100 x 100 m (10000 m²). Habitat diversity was derived by calculating the number of different habitats in each grid cell (Zonal tool – Variety, in Spatial Analyst Toolbox in ArcMap 10.4). Major cover was also derived directly from the habitat map (Zonal tool – Majority) and was used to test if the dominant benthic cover within the colonies' surroundings is a factor determining the distribution of milleporas in the area.

3.3.2.2.2 Topographic

Topographic layers were all derived from fine and medium resolutions bathymetric data (2 and 30 m/pixel, respectively) available for Tamandaré's coastal zone (Silveira *et al.*, 2019). From these datasets, four derivatives were calculated: Bathymetric Position Index (BPI), slope, rugosity and aspect. These seascape characteristics are known to influence coral reef zoning and species distribution (Lewis, 2006) and are frequently applied in distribution modelling studies (*e.g.* Bridge *et al.*, 2012; Etnoyer *et al.*, 2018; Poulos *et al.*, 2016). Topographic layers were derived using Benthic Terrain Modeler (BTM) version 3.0 extension for ArcGIS (Walbridge *et al.*, 2018).

BPI compares the depth of each pixel to the mean depth of a determined surrounding area (Yamamoto *et al.*, 2012; Secomandi *et al.*, 2016). In other words, it calculates where the pixel is (vertically) compared to its surroundings. As a result, BPI's positive values reflect how shallower a pixel is, in relation to the mean (such as reefs structures, reef crests). Contrarily, BPI's negative values reflect how deeper a pixel is (such as channels, intra-reef lagoons). Slope is given in degrees and is defined as the maximum rate of depth change, or the gradient of each cell using a 3x3 screening window. Rugosity was inferred using the vector Ruggedness Measure (VRM) tool in BTM, and it incorporates slope and aspect into a single unidimensional measure (Walbridge *et al.*, 2018). VRM calculates rugosity (*i.e.* terrain structural complexity) by measuring the dispersion of vectors orthogonal to the ground surface (Sappington *et al.*, 2007). It was derived using 5x5 window for the high-resolution bathymetric dataset and a 3x3 window for the medium-resolution data. Aspect, given in degrees (0 to 360°), reflects the compass direction of each cell's gradient (*i.e.* the orientation of the seabed in a given location) and can be an important predictor in areas where large-scale hydrodynamics and water flow are in place (Wilson *et al.*, 2007; Henry *et al.*, 2009; Henry *et al.*, 2013).

3.3.2.2.3 Local

Local environmental attributes that could affect distribution of *Millepora alcicornis* were distance to shore and turbidity. Distance to shore was determined by calculating the distance between each pixel in the WV3 image and a line drawn on the coast-sea boundary. It can affect the stability of the habitat, since areas closer to the coast usually suffer more impacts due to trampling, coastal erosion, pollution and tourist-related damage (Davenport and Davenport, 2006; Halpern *et al.*, 2008; Selig *et al.*, 2014). Turbidity (TSU) was derived from a Landsat 8 satellite image (July 20, 2016) showing an increased influx of sediment to the area. We used the algorithm of Dogliotti *et al.* (2015) in the software ACOLITE (Vanhellemont and Ruddick, 2016; 2018) to retrieve a relative measure of turbidity and sedimentation in the region.

3.3.3 Use Layers

The “use layers” considered in this study were fishing and tourism pressure. These activities occur on top of the reef structures, or in their immediate surroundings (Silveira, 2018), and thus can interact negatively with the settling and continuous growth of coral colonies.

The tourism layer was calculated using the maximum number of tourism-related vessels observed in the proximities of a reef area or reef lagoon on a given day (including speed boats, artisanal vessels called “jangadas, and catamarans). Three surveys were conducted in 2018, during Brazilian holidays or busy weekends (February 02; September 13, September 14), to allow the estimation of largest impacts.

Fishing data were collected during a twelve-month period (July 2016 to June 2017), on an average of two days each week, totalling 87 survey days (Silveira, 2018). Although the data used in this study only comprised 2016 and 2017, artisanal fisheries in Tamandaré have been surveyed since 2005 due to a multi-institutional collaboration of Instituto Recifes Costeiros and SOS Mata Atlântica Foundation. Following the same pattern of the tourism’s layer calculation, the fishing map was derived using the maximum number of fishers in a reef area on a given day.

3.4 Results

3.4.1 MaxEnt Input Parameters

3.4.1.1 *Millepora alcicornis* presence data

Millepora alcicornis colonies were found on 859 locations, out of the total 7437 points in the study area. Out of these, only 222 registers were of “large colonies”, following the proposed 100-cm diameter rule (2.98% of total points). As expected, almost all colonies (185 registers) were found on a consolidated reef structure, and usually on reef crests. Few specimens (37 points) were also associated to reef rubble, detached of a larger framework. All larger colonies in our survey data were on the central region of the study area (Campas Beach and Tamandaré Bay) and were of the type *fenestrata*, with a “fine branching” form (Figure 4).

Additionally, during the course of this study, we were able to register all 11 coral species described for the area: *Siderastrea* sp., *Millepora alcicornis*, *Agaricia humilis*, *Porites astreoides*, *Favia gravis*, *Millepora braziliensis*, *Mussismilia hispida*, *Montastraea cavernosa*, *Mussismilia harttii*, *Porites branneri* and *Scolymia welsii* (in order of occurrence).

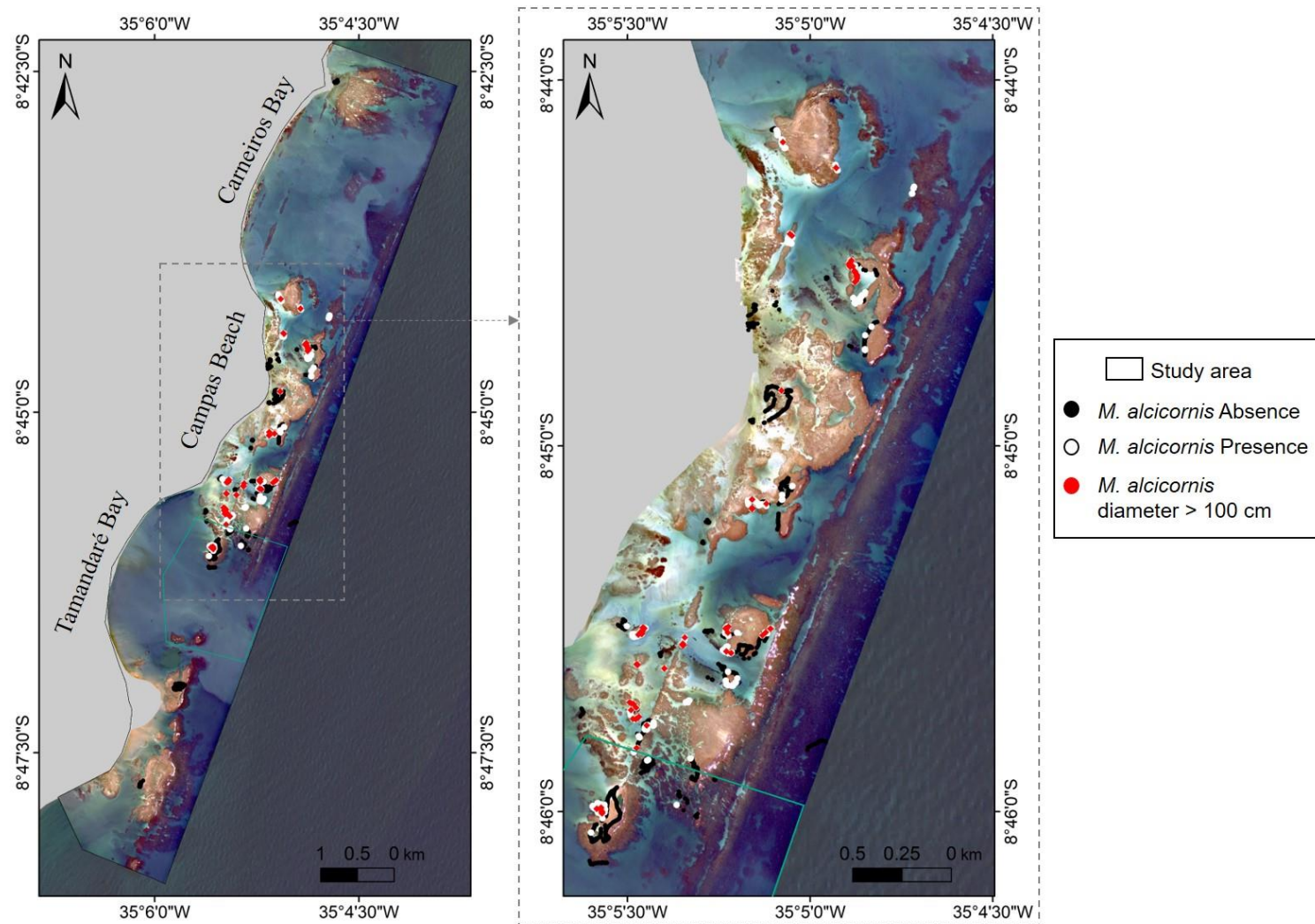


Figure 4 *Millepora alcicornis* presence data in Tamandaré-Brazil used as input in MaxEnt modelling. Red dots show locations where large colonies of the species were found (222). White dots show all *Millepora alcicornis* locations, considering smaller colonies (637). Black dots show all remaining field data (6578). Satellite image: WorldView-03 RGB431

3.4.1.2 Ecological layers

Using supervised classification of the WV3 scene, we were able to identify 15 benthic classes in the study area (Figure 5), which were: reef rubble; rock/algae and urchin; coral, rock and urchin; fore-reef/“Itapitangas”; macroalgae; *Millepora alcicornis*; algae turf (leafy); macroalgae and seagrass; *Palythoa caribaeorum*; hard substratum – reef flat; reef flat with algae; sand; seagrass; terrigenous sediment; turf (calcareous algae) (Table 1). Close-up maps and example photos of each class can be found in Supplementary Materials.

Table 1 Major composition of each benthic cover identified in the Habitat Mapping of Tamandaré's coastal area. Benthic cover identification was performed in CPCe software using 15 points per class. The class "Terrigenous sediment" was only identified remotely (due to high sedimentation in the area and thus, unfeasibility of mapping the bottom with satellite imagery)

Class	Benthic cover	Major Cover				
1	Reef Rubble	rubble (gravel)	turf algae	rock	<i>Halimeda</i> spp.	-
2	Algae, rock and urchin	rock	turf algae	<i>Echinometra lucunter</i>	encrusting coralline algae	-
3	Coral, rock and urchin	rock	coral (<i>Porites astreoides</i>)	<i>Echinometra lucunter</i>	<i>Palythoa caribaeorum</i>	-
4	Itapitanga/Fore-reef	<i>Palythoa caribaeorum</i>	rock	<i>Caulerpa</i> spp.	-	-
5	Macroalgae	<i>Sargassum</i> spp.	<i>Dictyota</i> spp.	<i>Caulerpa</i> spp.	turf algae	-
6	<i>Millepora alcicornis</i>	<i>Millepora alcicornis</i>	turf algae	-	-	-
7	Turf algae	turf algae	calcareous turf algae	<i>Sargassum</i> spp.	<i>Halimeda</i> spp.	rock
8	Seagrass and macroalgae	<i>Sargassum</i> spp.	Seagrass (<i>Halodule wrightii</i>)	sand	-	-
9	<i>Palythoa caribaeorum</i>	<i>Palythoa caribaeorum</i>	turf algae	-	-	-
10	Rock	rock	turf algae	<i>Palythoa caribaeorum</i>	-	-
11	Rock-algae flat	rock	turf algae	filamentous algae	<i>Halimeda</i> spp.	-
12	Sand	sand	gravel	-	-	-
13	Seagrass	Seagrass (<i>Halodule wrightii</i>)	sand	gravel	-	-
14	Terrigenous sediment	*	-	-	-	-
15	Calcareous turf	calcareous turf	algae turf	rock	sand	<i>Millepora alcicornis</i>

Most of the study area was covered by sand (61%) followed by algae turf (10%). This class is characterized by a multi-specific assembly of various algae (e.g. filamentous algae, *Caulerpa* spp., juvenile macroalgae) with a typical maximum height of 2 cm (Ferreira *et al.*, 2008). They were found covering most of the submerged parts of the reef structures in the area. As noted, *Millepora alcicornis* was considered a benthic cover, due to the joint size of some colonies and specific spectral signature. Areas where *Millepora alcicornis* was the main cover corresponded to 0.5% of the total study area. Most reefs had a very typical habitat zonation of: deeper regions covered by macroalgae, followed by algae turf, a reef crest (characterized by *Millepora alcicornis* and/or calcareous turf), *Palythoa caribaeorum* on the shallow area exposed during lower tides, and a reef flat of calcareous rock and/or rock covered by algae.

Habitat diversity maps showed that the highest variety can be found on the reef areas, mostly in grids which include the reef structure and the sea bottom. This trend could be observed in every grid resolution we used in this study (i.e. 30x30m, 50x50m and 100x100m).

It is possible to observe in the major cover map (Fig 5), that significant parts of the region correspond to algae-dominant covers, with macroalgae and algae turf covering the third reef line and the basal area of the northern and southern reefs. Also, we can see the seagrass areas almost attached to the coastline, and a region of significant reef rubble near the limits of the no-take zone.

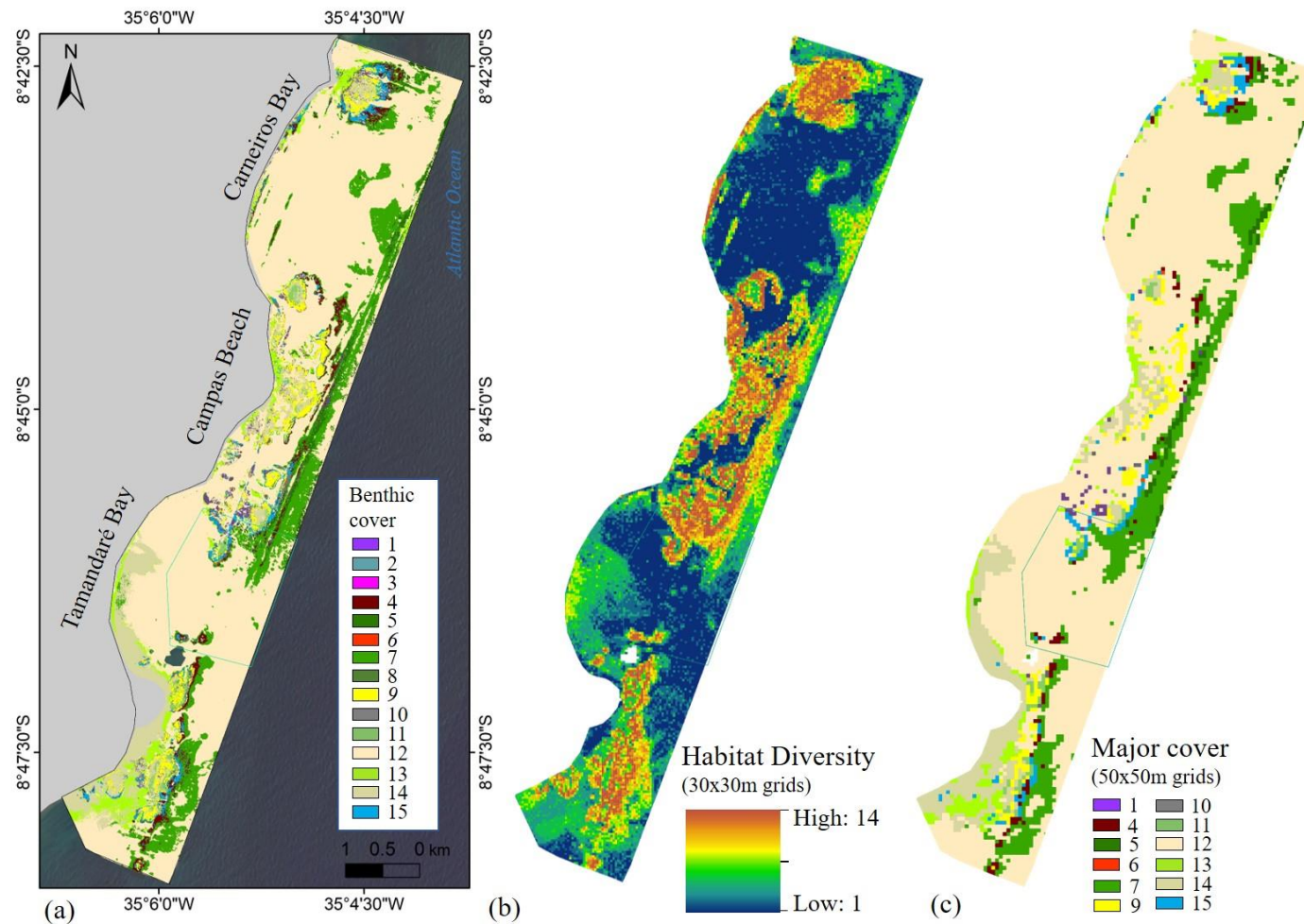


Figure 5 Ecological layers used as environmental variables in the predictive modelling of *Millepora alcicornis*. The hollow blue polygon on the three images shows the location of the no-take zone. **a)** Habitat map of the coastal reefs of Tamandaré-Pernambuco, with 15 classes: (1) reef rubble, (2) rock/algae and urchin (3) coral, rock and urchin, (4) fore-reef/“Itapitangas”, (5) macroalgae, (6) *Millepora alcicornis*, (7) Algae turf (leafy), (8) Macroalgae and seagrass, (9) *Palythoa caribaeorum*, (10) hard substratum – reef flat, (11) reef flat with algae, (12) sand, (13) seagrass, (14) terrigenous sediment, (15) calcareous algae turf. **b)** number of different habitats present in a 30x30m grid, or 900m² area. **c)** Major benthic cover calculated for a 50x50m grid, or 2500m² area.

3.4.1.3 Topographical and local layers

Figure 6 shows the topographical layers derived in this study. Depth values varied from -21 m in the deeper regions and 2 m, in the shallowest areas, exposed during the lowest tides (tide reference = 0.0 m). The overall tendency of mainly shallow areas (reefs) separated by deeper channels. It is possible to see the first reef line, almost attached to the coastline and the main channels occurring in front of the two bays (Tamandaré and Campas Bay). This observation can also be inferred by analysing the Broad BPI derivations, which show the negative values corresponding to the channels' areas and neutral/positive on the reefs.

Low values of slope and rugosity make the most of the study area and represent areas low topographic variation, mainly soft bottom (*e.g.* sand) without vegetation cover. Low rugosity and slope values are also noticeable in deeper regions, and in areas closer to the shore, even when reefs were present. Alternatively, the highest values of both variables, were correlated with reefs and areas surrounding them, mostly in the second and third reef bank lines. Also, the most complex regions were always surrounded by intermediate rugosity areas. Aspect maps show the variation in orientation across the area. A gradient oriented to the East seems to be the most constant throughout the region and is mainly registered in front of the bays and associated with the channels' southern borders. Additionally, frequent changes in orientation can be detected associated with the reefs in the area.

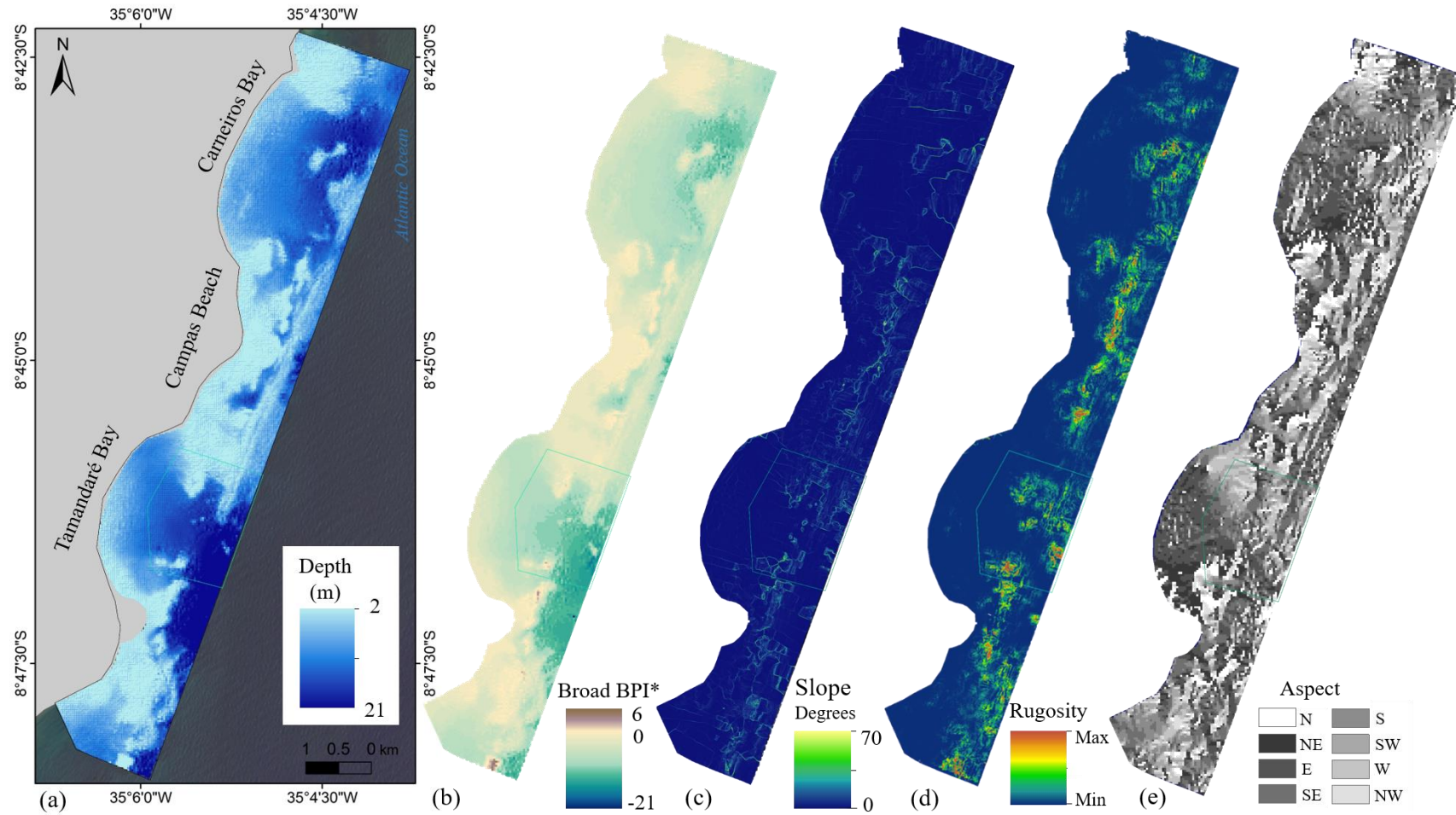


Figure 6 Topographical layers used as environmental variables in the predictive modelling of *Millepora alcicornis*. The hollow blue polygon on the images shows the location of the no-take zone. a) Bathymetric dataset; b) Broad Bathymetric Position Index (BPI); c) Slope; d) Rugosity; e) Aspect

The local layers are shown on Figure 7. Distance to shore of all points in our study area ranged from 7 m (closest to the coast) to 2122 m (furthest from the coast), with an average of 827 m. Out of all field data, the closest point was located 69 m from the shore, in a seagrass area, and the furthest point was 1398 m away from the coastline, on the fore-reef of the third reef line. Large *Millepora alcicornis* colonies were found as close as 200 m and as far as 930 m but were mostly observed within a 300-800m coast distance range. Turbidity varied greatly in the region, with higher values near the coast of the two rivers (northern and southern parts of the map). Also, increased turbidity can be seen in the regions occupied by channels and near the shore (central area of the image), probably associated with coastal sedimentation.

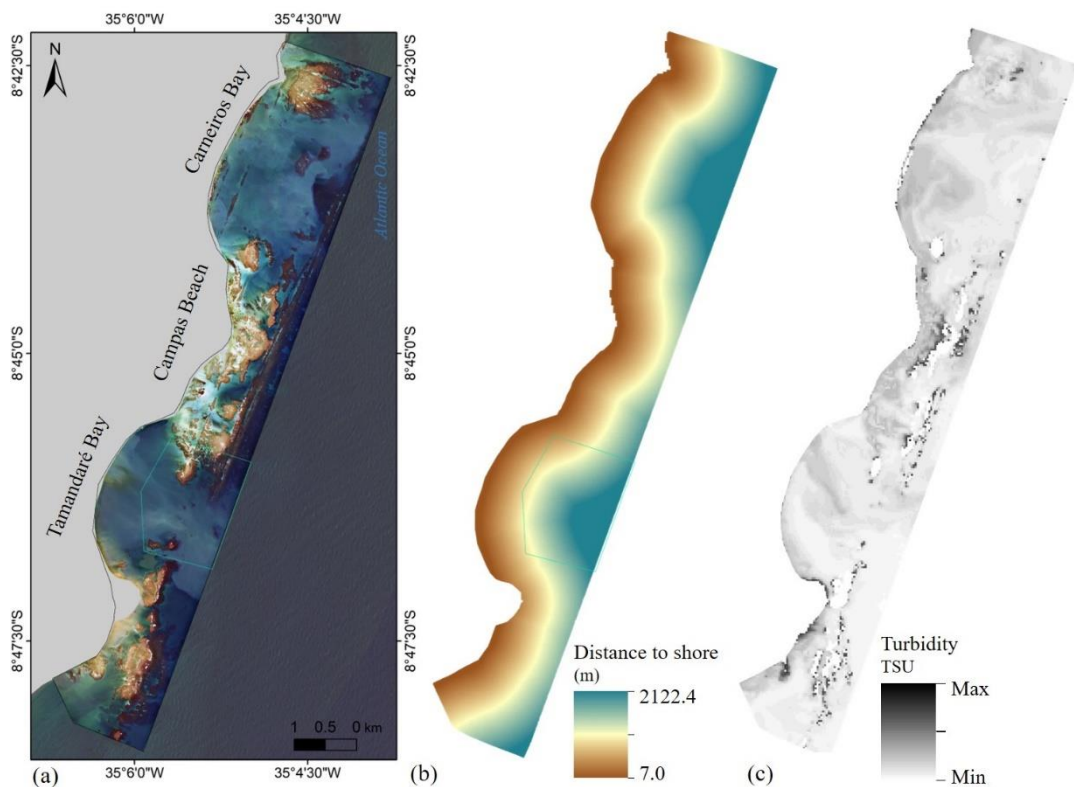


Figure 7 Local layers used as environmental variables in the predictive modelling of *Millepora alcicornis*. The hollow blue polygon on the images shows the location of the no-take zone. a) WorldView03 image RGB431 for visualization purposes; b) distance to shore; and c) Relative measures of turbidity.

3.4.2 Species Distribution Modelling Results

AUC model for training and testing datasets were considered high (>0.97). The results (Figure 8) are shown in a scale from 0 to 1; 0 being the most unsuitable habitats and 1, areas showing the best environmental features for the target species. The habitat suitability map suggests a limited availability of suitable habitats for large colonies of *Millepora alcicornis*.

Considering the entire mapped area (17.64 km²), 81% of the pixels exhibited values ranging from 0 to 0.1, indicating an area of more than 14 km² of highly unsuitable habitats. Alternatively, only 0.56% of the area (0.1 km²) showed habitat suitability values higher than 0.5.

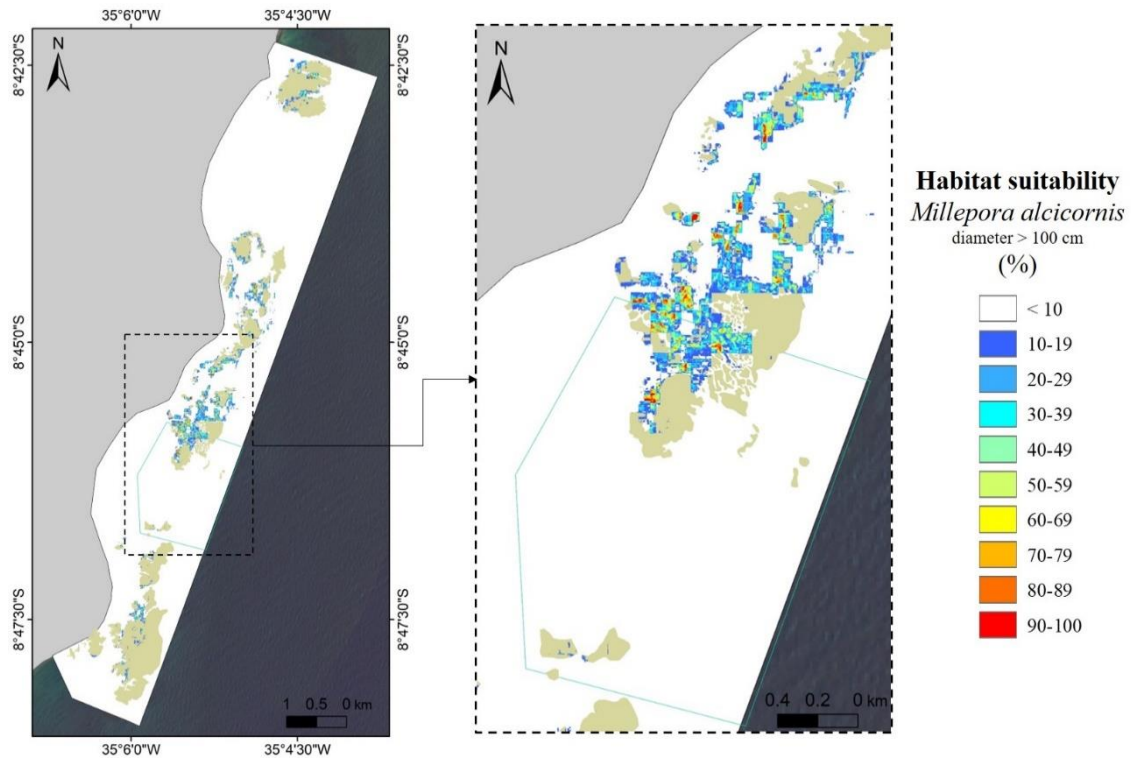


Figure 8 MaxEnt georeferenced output showing relative habitat suitability for large colonies of *Millepora alcicornis*. a) Complete map of habitat suitability in Tamandaré - PE; and b) Map focusing on the no-take zone and surrounding reefs. The reefs are pictured in light brown to enable the visualization of the results

Besides the habitat suitability map, MaxEnt offers jackknife tests and marginal and individual response curves (in probability of presence) for each variable. We used the jackknife on AUC test (Figure 9) and individual response curves (Figure 10) to analyse how each variable influenced the modelled presence of *Milleporas* and in what manner they determined occurrence.

The most important ecological factors for our predictive model included: habitat diversity (in all three grid-sizes) and habitat cover. The most influential topographic and local variables were bathymetry (in both spatial scales), broad BPI and distance to coast. On the other hand, aspect showed practically negligible influence on the predicted occurrence of *Millepora alcicornis*. We can also infer by the jackknife test analysis that the model was not dependant on any single variable, since the AUC did not decline when a determined variable was excluded from the model (light blue bars, in relation to the test's AUC, in red).

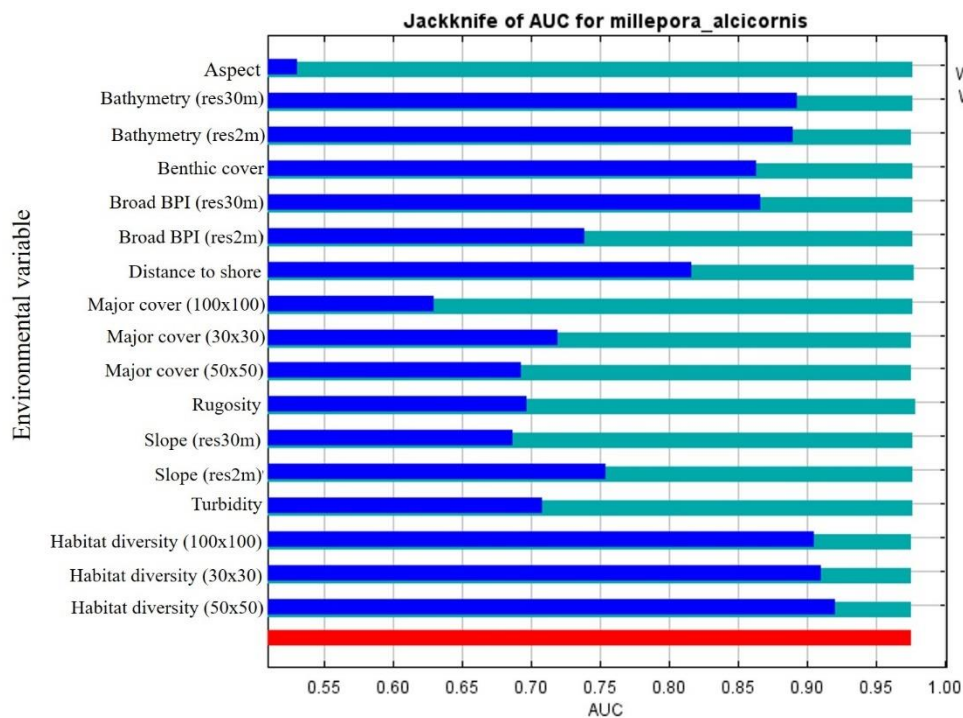


Figure 9 Jackknife test results exhibiting the influence of each variable on the final AUC (Area Under the receiver-operator Curve) value

The individual response curve for habitat diversity showed that large colonies of *Millepora alcicornis* are most likely to occur on areas with a higher variety of habitats, and thus, higher biological complexity. The probability of occurrence reaches 50% only in sites with 8 habitats (or more) in a 900m² area, with similar trends for the other grid windows. As expected, the highest relative probability of large *Millepora alcicornis*' occurrence is in areas where the benthic cover is *Millepora alcicornis*. The occurrence rates related to benthic classes are followed by "reef rubble" and "turf of calcareous algae". The bathymetric curve showed an optimum depth in which *Millepora alcicornis* are more likely to occur (-3 m), considering both the medium resolution analysis and the high-resolution data. The most suitable are in depths between -5 and -1 m. BPI's results showed the specie's preference for areas that are shallower than their surroundings, and that large colonies are less likely to occur in regions like channels and valleys. Additionally, a distance of about 650 meters from the coastline seems to be ideal, and areas too close or too distant from the coast are less likely to harbour large colonies of Milleporas.

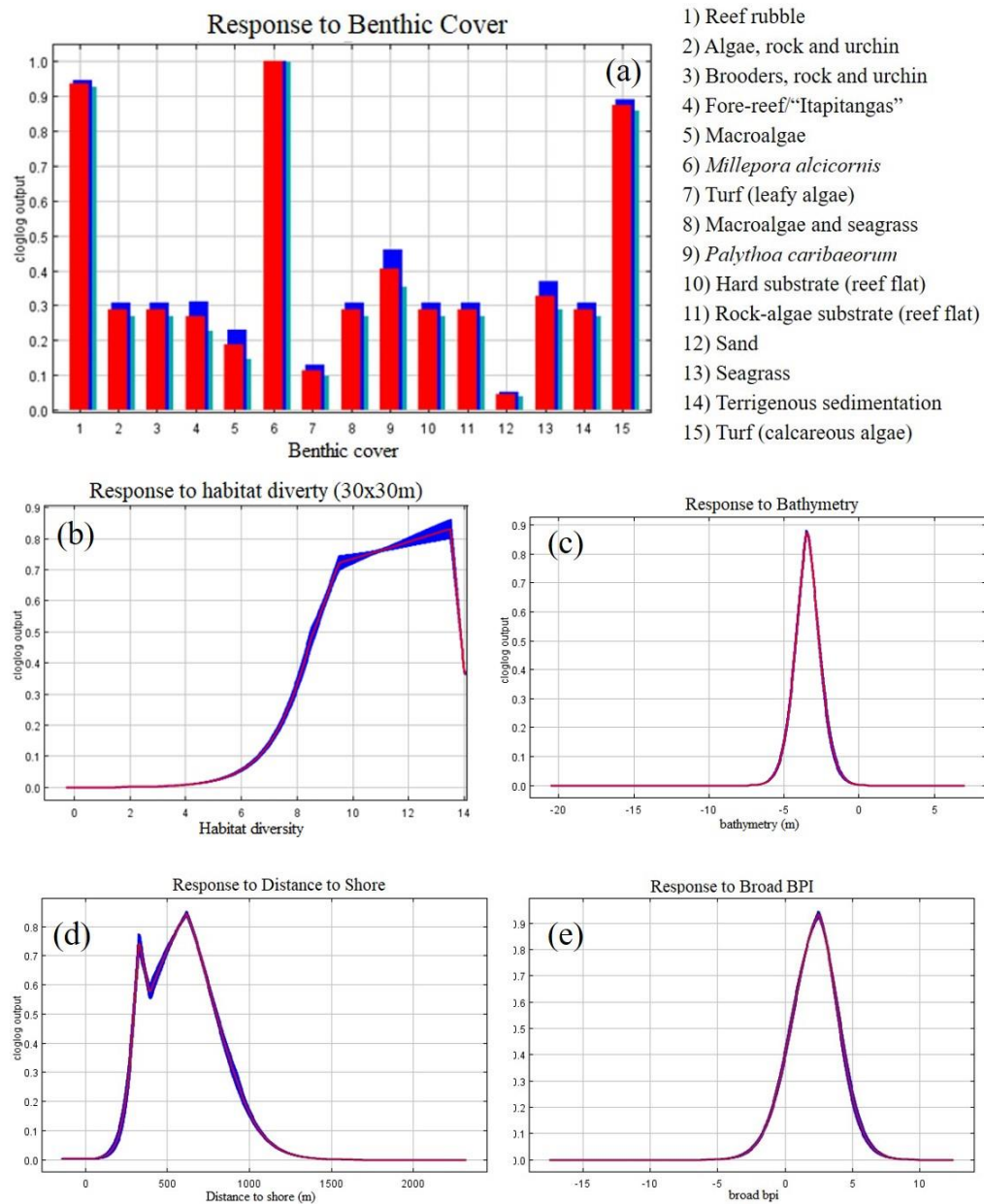


Figure 10 Response curves for the most influential variables of the model: a) Benthic cover; b) Habitat Diversity, c) Bathymetry, d) Broad Scale Bathymetric Position Index (BPI); and e) distance to shore.

3.4.3 Human use

Fishing and tourism density maps showed the broad distribution of these activities in the study area (Figure 11). Also, showed how related they are to the coral reefs, occurring on top of the reef structures, reef lagoons and areas surrounding the main reefs. Fishing had high densities in the Southern (Mamucabas and Tamandaré bay), central (Campas beach), and Northern regions (Carneiros Bay); contrastingly use in the southern area is much less intense. It is possible to notice increased use of both activities right on the boundaries of the no-take

zone. We were able to detect five main tourist spots, four of them in Campas Beach. Most tourist activities were in shallow reefs, and very close to the shore.

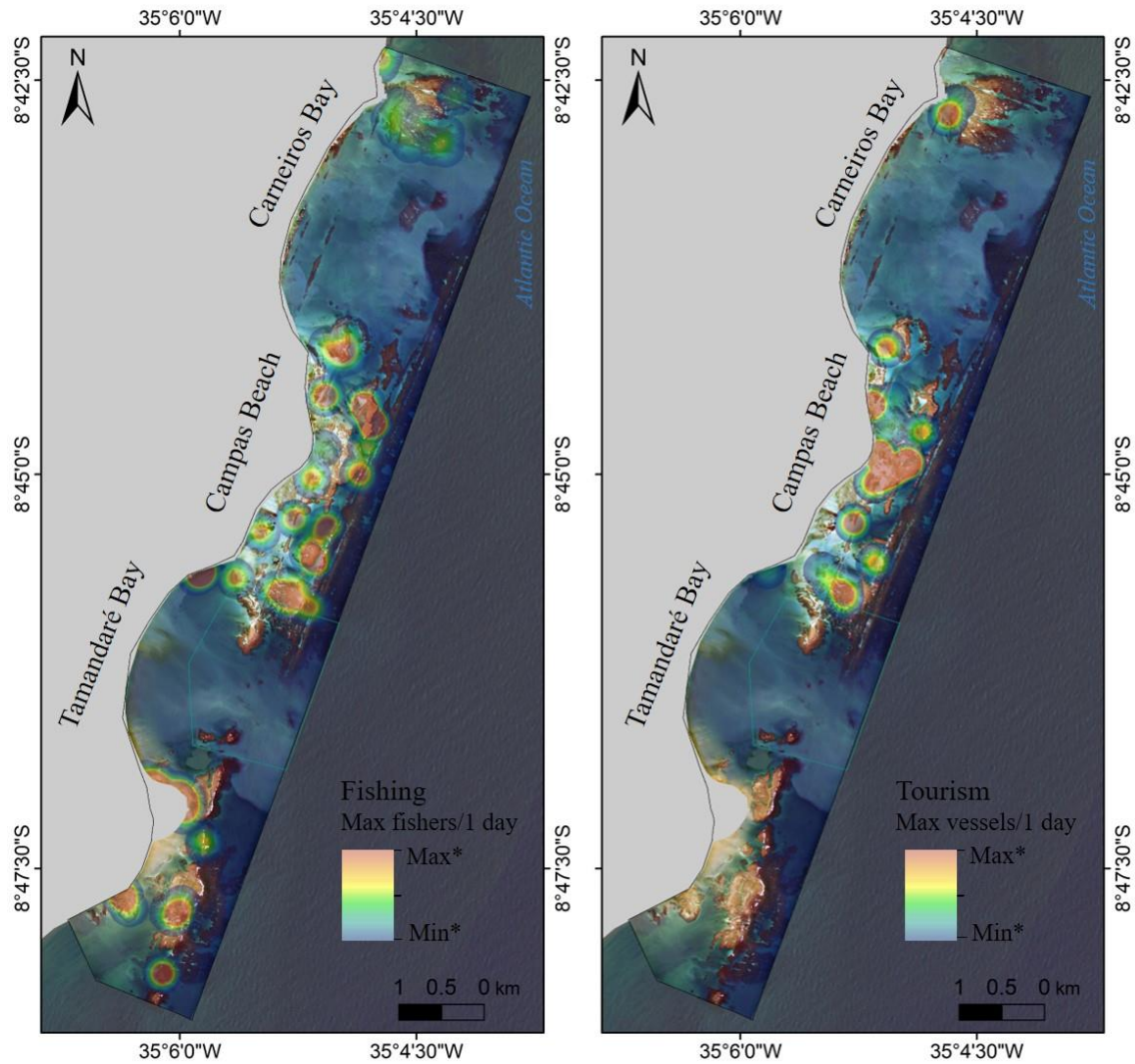


Figure 11 Use maps of the study area, including the main regions: Tamandaré Bay, Campas Beach and Carneiros Bay. a) Fishing pressure, calculated using the maximum number of fishers in the vicinities of a reef in a given day; b) Tourism activities map, calculated using the maximum number of tourism-related vessels on a reef or its proximities in a given day

3.5 Discussion

Millepora alcicornis had the second highest rate of occurrence (859 in 7437 total points), surpassed only by *Siderastrea* sp. (1392 in 7437 total points). Besides these numbers, the occupation of *Millepora alcicornis* on the reefs of the area can be considered higher than any other coral, especially due to their average size in comparison with Scleractinia corals like *Siderastrea* sp. and the other Millepore occurring in the area, *Millepora braziliensis*. For

example, out of almost 1400 colonies, only 15 colonies of *Siderastrea* sp. had diameters larger than 15 cm (5 of which occurred inside the *no-take* zone), and only one was larger than 100 cm. Indeed, larger colonies of *Siderastrea strelata* suffered intense mortality during the 1998 bleaching according to in situ observations at the time (Ferreira per obs), what can explain their rarity.

Since Laborel (1969), *Millepora alcicornis* has been described as one the main reef builders in the region and as a preferential occupant of shallow areas of the reefs (Maida and Ferreira, 1997; Ferreira *et al.*, 2006b). Although this preferential location may hinder reproductive advantages, due to greater recruitment rates in areas between 4 and 6 meters deep (Lewis 2006), it also has several possible drawbacks. In a region where tourism and fishing activities occur on top of the reefs or their immediate surroundings, direct physical impacts on the limits of the reef framework (and the framework itself) are expected. Breakage due to trampling, snorkelling, anchors, passage of the boats can be observed in the area and are common human-related impacts on coral reefs (Tratalos and Austin, 2001; Davenport and Davenport, 2006; Flynn and Forrester, 2019). *Millepora* colonies can use that to their advantage, though, as fragmentation and regeneration of broken colonies are important forms of asexual reproduction in the genera (Lewis, 2006; Rodríguez *et al.*, 2019). The branches' settlement post fragmentation usually occurs on other *Millepora alcicornis* colonies and rock substratum, but it has also been described to attach to soft substrate, such as sand (Edmunds, 1999; Lewis, 2006). On that note, this inherent capability of settling and colonizing different substrates from broken branches was the reason we chose to use only large colonies as input data on MaxEnt modelling. Thus, we believe that by using all available data (i.e. including recently settled branches) the resulting suitability map could suggest areas that are in fact, not suitable for occurrence in a long-term basis. Additionally, large colonies are not only valuable as individual organisms, but also as habitats, as we were able to see in the habitat map (Fig 4). *M. alcicornis* are usually found harbouring rich associated micro and macro fauna, including fish, Crustacea, Bryozoa, and other Cnidaria (Amaral *et al.*, 2008; Lewis, 2006; Ferreira *et al.*, 2006b).

Large colonies of *Millepora alcicornis* were not registered in the extreme North of the study area (Carneiros) nor in the South (Mamucabas). In Carneiros, field survey was limited due to high turbidity and we were not able to access many areas of the main reef, which might explain the lack of presence data. Even so, other authors have related the scarcity of *M. alcicornis* in this region (*e.g.* Correia *et al.*, 2018) with the few colonies registered occurring

in fore-reef regions. According to our field data, Milleporas were absent in the two Mamucabas reefs surveyed, and had very few coral colonies in general, a trend related in Reef Check monitoring in the area (coral cover < 1%) (Reef Check, *unpublished data*). Alternatively, the presence data was highly concentrated on the central area, which included Campas Bay and Tamandaré Beach and has a higher density of reef structures.

The benthic mapping of the area exposed the habitat complexity that still exists in Tamandaré's coastal reefs. Even considering the relatively low coral cover in general (10%) (Ferreira *et al.*, 2006b), colonies of *Millepora alcicornis* and small brooders (*Porites astreoides*, *Siderastraea* sp, *Agaricia humilis* and *Favia gravida*) were found covering large areas of substratum. In fact, two benthic classes directly reflected this dominance: “*Millepora alcicornis*” and “coral, rock and urchin”. The latter refers to a highly characteristic reef located only 200 meters from the coastline and easily accessed by swimmers, tourists and fishers. This specific reef also has the highest densities of seaurchin (*Echinometra lucunter*), which has been associated with human impacts such as fishing (Roberts, 1995; Hughes *et al.*, 2007; Topor *et al.*, 2019). The increased abundance of urchins in reefs experiencing overfishing is explained mainly by trophic replacement of herbivorous fish by urchins, especially with the removal of their predators from the region (*e.g.* lobsters, large fish) (McClanahan, 1994; Graham *et al.*, 2017).

Furthermore, the benthic mapping allowed a direct derivation of habitat-complexity measures, such as the habitat diversity per area. Considering the average area of the reefs in the region, and the size of the study area itself, we believe that 30x30, 50x50, and 100x100 grids provide insights on localities concentrating habitat diversity. Albeit some cover classes (*i.e.* sand, terrigenous sediment, rocky reef flat) are not direct indicators of biological diversity (Wedding *et al.*, 2008), the presence of various types of substrates in a small area is usually positively associated with increased niches availability. Most reef zones (with exception to reef tops), exhibited increased habitat diversity (10-13 different habitats in a 30x30m area), a pattern easily observed in areas within the no-take zone and its immediate surroundings.

MaxEnt modelling output showed the close association between the presence of large colonies and the diversity of habitats: areas with higher habitat variety were the most suitable for *M. alcicornis* presence. Since the presence of large Milleporas may be responsible for an increase of biodiversity (Garcia *et al.*, 2008; 2009), these results can be considered part of a feed-back succession process that is typical of coral reef ecosystems. Additionally, large colonies were mostly found on reef crests and fore-reefs, areas which, depending on the

spatial scale, can be considered “border areas” that limit the ecosystem and the open bottom. Bordering, or very close to main reef structures, we found cover classes that did not occur in the reef itself, such as seagrass.

Benthic cover on the site was the second most important variable for the model. Not surprisingly, large colonies were highly correlated with areas remotely interpreted as “*Millepora alcicornis*”. In fact, *M. alcicornis* and *Palythoa caribaeorum* were the only single-species substrata that could be detected by the 2-meter resolution satellite image used in this study. Interestingly, habitats classified as “reef rubble” showed strong correlation with *M. alcicornis*. This cover was found on several regions throughout the area, but in a more concise way, close to the shore and near the no-take zone. This corroborates this specie’s capability of settling in fragmented substrata, as this class is mostly composed by reef fragments, boulders covered by filamentous algae, macroalgae and sand. The proximity to the no-take zone (less than 70m) and its large colonies’ assemblages (400 m) may raise the hypothesis that the natural breakage of large colonies within the protected zone have been frequently supplying fragments for this rubble area. Additionally, no other reef rubble region had such high presence of Milleporas, except for these two near the no-take zone.

The other main correlation with habitat cover is a characteristic algae turf in Tamandaré reefs (Ferreira *et al.*, 2018), here classified as “calcareous turf”. This class represents a multi-specific assemblage of articulated calcareous algae (e.g. *Jania* spp., *Amphiroa* spp.) and is the dominant substrata in many parts of the reefs, notably on the reef crests. This alone might explain the high habitat suitability for the presence of *Millepora alcicornis* in areas classified as calcareous algae turf. Alternatively, it is generally known that coral species show a negative relation to algae cover mainly due to a decreased availability of substrate for settlement (Hughes *et al.*, 2007). Remotely classified classes usually depict the major cover (not necessarily a 100% dominance) of a determined pixel. Here, MaxEnt results imply that contrarily to other algae covers like “macroalgae” and “seagrass”, a high percentage of calcareous turf is not necessarily an indicator of unsuitable habitats.

Topographical values showed narrow response curves in general, implying that *Millepora alcicornis* can be highly dependable on seascape relief. Bathymetry’s results were partly corresponded to those of other studies which related the species’ depth of occurrence (e.g. 0 to 15m in Amaral *et al.*, 2008; 0 to 10 m in Leao and Kikuchi, 2001). The optimal depths estimated by our modelling ranged between 0 and 5 meters. Indeed, we were able to see large colonies which grew vertically to reach the upper water column limits, causing a

localized mortality on these colonies tops due to aerial exposure. Broad BPI's results showed the high correspondence of presence of large colonies and areas shallower than the surroundings, limiting the suitable habitats to "peak-like" areas such as reef crests and on a broader scale, the reef framework. The negative values of BPI were characterized by the two main channels in the area, which are highly unsuitable for the settlement and growth of coral colonies in general, since these regions exhibit high turbidity, increased depth and mostly sand substrata.

Distance to shore was also an important limiting factor, registering low suitability in areas too close or too far from the coastline. The highest occurrence peak (650 m) coincide with the second reef-line, described as having the highest coral cover and biological complexity (Maida and Ferreira, 1997). The second peak, at about 350 m from the coast, seems to be related with the occurrence of large colonies on reef rubble areas and some extended backreefs. The low habitat suitability in areas close to the shore seems to disagree with the bathymetric curve, since this is the distance range in which most shallow areas occur. This conflict infers limiting impacts of other variables, which can in this case, be caused by human activities. In an extensive study of the Brazilian coast, Ferreira *et al.* (2004) concluded that pollution, fishing and tourism-related impacts typically decrease with distance from the coast. As a particular regional issue, the reefs closer to the shore are easily accessed by foot, swimming and by all kinds of vessels, which can cause a range of direct impacts to the corals and may suppress and impede growth. Additionally, higher levels of pollution and coastal sedimentation can influence coral colonies both chemically and physically (Zaneveld *et al.*, 2016). On the other hand, low correlations of areas further than 1000 m from shore may be highly related to depth. This variable may also be acting as a proxy for hydrodynamical factors, which were not considered in our model. Branching colonies of *Millepora* genera as the ones mapped in this study, are usually related to low to moderate wave energy (Lewis, 2006; Dubé *et al.*, 2017). The third reef-line, furthest from the shore, is an area of high wave energy and turbulence, (which in fact, impeded field survey several times) and showed little to no habitat suitability. In future studies, researches may consider using oceanographical variables to test this theory.

The fact that we used only points where large colonies occurred and did not input background points with absence data in the model, enabled the comparison of the model results with human use variables. The tourism and fishing maps clearly show that most reef structures of Tamandare's coastal zone suffer with either one or both kinds human impact,

with the exception of the no-take zone. Overfishing, uncontrolled tourism and high pollution rates have been constantly described as the major source of impacts in Tamandaré (Castro *et al.*, 2001; Ferreira *et al.*, 2006a; Chaves *et al.*, 2013) and may act as limiting factors of coral settlement and growth. Apart from direct impacts to the structure (*e.g.* anchoring, physical damages due to fishing gear), overfishing may cause chronic impacts to coral reef areas, with the removal of herbivores and thus increasing competition between macroalgae and corals (Hughes *et al.*, 2007).

Tourism was higher on shallow, reef lagoons, with a maximum of 74 people and 18 vessels in a day in one reef lagoon. We observed that local tourist guides usually take the tourists using small artisanal vessels called “jangadas”, to practice diving activities in the shallow reefs, mostly close to the shore. On the other hand, large speed boats and catamarans were also seen in the area and on top of reefs. One may infer that they must cause larger impacts to the structures than the jangadas but, according to the Management Plan for the area, there are few differences on the rules regulating vessels used for tourism activities on the Sustainable Use zone (ICMBio, 2012).

MaxEnt modelling was mostly accurate in relation to where the most suitable and unsuitable habitats were in the study area, as confirmed by field data. In the few areas where it was not, negative synergies between human use maps and the occurrence of large colonies of *Milleporas* were registered. These instances occurred only on the Sustainable Use Zone, which is the whole area except from the no-take zone. Alternatively, large *Milleporas* were registered in all modelled suitable habitats inside the no-take area. We considered this a strong indicator that topography and physical variables may provide the threshold features within which a coral species may occur, but ecological features and conservation measures in place allow these animals to thrive. Meanwhile, some ecological variables in this study may also reflect this evaluation, such as the benthic cover and a high diversity of habitats.

Species distribution modelling results may be extremely helpful when selecting areas for the application of conservational measures and evaluating the performance of those already in place (*e.g.* Pawar *et al.*, 2007; Carrol, 2010; Pittman and Brown, 2011; Bridge *et al.*, 2012). Considering the wide range of impacts the coral reefs are subjected to, including global re-occurring threats like El-Niño related bleaching and climate change, it is imperative to at least, act locally to avoid mass mortality (Hughes *et al.*, 2007). This study shows areas that are highly suitable for settlement, growth and development of *Millepora alcicornis* and probably, other coral colonies. These areas should be considered as high priority and

monitored closely. We recommend that, when faced with options, decision makers and managers should protect areas with high diversity and coral cover, which can be biological suppliers to other areas, if needed. Indeed, we believe that the variables derived here can be applied in other predictive models and that further studies should be conducted in the area using this methodology. This would provide a rich perspective on ecologically important areas, and whether Tamandaré's coastal zone needs of additional conservation efforts than the ones currently in place. Notably, our analyses reinforce the importance of a no-take zone for the maintenance of local biodiversity and suggest the implementation of improved use management measures of the reef areas.

3.6 Acknowledgments

The authors thank the Center for Research and Conservation of Marine Biodiversity of the Northeast (CEPENE) of the Chico Mendes Brazilian Institute of Biodiversity (ICMBIO) and Projeto Recifes Costeiros, Fundação Toyota do Brasil, Fundação SOS Mata Atlântica for supporting the field work. The authors are grateful to all volunteers, specially Gaspar A.L.B, Lippi, D., and Coxey, M., for their great help with the field work and helpful insights. This research is a contribution of the Long-Term Ecological Research Program (PELD-CNPq 441632/2016-5 ILTER-Brazil -Tamandaré site 18), and Ciências do Mar II, AUXPE 1979/2014. This study was financed in part by the Coordenação de Aperfeiçoamento de Pessoal de Nível Superior – Brasil (CAPES) – Finance Code 001.

References

- Adam, T. C., Burkepile, D. E., Ruttenberg, B. I., & Paddock, M. J. (2015). Herbivory and the resilience of Caribbean coral reefs: knowledge gaps and implications for management. *Marine Ecology Progress Series*, 520, 1-20.
- Agardy, T., Di Sciara, G. N., & Christie, P. (2011). Mind the gap: addressing the shortcomings of marine protected areas through large scale marine spatial planning. *Marine Policy*, 35(2), 226-232.
- Amaral, F. M., Steiner, A. Q., Broadhurst, M. K., & Cairns, S. D. (2008). An overview of the shallow-water calcified hydroids from Brazil (Hydrozoa: Cnidaria), including the description of a new species. *Zootaxa*.
- Andréfouët, S., Kramer, P., Torres-Pulliza, D., Joyce, K. E., Hochberg, E. J., Garza-Pérez, R., Mumby, P. J., Riegl, B., Yamano, H., White, W. H., Zubia, M., Brock, J. C., Phinn, S. R., Naseer, A., Hatcher, B. G., Muller-Karger, F. E. (2003). Multi-site evaluation of IKONOS

data for classification of tropical coral reef environments. *Remote sensing of environment*, 88(1-2), 128-143.

Bargain, A., Marchese, F., Savini, A., Taviani, M., & Fabri, M. C. (2017). Santa Maria di Leuca Province (Mediterranean Sea): Identification of suitable mounds for cold-water coral settlement using geomorphometric proxies and Maxent methods. *Frontiers in Marine Science*, 4, 338.

Bellwood, D. R., Hughes, T. P., Folke, C., & Nyström, M. (2004). Confronting the coral reef crisis. *Nature*, 429(6994), 827.

Bridge, T., Beaman, R., Done, T., & Webster, J. (2012). Predicting the location and spatial extent of submerged coral reef habitat in the Great Barrier Reef World Heritage Area, Australia. *PLoS One*, 7(10), e48203.

Burke, L. M., Reyttar, K., Spalding, M., & Perry, A. (2017). Reefs at risk revisited: World Resources Institute

Carroll, C. (2010). Role of climatic niche models in focal-species-based conservation planning: assessing potential effects of climate change on Northern Spotted Owl in the Pacific Northwest, USA. *Biological Conservation*, 143(6), 1432-1437.

Castro, C. B., & Pires, D. O. (2001). Brazilian coral reefs: what we already know and what is still missing. *Bulletin of Marine Science*, 69(2), 357-371.

Chaves, L. T. C., Pereira, P. H. C., & Feitosa, J. L. L. (2013). Coral reef fish association with macroalgal beds on a tropical reef system in North-eastern Brazil. *Marine and Freshwater Research*, 64(12), 1101-1111.

Collin, A., & Hench, J. L. (2012). Towards deeper measurements of tropical reefscape structure using the WorldView-2 spaceborne sensor. *Remote Sensing*, 4(5), 1425-1447.

Correia, J. R. M., Oliveira, W. D., Pereira, P. S., de Camargo, J. M. R., & de Araújo, M. E. (2018). Substrate Zonation as a Function of Reef Morphology: A Case Study in Carneiros Beach, Pernambuco, Brazil. *Journal of Coastal Research*, 81(sp1), 1-9.

Costa, B., Kendall, M. S., Parrish, F. A., Rooney, J., Boland, R. C., Chow, M., Lecky, J., Montgomery, A., & Spalding, H. (2015). Identifying suitable locations for mesophotic hard corals offshore of Maui, Hawai 'i. *PLoS One*, 10(7), e0130285.

Couce, E., Ridgwell, A., & Hendy, E. J. (2012). Environmental controls on the global distribution of shallow-water coral reefs. *Journal of Biogeography*, 39(8), 1508-1523.

Dalleau, M., Andréfouët, S., Wabnitz, C. C., Payri, C., Wantiez, L., Pichon, M. & Benzoni, F. (2010). Use of habitats as surrogates of biodiversity for efficient coral reef conservation planning in Pacific Ocean islands. *Conservation Biology*, 24(2), 541-552.

Davenport, J. & Davenport, J. L. (2006). The Impact of Tourism and Personal Leisure Transport on Coastal Environments: A Review. *Estuarine, Coastal and Shelf Science*, 67(1-2), 280-92. doi:10.1016/j.ecss.2005.11.026.

Deidda, M., & Sanna, G. (2012). Pre-processing of high resolution satellite images for sea bottom classification. *Italian Journal of Remote Sensing/Rivista Italiana di Telerilevamento*, 44(1).

- Dogliotti, A. I., Ruddick, K. G., Nechad, B., Doxaran, D., & Knaeps, E. (2015). A single algorithm to retrieve turbidity from remotely-sensed data in all coastal and estuarine waters. *Remote Sensing of Environment*, 156, 157-168.
- Dubé, C. E., Mercière, A., Vermeij, M. J., & Planes, S. (2017). Population structure of the hydrocoral *Millepora platyphylla* in habitats experiencing different flow regimes in Moorea, French Polynesia. *PloS one*, 12(3), e0173513.
- Edmunds, P. J. (1999). The role of colony morphology and substratum inclination in the success of *Millepora alcicornis* on shallow coral reefs. *Coral Reefs*, 18(2), 133-140.
- Elith, J., Phillips, S. J., Hastie, T., Dudík, M., Chee, Y. E., & Yates, C. J. (2011). A statistical explanation of MaxEnt for ecologists. *Diversity and distributions*, 17(1), 43-57.
- Etnoyer, P. J., Wagner, D., Fowle, H. A., Poti, M., Kinlan, B., Georgian, S. E., & Cordes, E. E. (2018). Models of habitat suitability, size, and age-class structure for the deep-sea black coral *Leiopathes glaberrima* in the Gulf of Mexico. *Deep Sea Research Part II: Topical Studies in Oceanography*, 150, 218-228.
- Eugenio, F., Marcello, J., Martin, J., & Rodríguez-Esparragón, D. (2017). Benthic Habitat Mapping Using Multispectral High-Resolution Imagery: Evaluation of Shallow Water Atmospheric Correction Techniques. *Sensors*, 17(11), 2639.
- Ferreira, B. P., Maida, M., & Cava, F. (2001). Características e perspectivas para o manejo da pesca na APA Marinha Costa dos Corais. In *Congresso Brasileiro de Unidades de Conservação* (pp. 50-58).
- Ferreira, B. P., Maida, M., Castro, C. B., Pires, D. O., Damico, T. M., Prates, A. P., & Marx, D. (2006b). The status of coral reefs in Brazil. In *Proc. 10th Int. Coral Reef Symp* (Vol. 1, pp. 1011-1015).
- Ferreira, B. P., Messias, L. T., & Maida, M. (2006a). The environmental municipal councils as an instrument in coastal integrated management: the Area de Proteção Ambiental Costa dos Corais (AL/PE) experience. *Journal of Coastal Research*, 1003-1007.
- Ferreira, B. P.; Gaspar, A. L. B.; Coxey, M. S.; Monteiro, A. C. G. (2018). Manual de Monitoramento Reef Check Brasil 2018. Ministério do Meio Ambiente, Brasília, DF. Disponível em: <http://www.mma.gov.br/publicacoes/>
- Ferreira, B.P. & Maida M. (2006). Monitoramento dos recifes de coral do Brasil: situação atual e perspectivas. Brasília: MMA (Environmental Ministry)/SBF.
- Ferreira, C. E. L., Floeter, S. R., Gasparini, J. L., Ferreira, B. P., & Joyeux, J. C. (2004). Trophic structure patterns of Brazilian reef fishes: a latitudinal comparison. *Journal of Biogeography*, 31(7), 1093-1106.
- Flynn, R. L., & Forrester, G. E. (2019). Boat anchoring contributes substantially to coral reef degradation in the British Virgin Islands. *PeerJ*, 7, e7010.
- Freeman, L. A., Kleypas, J. A., & Miller, A. J. (2013). Coral reef habitat response to climate change scenarios. *PloS one*, 8(12), e82404.
- Garcia, T. M., Cascon, H., & Franklin-Junior, W. (2008). Macrofauna associated with branching fire coral. *Thalassas*, 24(1), 11-19.

- Garcia, T. M., Matthews-Cascon, H., & Franklin-Junior, W. (2009). *Millepora alcicornis* (Cnidaria: Hydrozoa) as substrate for benthic fauna. *Brazilian Journal of Oceanography*, 57(2), 153-155.
- González-Rivero, M., Harborne, A. R., Herrera-Reveles, A., Bozec, Y. M., Rogers, A., Friedman, A. & Hoegh-Guldberg, O. (2017). Linking fishes to multiple metrics of coral reef structural complexity using three-dimensional technology. *Scientific reports*, 7(1), 13965.
- Graham, N. A. J., & Nash, K. L. (2013). The importance of structural complexity in coral reef ecosystems. *Coral Reefs*, 32(2), 315-326.
- Graham, N. A., McClanahan, T. R., MacNeil, M. A., Wilson, S. K., Cinner, J. E., Huchery, C., & Holmes, T. H. (2017). Human disruption of coral reef trophic structure. *Current Biology*, 27(2), 231-236.
- Green, E. P., Mumby, P. J., Edwards, A. J., & Clark, C. D. (1996). A review of remote sensing for the assessment and management of tropical coastal resources. *Coastal management*, 24(1), 1-40.
- Green, E. P., Mumby, P. J., Edwards, A. J., & Clark, C. D. (2000). *Remote Sensing: Handbook for Tropical Coastal Management*. United Nations Educational, Scientific and Cultural Organization (UNESCO).
- Halpern, B. S., Walbridge, S., Selkoe, K. A., Kappel, C. V., Micheli, F., D'agrosa, C. & Fujita, R. (2008). A global map of human impact on marine ecosystems. *Science*, 319(5865), 948-952.
- Henry, L. A., Davies, A. J., & Roberts, J. M. (2010). Beta diversity of cold-water coral reef communities off western Scotland. *Coral Reefs*, 29(2), 427-436.
- Henry, L. A., Moreno Navas, J., & Roberts, J. M. (2013). Multi-scale interactions between local hydrography, seabed topography, and community assembly on cold-water coral reefs. *Biogeosciences*, 10(4), 2737-2746.
- Hughes, T. P., Rodrigues, M. J., Bellwood, D. R., Ceccarelli, D., Hoegh-Guldberg, O., McCook, L., Moltschaniwskyj, N., Pratchett, M. S., Steneck, R. S., & Willis, B. (2007). Phase Shifts, Herbivory, and the Resilience of Coral Reefs to Climate Change. *Current Biology* 17(4): 360–65. doi:10.1016/j.cub.2006.12.049.
- Instituto Chico Mendes de Conservação a Biodiversidade – ICMBio, 2012. Plano de Manejo da APA Costa dos Corais. Tamandaré-PE, 1, 74p. Available online: http://www.icmbio.gov.br/apacostadoscorais/images/stories/plano_de_manejo/PM_APACC_2013_JANEIRO.pdf.
- Jameson, S. C., Tupper, M. H., & Ridley, J. M. (2002). The three screen doors: can marine “protected” areas be effective?. *Marine Pollution Bulletin*, 44(11), 1177-1183.
- Kohler, K. E., & Gill, S. M. (2006). Coral Point Count with Excel extensions (CPCe): A Visual Basic program for the determination of coral and substrate coverage using random point count methodology. *Computers & Geosciences*, 32(9), 1259-1269.
- Laborel, J., 1969. Madreporaires et hydrocoralliaires recifaux des cotes Bresiliennes. Systematique, ecologie repartition verticale et geographique. Results Scientifique du Campagne de Calypso, 9(25), 171-229.

- Lai, S., Loke, L. H., Hilton, M. J., Bouma, T. J., & Todd, P. A. (2015). The effects of urbanisation on coastal habitats and the potential for ecological engineering: A Singapore case study. *Ocean & Coastal Management*, 103, 78-85.
- Leão, Z. M. A. N.; Kikuchi, R. K. P. & Testa, V. (2003). Corals and coral reefs of Brazil. In: *Latin American Coral Reefs*, ed. J. Cortés. Elsevier, Amsterdam, pp. 9-52.
- Ledlie, M. H., Graham, N. A. J., Bythell, J. C., Wilson, S. K., Jennings, S., Polunin, N. V., & Hardcastle, J. (2007). Phase shifts and the role of herbivory in the resilience of coral reefs. *Coral Reefs*, 26(3), 641-653.
- Lewis, J. B. (2006). Biology and ecology of the hydrocoral *Millepora* on coral reefs. *Advances in Marine Biology*, 50, 1-55.
- Lundblad, E. R., Wright, D. J., Miller, J., Larkin, E. M., Rinehart, R., Naar, D. F., Donahue, B. T., Anderson, S. M. & Battista, T. (2006). A benthic terrain classification scheme for American Samoa. *Marine Geodesy*, 29(2), 89-111.
- Macedo, E.C., 2009. Um ensaio sobre a sedimentação e suas implicações ecológicas nos recifes costeiros da baía de Tamandaré/PE. Recife, Pernambuco: Universidade Federal de Pernambuco (Federal University of Pernambuco), Master's thesis, 144p.
- Magris, R. A., Treml, E. A., Pressey, R. L., & Weeks, R. (2016). Integrating multiple species connectivity and habitat quality into conservation planning for coral reefs. *Ecography*, 39(7), 649-664.
- Maida, M. & Ferreira, B. P. (1997), Coral Reefs of Brazil: Overview and Field Guide. Proc. 8th Int. Coral Reef Symp., Panamá, pp. 263-274
- McClanahan, T. R., Nugues, M., & Mwachireya, S. (1994). Fish and sea urchin herbivory and competition in Kenyan coral reef lagoons: the role of reef management. *Journal of Experimental Marine Biology and Ecology*, 184(2), 237-254.
- McManus, L. C., Watson, J. R., Vasconcelos, V. V., & Levin, S. A. (2019). Stability and recovery of coral-algae systems: the importance of recruitment seasonality and grazing influence. *Theoretical Ecology*, 12(1), 61-72.
- Merow, C., Smith, M. J., & Silander Jr, J. A. (2013). A practical guide to MaxEnt for modeling species' distributions: what it does, and why inputs and settings matter. *Ecography*, 36(10), 1058-1069.
- Pawar, S., Koo, M. S., Kelley, C., Ahmed, M. F., Chaudhuri, S., & Sarkar, S. (2007). Conservation assessment and prioritization of areas in Northeast India: priorities for amphibians and reptiles. *Biological Conservation*, 136(3), 346-361.
- Phillips, S. J., & Dudík, M. (2008). Modeling of species distributions with Maxent: new extensions and a comprehensive evaluation. *Ecography*, 31(2), 161-175.
- Phillips, S. J., Dudík, M., Schapire, R. E. [Internet] Maxent software for modeling species niches and distributions (Version 3.4.1). Available from url: http://biodiversityinformatics.amnh.org/open_source/maxent/. Accessed on 2019-10-1.
- Pittman, S. J., & Brown, K. A. (2011). Multi-scale approach for predicting fish species distributions across coral reef seascapes. *PloS one*, 6(5), e20583.

- Pittman, S. J., Christensen, J. D., Caldow, C., Menza, C., & Monaco, M. E. (2007). Predictive mapping of fish species richness across shallow-water seascapes in the Caribbean. *Ecological modelling*, 204(1-2), 9-21.
- Pittman, S. J., Kneib, R., Simenstad, C., & Nagelkerken, I. (2011). Seascape ecology: application of landscape ecology to the marine environment. *Mar. Ecol. Prog. Ser.*, 427, 187-302.
- Poulos, D. E., Gallen, C., Davis, T., Booth, D. J., & Harasti, D. (2016). Distribution and spatial modelling of a soft coral habitat in the Port Stephens–Great Lakes Marine Park: implications for management. *Marine and Freshwater Research*, 67(2), 256-265.
- Radosavljevic, A., & Anderson, R. P. (2014). Making better Maxent models of species distributions: complexity, overfitting and evaluation. *Journal of biogeography*, 41(4), 629-643.
- Reshitnyk, L., Costa, M., Robinson, C., & Dearden, P. (2014). Evaluation of WorldView-2 and acoustic remote sensing for mapping benthic habitats in temperate coastal Pacific waters. *Remote Sensing of Environment*, 153, 7-23.
- Roberts, C. M. (1995). Effects of fishing on the ecosystem structure of coral reefs. *Conservation biology*, 9(5), 988-995.
- Rodríguez, L., López, C., Casado-Amezua, P., Ruiz-Ramos, D. V., Martínez, B., Banaszak, A., Tuya, F., García-Fernández, A. & Hernández, M. (2019). Genetic relationships of the hydrocoral *Millepora alcicornis* and its symbionts within and between locations across the Atlantic. *Coral Reefs*, 38(2), 255-268.
- Roelfsema, C. M., & Phinn, S. R. (2010). Integrating field data with high spatial resolution multispectral satellite imagery for calibration and validation of coral reef benthic community maps. *Journal of Applied Remote Sensing*, 4(1), 043527.
- Roelfsema, C., Lyons, M., Dunbabin, M., Kovacs, E. M., & Phinn, S. (2015). Integrating field survey data with satellite image data to improve shallow water seagrass maps: the role of AUV and snorkeller surveys?. *Remote Sensing Letters*, 6(2), 135-144.
- Sappington, J. M., Longshore, K. M., & Thompson, D. B. (2007). Quantifying landscape ruggedness for animal habitat analysis: a case study using bighorn sheep in the Mojave Desert. *The Journal of wildlife management*, 71(5), 1419-1426
- Secomandi, M., Owen, M. J., Jones, E., Terente, V., & Comrie, R. (2016). Application of the Bathymetric Position Index Method (BPI) for the purpose of defining a reference seabed level for cable burial.
- Selig, E. R., Turner, W. R., Troëng, S., Wallace, B. P., Halpern, B. S., Kaschner, K., Lasceller, B. G., Carpenter, K. E. & Mittermeier, R. A. (2014). Global priorities for marine biodiversity conservation. *PloS one*, 9(1), e82898.
- Silveira, C.B.L.; Strenzel, G.M.; Maida, M., Araújo T.C.M.; Ferreira, B.P. (2019). Multi Resolution Satellite-Derived Bathymetry in Shallow Coral Reefs: Improving linear algorithms with geographical analysis. *Journal of Coastal Research (in press)*.
- Silveira, M. F. D. (2018). *Pesca artesanal e manejo: uma abordagem temporal comparativa em Tamandaré-PE* (Master's thesis, Universidade Federal de Pernambuco)

- Topor, Z. M., Rasher, D. B., Duffy, J. E., & Brandl, S. J. (2019). Marine protected areas enhance coral reef functioning by promoting fish biodiversity. *Conservation Letters*, e12638.
- Tratalos, J. A., & Austin, T. J. (2001). Impacts of recreational SCUBA diving on coral communities of the Caribbean island of Grand Cayman. *Biological Conservation*, 102(1), 67-75.
- Vanhellemont, Q., & Ruddick, K. (2016). Acolite for Sentinel-2: Aquatic applications of MSI imagery. In *Proceedings of the 2016 ESA Living Planet Symposium, Prague, Czech Republic* (pp. 9-13).
- Vanhellemont, Q., & Ruddick, K. (2018). Atmospheric correction of metre-scale optical satellite data for inland and coastal water applications. *Remote Sensing of Environment*, 216, 586-597.
- Walbridge, S., Slocum, N., Pobuda, M., & Wright, D. (2018). Unified geomorphological analysis workflows with Benthic Terrain Modeler. *Geosciences*, 8(3), 94.
- Wedding, L. M., Friedlander, A. M., McGranaghan, M., Yost, R. S., & Monaco, M. E. (2008). Using bathymetric lidar to define nearshore benthic habitat complexity: Implications for management of reef fish assemblages in Hawaii. *Remote Sensing of Environment*, 112(11), 4159-4165.
- Wilkinson, C., & Salvat, B. (2012). Coastal resource degradation in the tropics: does the tragedy of the commons apply for coral reefs, mangrove forests and seagrass beds. *Marine Pollution Bulletin*, 64(6), 1096-1105.
- Wilson, M. F., O'Connell, B., Brown, C., Guinan, J. C., & Grehan, A. J. (2007). Multiscale terrain analysis of multibeam bathymetry data for habitat mapping on the continental slope. *Marine Geodesy*, 30(1-2), 3-35.
- Wirtz, P., & Zilberberg, C. (2019). Fire! The spread of the Caribbean fire coral *Millepora alcicornis* in the Eastern Atlantic. *bioRxiv*, 519041.
- Yamamoto, K. H., Powell, R. L., Anderson, S., & Sutton, P. C. (2012). Using LiDAR to quantify topographic and bathymetric details for sea turtle nesting beaches in Florida. *Remote Sensing of Environment*, 125, 125-133.
- Zaneveld, J. R., Burkepile, D. E., Shantz, A. A., Pritchard, C. E., McMinds, R., Payet, J. P. & Fuchs, C. (2016). Overfishing and nutrient pollution interact with temperature to disrupt coral reefs down to microbial scales. *Nature communications*, 7, 11833.

3.7 Supplementary Material

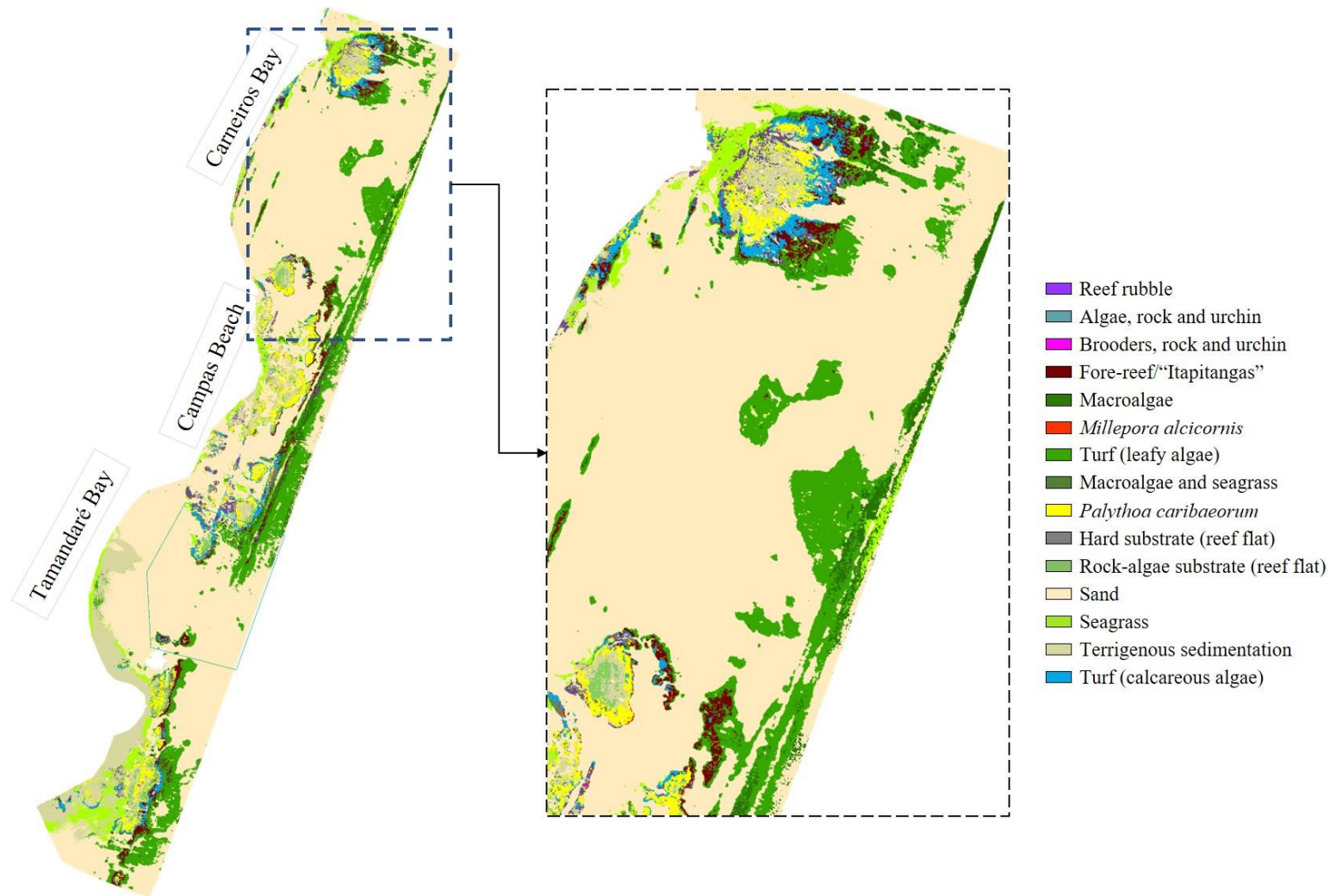


Fig S 1 Habitat map of the coastal reefs of Tamandaré – Pernambuco. The hollow blue polygon shows the location of the no-take zone. The dotted square shows a close-up of the reefs in Carneiros Bay, in the North of the study area.

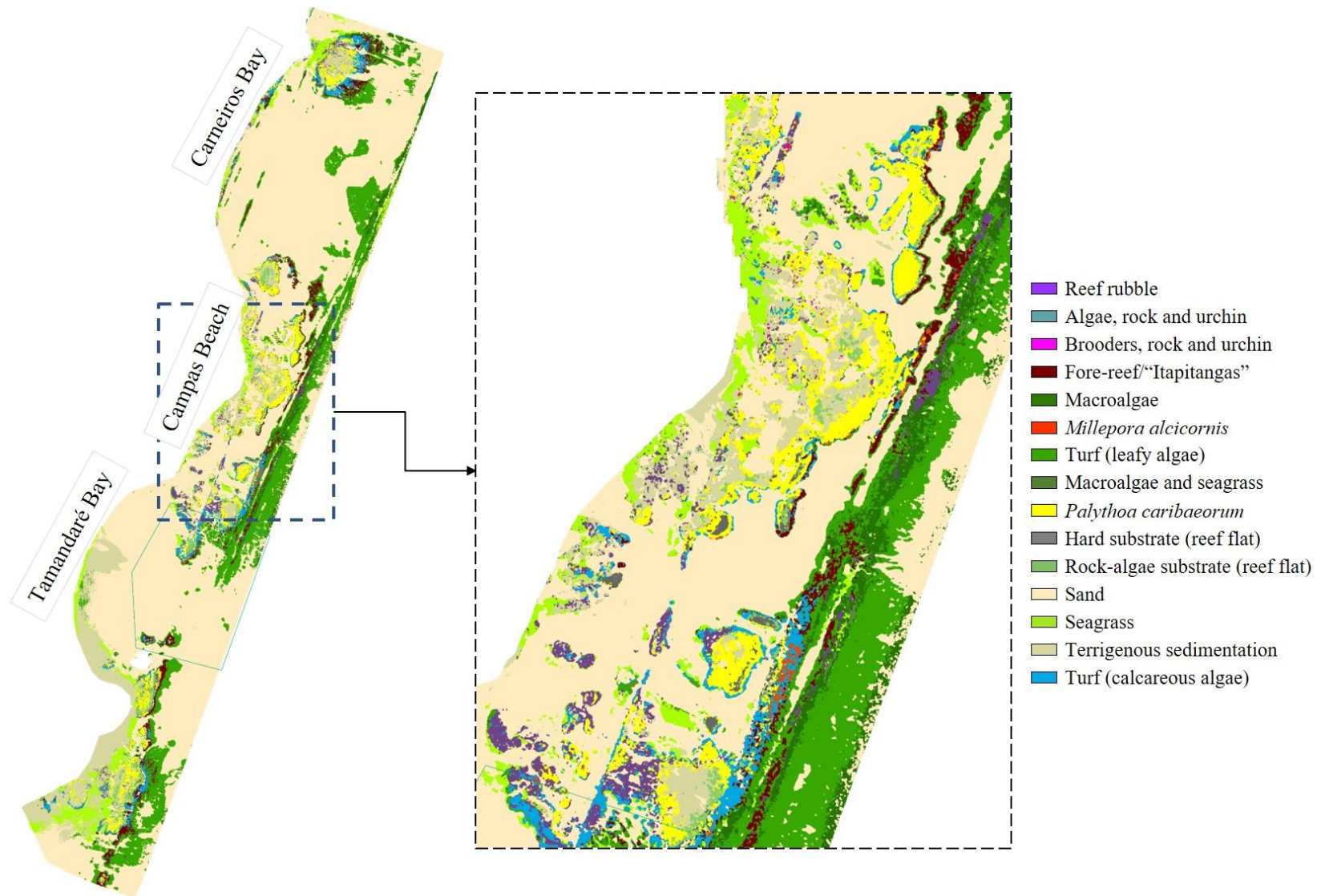


Fig S 2 Habitat map of the coastal reefs of Tamandaré – Pernambuco. The hollow blue polygon shows the location of the no-take zone. The dotted square shows a close-up of the reefs in Campas Beach, in the central region of the study area.

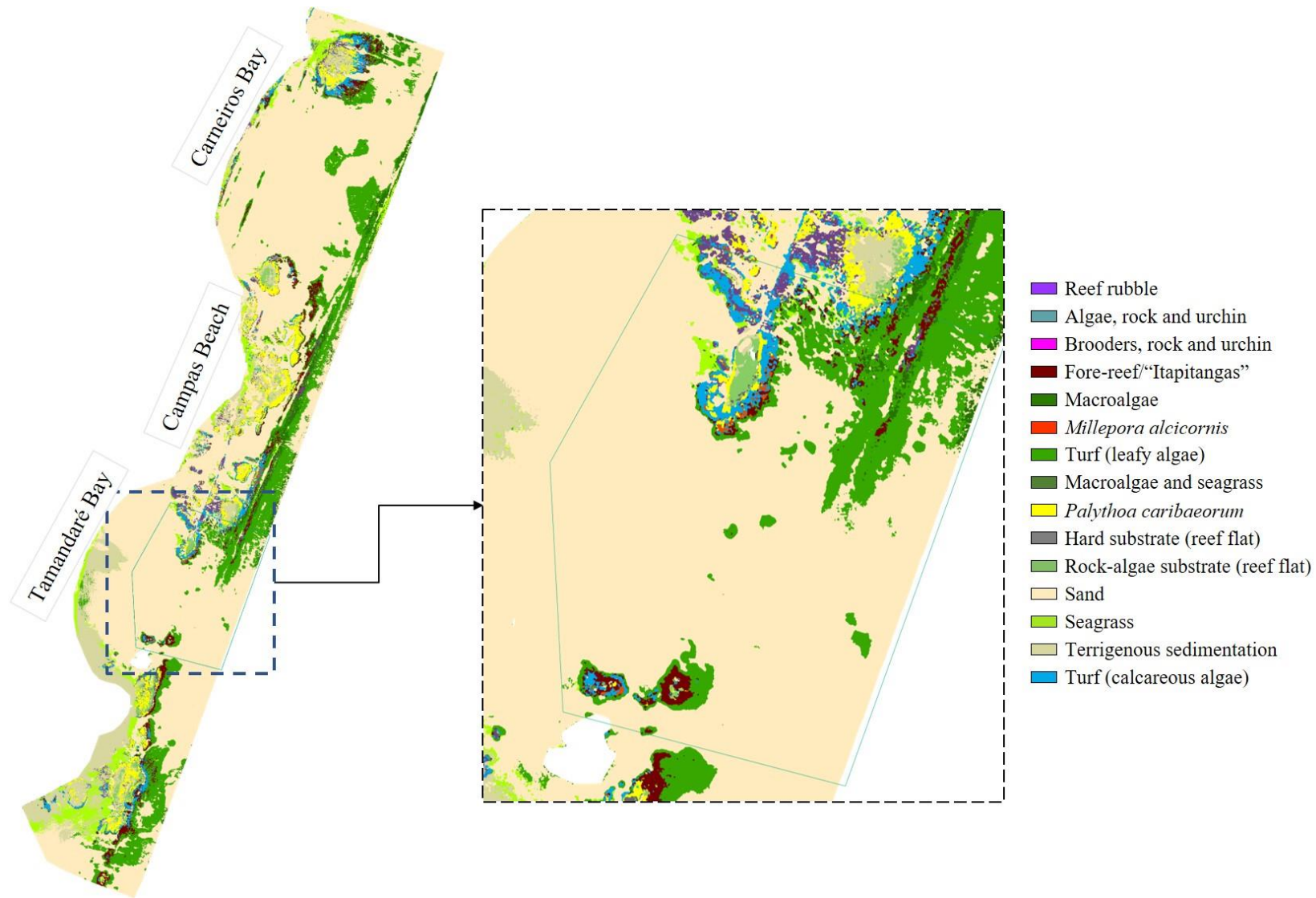








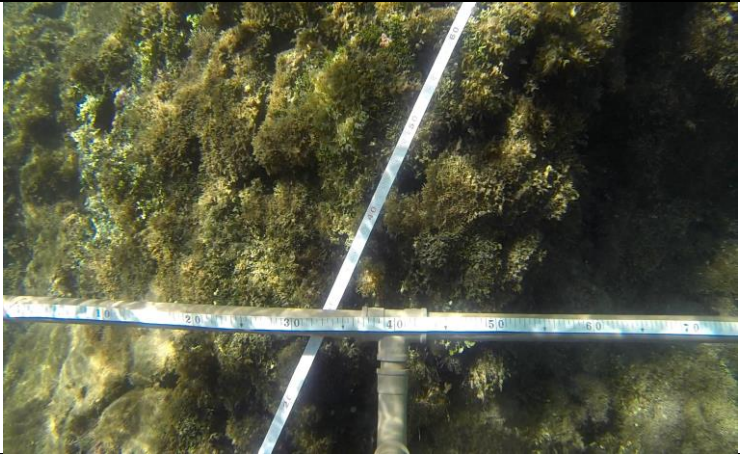

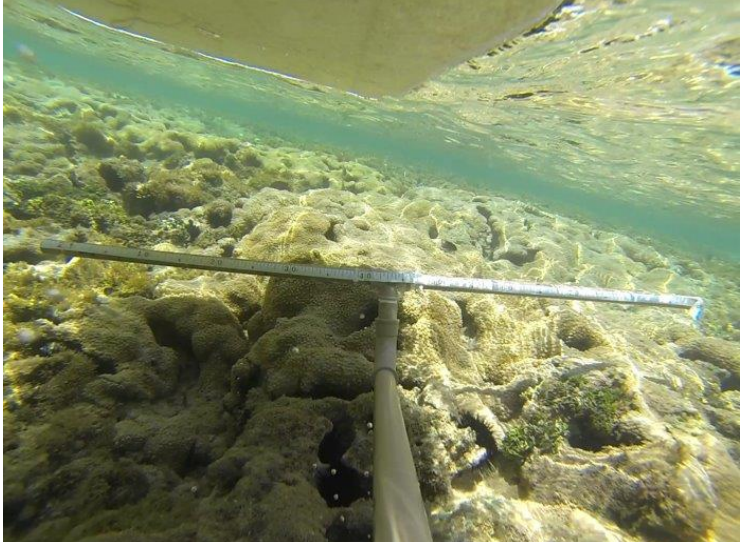
Fig S 3 Habitat map of the coastal reefs of Tamandaré – Pernambuco. The hollow blue polygon shows the location of the no-take zone. The dotted square shows a close-up of the reefs in Campas Beach, in the central region of the study area.




Example photos of the benthic covers found in the coastal reefs of Tamandaré



Below we present the 14 benthic covers found in the coral reefs of the study area, pictured by representative video-frames taken during field survey:

	<p>Fig S4 Class 1: “Reef rubble” Substrate cover characterized by gravel, usually covered by turf algae and/or filamentous algae. Fragmented parts of the reef.</p>
	<p>Fig S5 Class 2: “Algae, rock and urchin” Consolidated substrate with regions showing bare rock and encrusting coralline algae. Turf algae is also present. High density of sea-urchin (<i>Echinometra lucunter</i>).</p>
	<p>Fig S6 Class 3: “Coral, rock and urchin” Region with high densities of (mainly) brooding corals such as <i>Porites astreoides</i>, <i>Agaricia humilis</i> and <i>Favia gravida</i>. High density of sea-urchin (<i>E. lucunter</i>). Large areas with bare rock and encrusting coralline algae.</p>

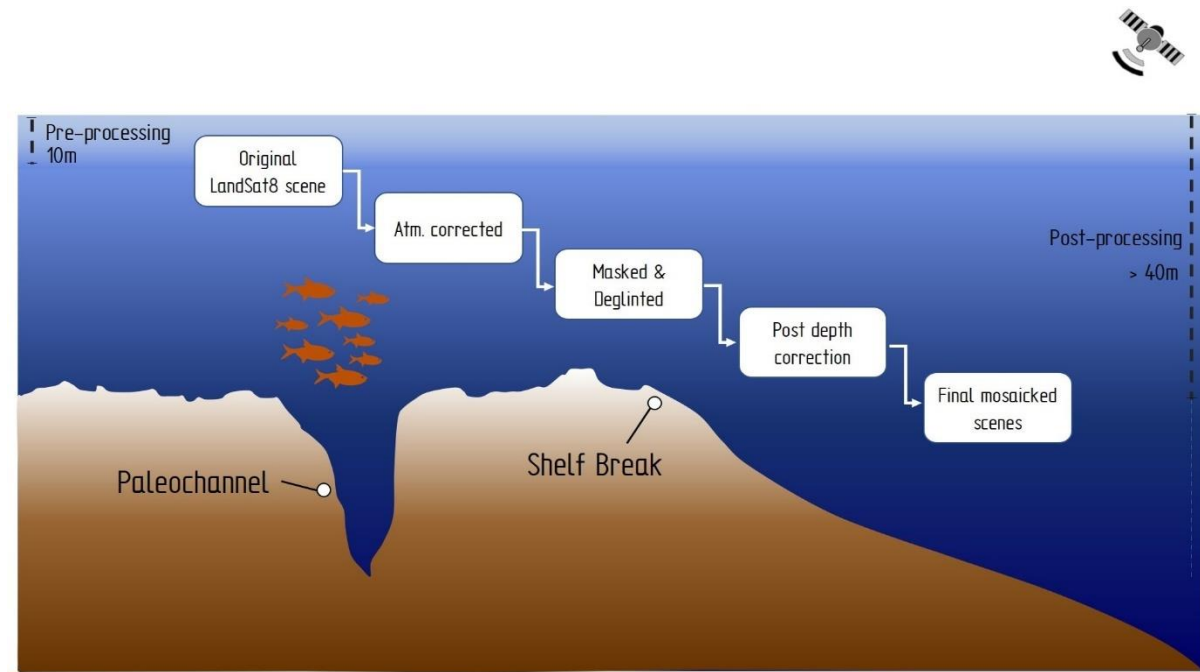
	<p>Fig S7 Class 4: “Fore reef/Itapitangas”</p> <p>Areas of high wave energy, mostly on the third reef line in the study area. Isolated rocks, covered by <i>Palythoa caribaeorum</i> on the base and green algae, encrusting coralline algae on the top. It is also possible to observe <i>Millepora alcicornis</i> on the top, usually showing a flat structure.</p>
	<p>Fig S8 Class 5: “Macroalgae”</p> <p>High density of brown algae, mostly <i>Sargassum</i> spp. and <i>Dycliota</i> spp.</p>
	<p>Fig S9 Class 6: “<i>Millepora alcicornis</i>”</p> <p>Areas mostly covered by colonies of the coral <i>Millepora alcicornis</i>.</p>

	<p>Fig S10 Class 7: “Turf algae” Multi-specific assembly of various algae (e.g. filamentous algae, <i>Caulerpa</i> spp., <i>Halimeda</i> spp., juvenile macroalgae) with a typical maximum height of 2 cm.</p>
	<p>Fig S11 Class 8: “Macroalgae and seagrass” Areas of seagrass (<i>Halodule wrightii</i>) with associated macroalgae covering most of the substrate.</p>
	<p>Fig S12 Class 9: “<i>Palythoa caribaeorum</i>” Consolidated substrate, mostly reef flats, covered by <i>Palythoa caribaeorum</i></p>

	<p>Fig S13 Class 10: “Rock” Consolidated substrate (<i>i.e.</i> calcareous rock), mostly emerged reefs. Turf algae and <i>Palythoa caribaeorum</i> may also be observed covering the substrate</p>
	<p>Fig S14 Class 11: “Rock-algae flat” Consolidated substrate (<i>i.e.</i> calcareous rock), mostly emerged reefs covered by turf and filamentous algae.</p>
	<p>Fig S15 Class 12: “Sand” Unconsolidated substrate: sand and in smaller proportions, gravel. Usually found surrounding each reef structure throughout the study area</p>

	<p>Fig S16 Class 13: “Seagrass”</p> <p>Seagrass beds mostly comprised by <i>Halodule wrightii</i>. The species <i>Halophila decipiens</i> was also registered in the study region.</p>
	<p>Fig S17 Class 15: “Calcareous turf”</p> <p>Multi-specific assemblage of articulated calcareous algae (e.g. <i>Jania</i> spp., <i>Amphiroa</i> spp.). It is a dominant substratum in many parts of the reefs, notably on the reef crests.</p>

4 PUSHING SATELLITE IMAGERY TO NEW DEPTHS: seascape feature mapping in a tropical shelf



4.1 Abstract

The Brazilian Northeast Continental shelf harbours a variety of geo and benthic habitats, including coral and algal reefs, beachrocks, mesophotic reefs, shelf valleys, canyons, and paleochannels. Due to the low sediment budget that reaches this platform, it is classified as a “sediment-starved shelf”. In spite of the intense use, there is a lack of studies directed to habitat mapping in many tropical shelves, mainly due to the high costs associated with surveying large marine areas with traditional techniques. Thus, this study tested the applicability of Landsat-8 (L8) imagery to detect bottom features in the Brazilian Northeast Continental Shelf. Nine scenes were tested and processed following the same steps: radiometric and atmospheric correction, masking, glint removal, water column correction and individual image adjustments. Out of the nine, two were deemed the best to portray targeted features. We detected 14 paleochannels in a 9700 km² area, as well as the shelf break. Bathymetric field data were used to validate a set of the identified features. We were able to offer a detailed view of submerged valleys including previously unmapped channels, and the shelf break. Mapped features were distributed up to areas deeper than 100 meters using free of charge, medium resolution satellite imagery. Some of these channels are known fishing grounds and fish spawning aggregation areas, making them priority zones for the application of management and monitoring efforts. To the best of our knowledge, this represents the first study applying Landsat imagery to map paleochannels in submerged areas, and most importantly, in areas deeper than 30 meters. We believe this research can help focusing future mapping efforts and may advance the general knowledge of the area.

Keywords: Landsat 8. Satellite imagery. Continental shelf. Ocean. Paleochannels. Shelf valleys.

4.2 Introduction

The Brazilian Continental Shelf and its water column have been studied for almost six decades (*i.e.* Emílsson, 1961; Martins and Coutinho, 1981). Researches describing the geological framework (Ponte and Asmus, 1978; Ojeda, 1982; Cainelli and Mohriak, 1999; Mahiques *et al.*, 2010), structure, hydrodynamics (*e.g.* Bittencourt *et al.*, 2002), and biological characteristics are extensive (*e.g.* Bastos *et al.*, 2015), but are mainly focused on the Southern, South-eastern, Eastern and Northern margins. There is a lack of studies directed to the tropical shelf, which includes the Northeast (NE) Continental Shelf (Vital *et al.*, 2010; Camargo *et al.*, 2015; Gomes *et al.*, 2016). This bias has been associated with the oligotrophic characteristics of the region, and to the low sediment budget that reaches this platform, which renders it a “sediment-starved shelf” (Vital, 2014). Diversely, this region has also been associated with a variety of geo and benthic habitats, including coral and algal reefs, beachrocks, shelf valleys, canyons, and paleochannels (Leao *et al.*, 2003; Ferreira and Maida, 2006; Gomes *et al.*, 2015; Camargo *et al.*, 2015; Fontes *et al.*, 2019).

Paleochannels are indicators of their margins’ evolutionary history (Conti and Furtado, 2009; Wang *et al.*, 2012), and thus can provide insights on sea-level changes, paleoclimate and oceanographic conditions. Most of the paleo-valleys are geologic vestiges of rivers that were in-land in previous periods (Vervoort and Annen, 2006). The paleochannels found on NE Continental Shelf have been linked to the Last Regressive Period (18000 years BP), when the presently submerged continental shelves were exposed to subaerial processes due to sea-level lowstands (approximately 120m lower than today) (Michelli *et al.*, 2001; Vital, 2014; Camargo *et al.*, 2015). During the following sea-level rise, most of these rivers were submerged and filled with sediments. On the NE Continental Shelf, due to the low capacity of rivers in the region (Knoppers *et al.*, 1999; Vital, 2014), some paleochannels remain unfilled, preserving an incision-like shape. These areas harbour a higher diverse of features, including mesophotic reefs (Camargo *et al.*, 2015) associated with increased biological activity (Baro *et al.*, 2011; Bourguignon *et al.*, 2018) and spawning aggregations (Ferreira *et al.*, 2017), making them important fishing grounds in an otherwise oligotrophic region.

The bottom topography and the continental shelf itself are currently investigated using a range of possible technologies (Harris *et al.*, 2013; Harris and Baker, 2012). In the shallow clear waters of the coastal zone and inner continental shelf, remote sensing based on satellite imagery has been widely applied (*e.g.* Silveira *et al.*, 2019; Andréfouët *et al.*, 2003; Eugenio *et al.*, 2017). Laser-light detection and ranging (LIDAR) is also an option for waters shallower

than 50 meters and with low turbidity, though budgetary restraints can limit its applicability (Su *et al.*, 2015). Single and multi-beam echosounders can survey areas of depths ranging from 10 to 2000 meters (Harris and Baker, 2012) and thus are frequently applied in the continental shelf. Considering the size of our study area, and the cost associated with field surveys (*i.e.* acoustic, sonar, video techniques), most bottom features in the deeper regions of the NE Continental Shelf remain unmapped.

This study aims to test the possibility of using satellite imagery to detect bottom features of the continental shelf. Most specifically, we intend to use Landsat-8 OLI processed scenes to map paleochannels that have been reported to occur throughout the external NE Brazilian margin. This technique is budget-friendly, as Landsat's database can be downloaded free of charge (USGS). Additionally, currently available datasets are able to cover the entire tropical continental shelf. Satellite imagery are rarely used in areas deeper than 30 meters, due to limited light penetration in water (Gao, 2009; Harris and Baker, 2012). Although paleochannels may be in waters exceeding this limit, we believe that due to the targeted area's typical characteristics (*i.e.* relatively shallow, low sediment influx) some features may be registered post image processing. Once proven successful, this methodology may be an invaluable tool to help managing ecologically and geologically important areas.

4.3 Methods

4.3.1 Study Area

The study area is located on the Brazilian Northeast Continental Shelf, between Pernambuco and Alagoas states (35°37'24''W - 34°30'06''W; 9°32'49''S - 7°55'09''S). Within its 9700 km², an International Long-Term Ecological Research site, PELD-Tams that include MPAs such as Costa dos Corais Marine Protected Area (MPA), Guadalupe Environmental Protected Area, and the recently declared Serrambi MPA, (Figure 1). These areas were created in an effort to promote the sustainable use and conservation of the region's marine biodiversity and seascape, and thus maintain the socio-economic and ecological status of the area.

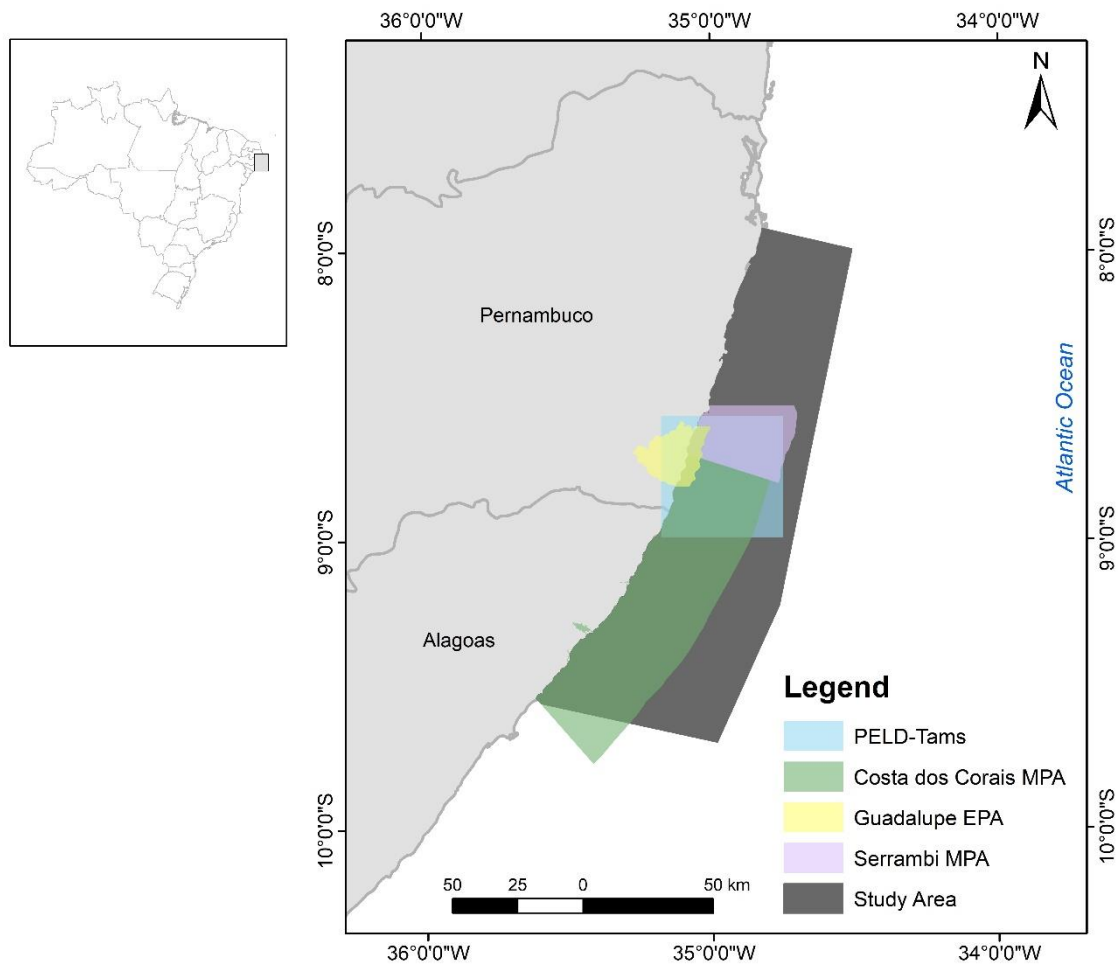


Figure 1 Study area (grey polygon), located between the Brazilian states of Pernambuco and Alagoas and the Environmental Protected Areas in the region: Long Term Ecological Research Site (PELD) – Tams (in blue); Costa dos Corais Marine Protected Area (in green); Guadalupe Environmental Protected Area (in yellow); and Serrambi Marine Protected Area (in light purple)

The Brazilian Continental Shelf is a tectonically passive margin (Martins and Coutinho, 1981). The Northeast region is relatively shallow (shelf breaks at 40 to 80 meters of depth), and flat (Martins and Coutinho, 1981; Vital *et al.*, 2010), reaching a maximum width of approximately 40 km. On the inner part of the shelf, closer to the continent, the most prominent features are sandstone reefs (beach rocks and coral-algal reefs) that occur in lines parallel to the coast (Maida and Ferreira, 1997; Ferreira and Maida, 2006). The presence of incised valleys, paleochannels and canyons associated with submerged reefs can be observed throughout the medium and outer part of the shelf (Camargo *et al.*, 2007; Vital, 2014; Camargo *et al.*, 2015; Fontes *et al.*, 2019). The area is oligotrophic and most of its sediment cover are biogenic carbonates (Vital, 2014; Assis *et al.*, 2016). Due to the low sediment budget and reduced continental sedimentation, this area is typically considered a sediment starved shelf (Vital, 2014; Camargo *et al.*, 2015).

However, habitat diversity is reflected by a diversity of species that sustain many fisheries typologies (Frédou *et al.*, 2006) with higher catches associated to higher feature complexity (Olavo *et al.*, 2011). The outer shelf in particular, where channels meet the shelf break, have been declared of environmental and ecological importance by the Convention on Biological diversity (EBSAS in CDB) (Druel, 2012; Bax *et al.*, 2016).

4.3.2 Image Processing

We selected nine Landsat-8 OLI scenes (2015-2019) with relatively low cloud cover in the study area to try and visualize the continental shelf (Table 1). Each scene was submitted to the following image processing steps:

Table 1 Details of the Landsat-8 OLI scenes used in this study. The table exhibits the following information: Scene ID, date of scene acquisition, total cloud cover (%), sun azimuth, sun elevation, and Earth-sun distance (astronomic unit).

Scene ID	Date YYYYMMDD	Cloud cov. (%)	Sun az.	Sun el.	Earth- sun dist.
LC82140662015311LGN01	2015-11-07	33.61	110.29	65.38	0.99
LC82140662016042LGN00	2016-02-11	9.14	102.87	58.47	0.99
LC82140662018223LGN00	2018-08-11	15.68	51.03	52.18	1.01
LC82140662016346LGN00	2016-12-11	15.57	122.66	60.86	0.98
LC82140662016202LGN00	2016-07-20	35.87	44.74	48.66	1.02
LC82140662018143LGN00	2018-05-23	12.18	42.51	50.05	1.01
LC82140662016298LGN00	2016-10-24	28.90	100.06	66.06	0.99
LC82140662016026LGN01	2016-01-26	27.62	111.76	58.07	0.98
LC82140662018319LGN00	2018-11-15	37.23	115.22	64.42	0.99

4.3.2.1 Atmospheric correction

Atmospheric and radiometric corrections were carried out to minimize the scattering and absorption effects caused by molecules in the atmosphere (De Keukelaere *et al.*, 2018). We used ATCOR II module in ERDAS IMAGINE software to produce the corrected datasets, using each scene's parameters as inputs.

4.3.2.2 Land masking

We manually defined a land mask that was applied to all atmospherically corrected datasets. Clouds, vessels, off-land constructions, piers, and coastal, saturated regions were also masked off the scene, to allow better visualisation of the targeted areas.

4.3.2.3 Sun-glint removal

Sun-glint removal (*i.e.* deglint) was carried out to minimize the effects of light reflection on sea surface. Sun-glint can cause the sea surface to appear very rough, preventing a good visualization of the bottom features. We followed the methodology proposed by Hedley *et al.* (2005) to deglint each visible band separately (*i.e.* coastal aerosol, blue, green and red), which were then stacked to produce each deglinted dataset.

4.3.2.4 Water Column Correction

Water column correction algorithms are applied to compensate for the confounding effects that varying depths have over underwater substratum (Green and Edwards, 2000). This additional step improves the accuracy of benthic mapping (*i.e.* Andréfouët *et al.*, 2003; Manessa *et al.*, 2016; Fritz *et al.*, 2017) and aids in the differentiation of each underwater habitat' spectra. We implemented water column correction by generating depth-invariant index (DII) of bottom type, as proposed by Green & Edwards (2000). For the present study, we selected a number of "sand" pixels in different depths to create the DII. Sand is usually the bottom type chosen for this type of correction since this substrate is easily recognizable even in the absence of field samples.

In this methodology, first, pairs of bands with good water penetration are selected. We considered all Landsat-8 OLI visible bands in this step, which totalled six band pairs: coastal aerosol/blue, coastal aerosol/green, coastal aerosol/red, blue/green, blue/red, green/red. After implementing the depth-invariant algorithm, we analysed each depth-corrected pair of bands of the datasets to verify its potential to map the bottom features. It was possible to verify that the pairs with the red band added provided no valuable information on the substrate. For each scene, the bands that were able to perceive the channels (*i.e.* 1: coastal aerosol/blue, 2: coastal aerosol/green, 3: blue/green) were stacked to produce a 3-band composite.

4.3.2.5 Individual Image Adjustments

We applied different image correction techniques and algorithms to try to reduce noise and amplify the differences between the valleys and other possible features. Contrast, light adjustments, low pass filtering and histogram editions were made in ArcMap 10.4 using the Image Processing and Spatial Analyst toolsets. In addition, we tested the Noise Reduction and

Radar Speckle Suppression filters in ERDAS Imagine 2014 to try to enhance the final mosaic of the area.

4.3.3 Ground Truth

Three bathymetric datasets were used to verify if the bottom features observed in the satellite imagery were indeed submerged valleys or paleochannels. Both datasets were collected using a single-beam echosounder coupled with GPS and sonar softwares.

Camargo *et al.* (2015) compiled and complemented a set of bathymetric data from two different projects (“Pro-Arribada – Reef Fishes Spawning Aggregations in Brazil” and “Mapping and Characterization of Emerged and Submerged Coral Reefs and Beachrocks at the Pernambuco Shore”) and researches (Michelli *et al.*, 2001 and Camargo *et al.*, 2007). The first surveys followed pre-set profiles from the coastline to the shelf break. Following field surveys focused efforts on the identified “Zieta Channel”, a well-known fishing ground for the artisanal fishers of the area. These latter field studies, from 2001 to 2015, resulted in 102.334 depth values.

In 2016 and 2018, separate field surveys were conducted (CMAR-II/PELD-TAMs), including more profiles using a Garmin GPSMAP 521 echosounder coupled with Furuno Network Sounder DFF. These surveys added important field data on two other channels, totalling 433.216 depth points (Fig 2). All depth values were interpolated using natural neighbours interpolation method to produce a final 10-meter resolution raster.

In addition, to confirm the location of the shelf break throughout the area, we overlaid vectorized isobaths from the official rasterized Nautical Chart produced by the Brazilian Navy, Chart number 01 “Costa e Ilhas ao Largo” (DHN, 2017) on top of our final map.

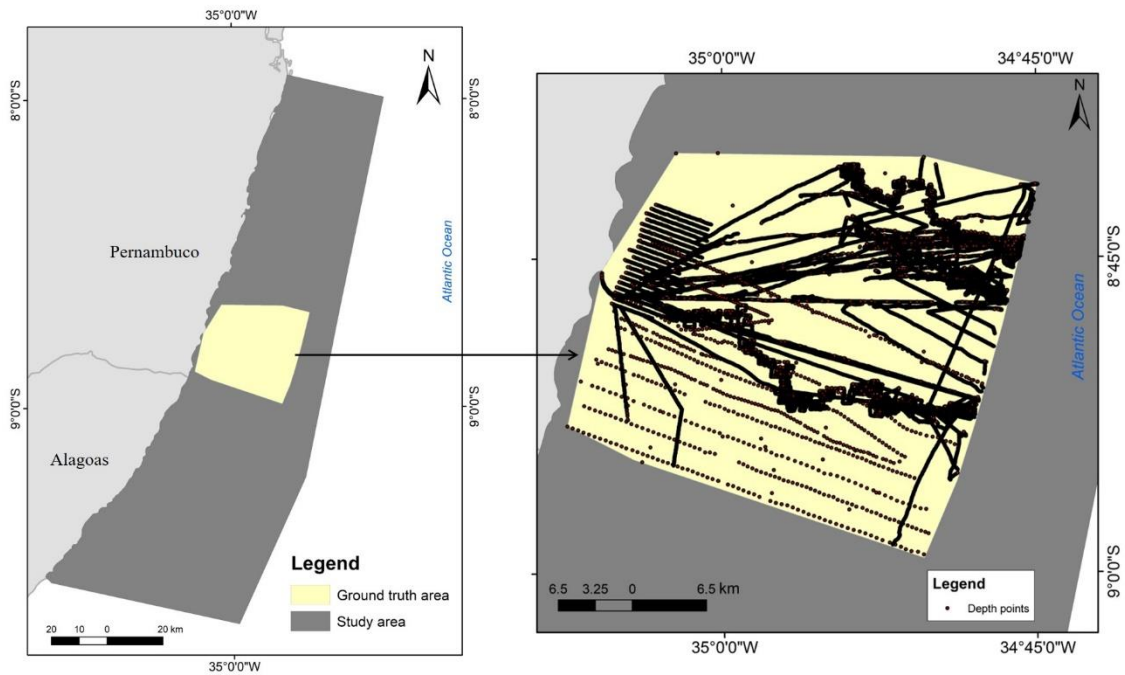


Figure 2 Ground truth points used to produce the bathymetric raster used to verify the true depth of the mapped features

4.4 Results

Out of the nine processed scenes, two were selected to produce a mosaic to picture the targeted features in the study area. Criteria was based on the best possible representation of the channels and shelf break, since one dataset was deemed best to represent the Northern area and another one for the Southern area (Table 2). Four scenes were not able to depict any bottom features, even though all imagery were subjected to the same processing techniques and methodologies.

The results of each processing step for the selected datasets are shown below.

4.4.1 Atmospheric Correction

Radiometric and atmospheric correction made in ATCOR2 module in ERDAS-Imagine software (Richter and Schlöpfer, 2013) enabled the visualization of some bottom features (Fig 3 and 4). On both scenes, it is possible to detect what is, apparently, the boundary between deep and shallow water at about 30 km and 41 km from the coastline on the Northern and Southern regions, respectively. From this border on (oceanwards), the satellite signal is lost due to the depth-limiting characteristics of light penetration. In addition, we can observe a great number of channel-like features on the continental shelf (Fig 3c and 4c). These results, and best imagery visual parameters were obtained using Histogram Equalize as stretch type (RGB 321) in ArcMap 10.4.

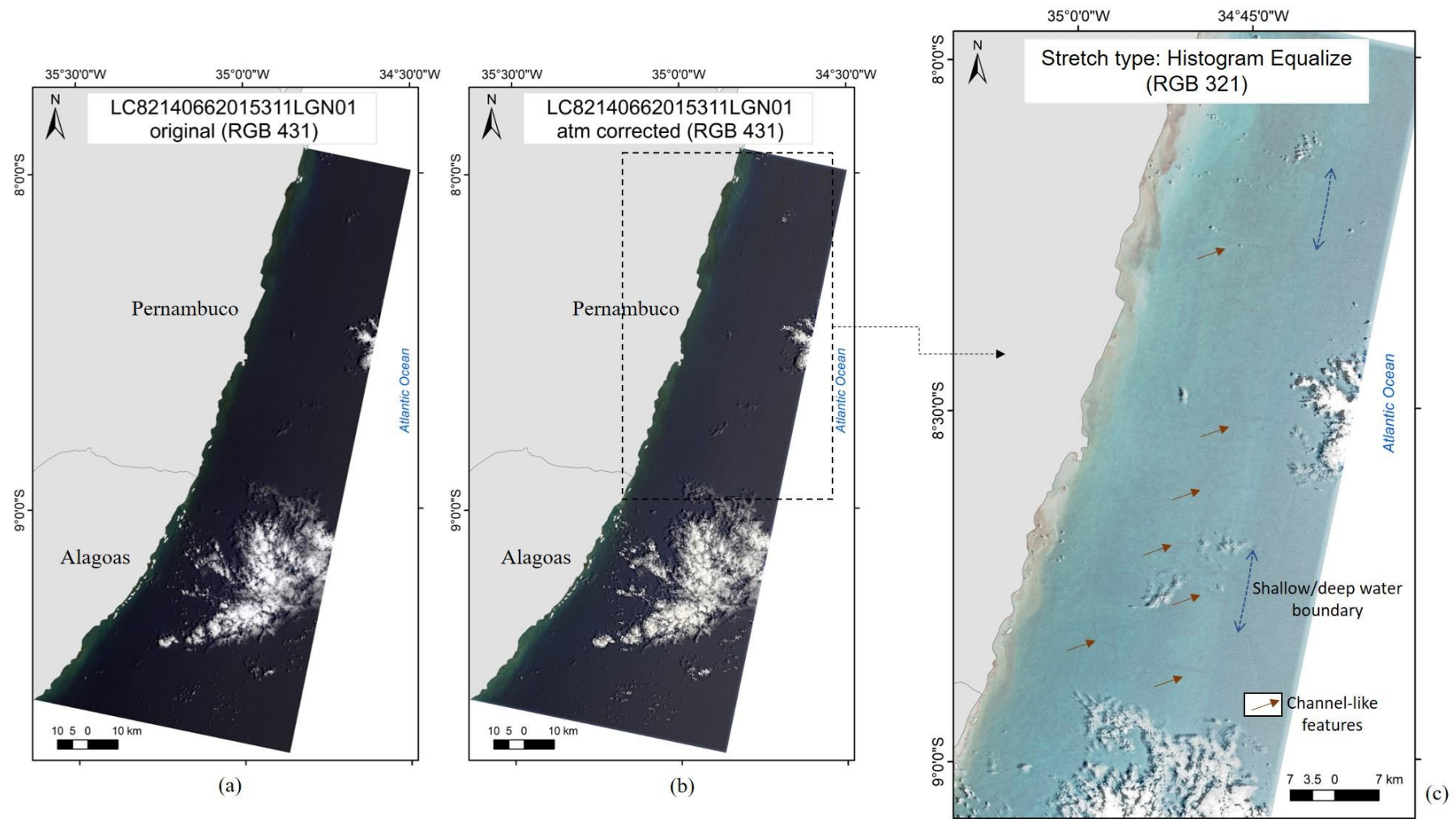


Figure 3 Atmospheric correction process for the Landsat-8 OLI image used for the Northern region. a) Original image, pre atmospheric correction; b) atmospherically corrected scene; c) histogram equalized, atmospherically corrected scene, RGB321 with arrows indicating possible shelf break and channel-like indentations on the bottom.

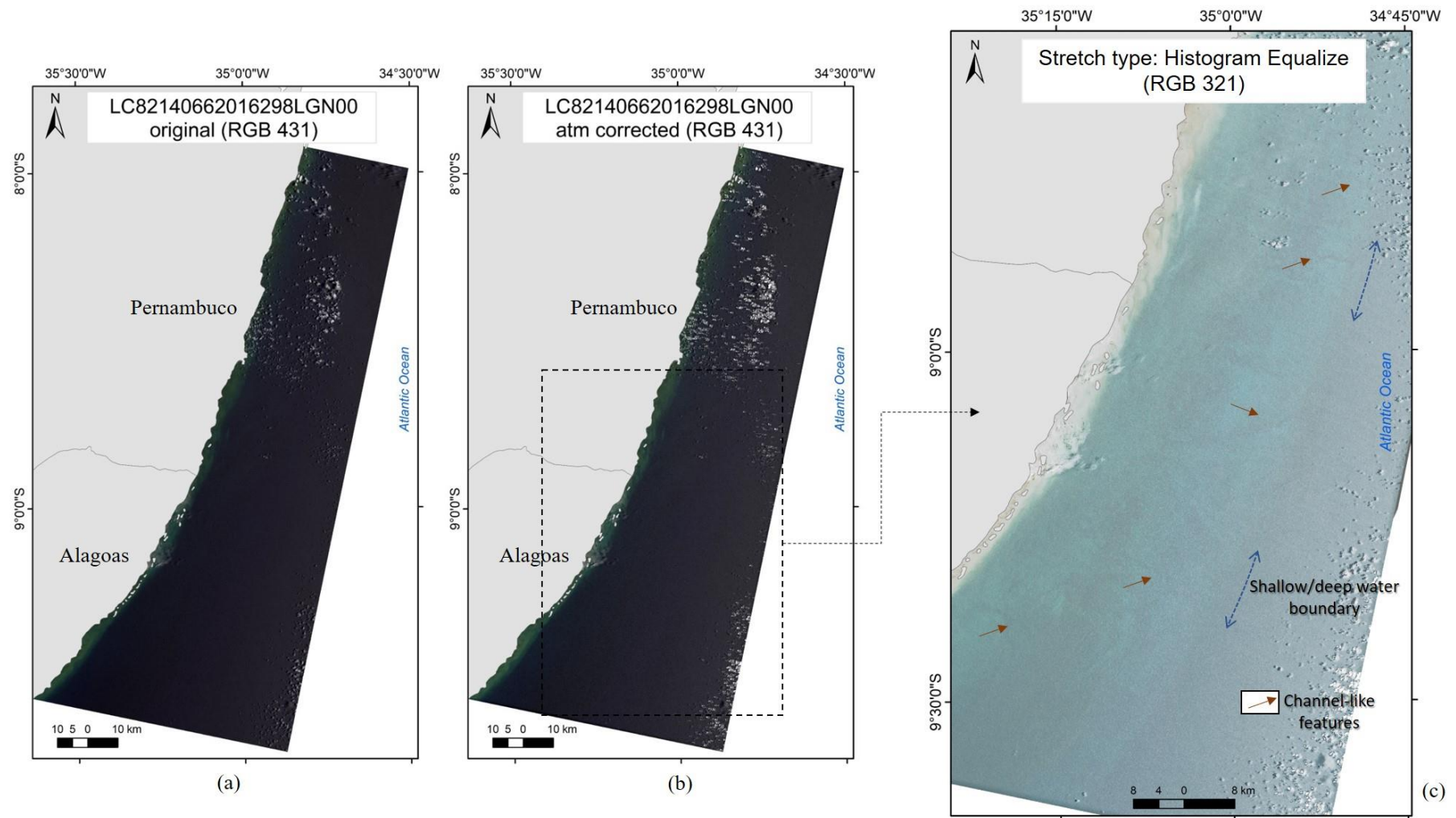


Figure 4 Atmospheric correction process for the Landsat-8 OLI image used for the Southern region. a) Original image, pre atmospheric correction; b) atmospherically corrected scene; c) histogram equalized, atmospherically corrected scene, RGB321 with arrows indicating possible shelf break and channel-like indentations on the bottom.

4.4.2 Masking and Sun-glnt Removal

The combination of masking out land and cloud pixels and glint removal significantly improved the visualization of the benthic features in both images. Using composites of the deglinted coastal aerosol, blue and green bands, we were able to easily identify eleven channel-like features on scene “LC82140662015311LGN01” (*i.e.* North) and three on scene “LC82140662016298LGN00” (*i.e.* South). The composites did not include the red band, since it showed no useful information on the water column or substrate. Both targeted features (*i.e.* channels and she shelf break) were visually enhanced and identifiable throughout the processed scenes (Fig 5).

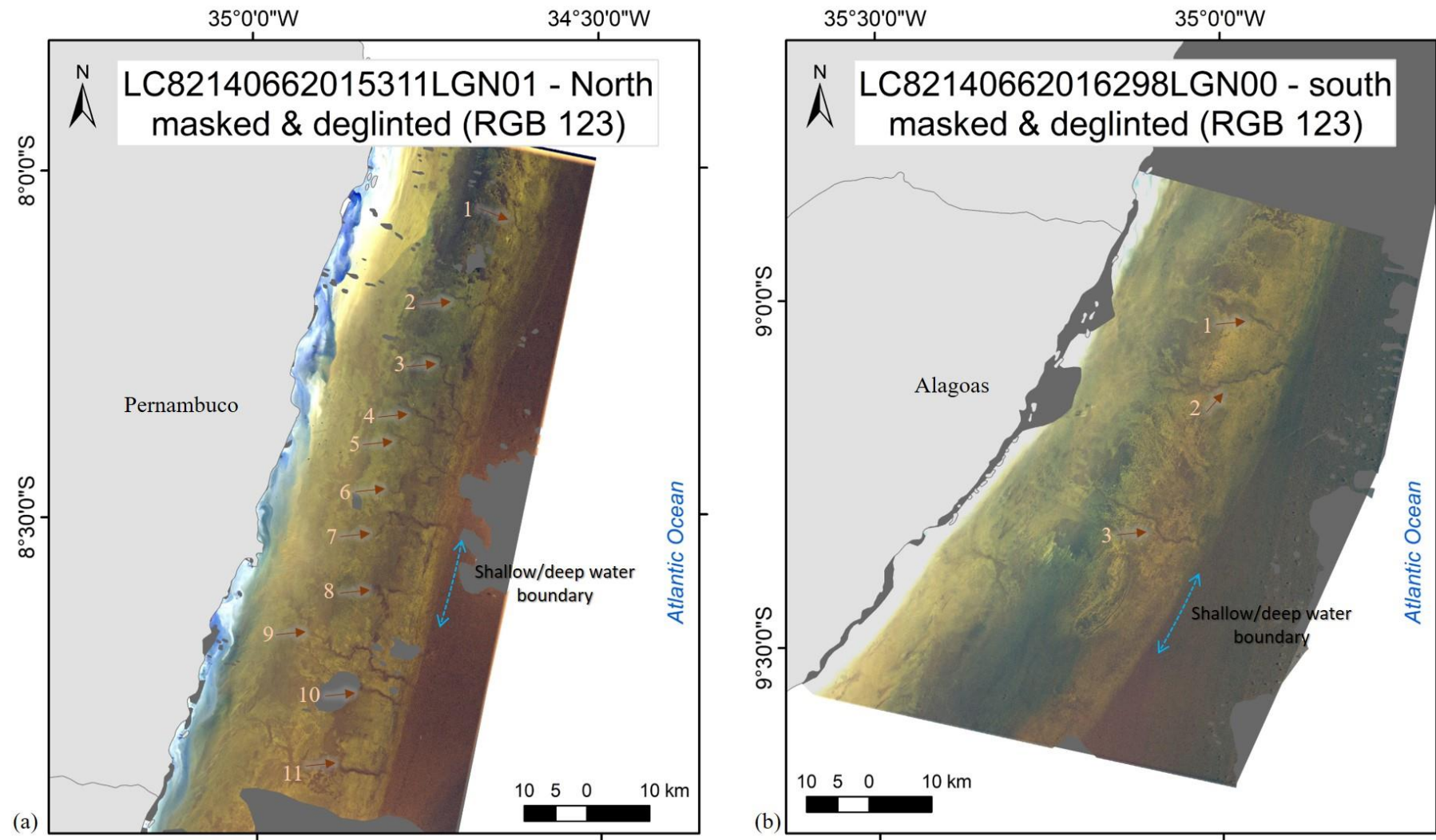


Figure 5 Landsat 8 imagery used in this study after cloud and land masking, and sunglint correction. a) North image; b) South image

4.4.3 Final Corrections and Filters

Final image corrections were applied to visually enhance the quality of the scenes. Water column correction is carried out by estimating the ratio of attenuation coefficients (k_i/k_j) for each pair of visible bands and thus, theoretically making each pixel value independent of depth. The parameters and results can vary from scene to scene, as shown in Table 3.

Table 3 Depth invariant index for the water column correction of scenes LC82140662015311LGN01 (North) and LC82140662015311LGN01 (South). B1: Coastal aerosol, B2: blue, B3: green, B4: red.

Scene	Pixels (<i>n</i>)	k_i/k_j					
		B1 / B2	B1 / B3	B1 / B4	B2 / B3	B2 / B4	B3 / B4
<i>North</i>	1440	0.818	0.761	10.819	1.085	894.731	3.162
<i>South</i>	1198	0.551	0.231	9.162	1.080	1973.381	2.451

Considering the results of the water-column correction and each band pairs' performance, a composite was built using bands 1, 2 and 4 (pairs: coastal aerosol/blue; coastal aerosol/green; and blue/green) for each image. The results of the individual scenes were mosaicked together and subjected to a Radar Speckle Suppression filter, implemented on ERDAS-Imagine *software*. The final mosaic still exhibits the seamline and the colour differences between the two scenes. This effect was not corrected since further manipulation of the pixels (*e.g.* histogram matching) caused a great loss of detail and obscured the representation of bottom features.

The previous processing techniques provided the best results and allowed the depiction of the channels and depressions in the area in remarkable detail. The channel-like features and the shelf break were vectorized to produce the final map of the study area (Fig 6).

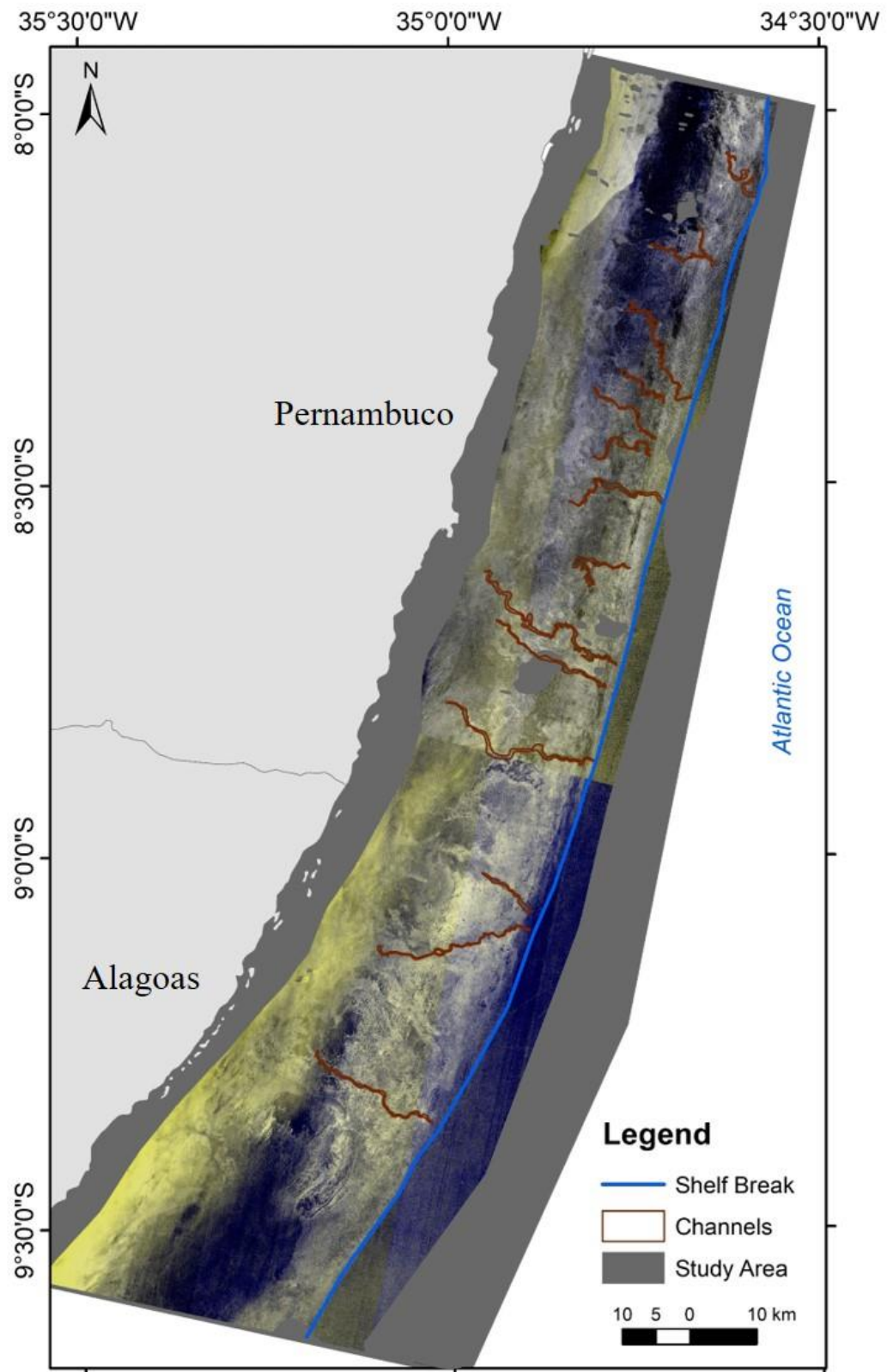


Figure 6 Composite of both Landsat-8 imagery post-processing. The blue line shows the suggested shelf break location and brown polygons mark the channel-like features in the study area.

4.4.4 Ground Truth

We analysed our results by overlaying the vectorized channels and shelf break identified by remote sensing on the official Brazilian Nautical Chart (DHN, 2017) and on the rasterized bathymetric model of the area.

The satellite imagery was able to detect the boundary between deep and shallow water at the shelf break's location (Fig 7, left). The shelf break detected in this study matches with the limits of the continental shelf and beginning of continental slope on the Nautical Chart. One apparent exception is a region in the north end of the line, where the remotely identified shelf break appears in a shallower area, deflecting to the continent. According to the Nautical Chart, the continental slope starts at a depth of about 44 meters and most of the study area is inserted between the 30 and 50 meters isobaths.

The results also showed that the indentations on the imagery were indeed channels, or underwater valleys, as they represent features that are deeper than the adjacent areas (Fig 7, right). The depth in the areas surrounding the channels on the outer part of the shelf (blue colours on the bathymetric model) varied from 40 to 50 meters. The maximum depth observed in the channels mapped by *in situ* surveys was 87 meters and the average depth was approximately 60 meters.

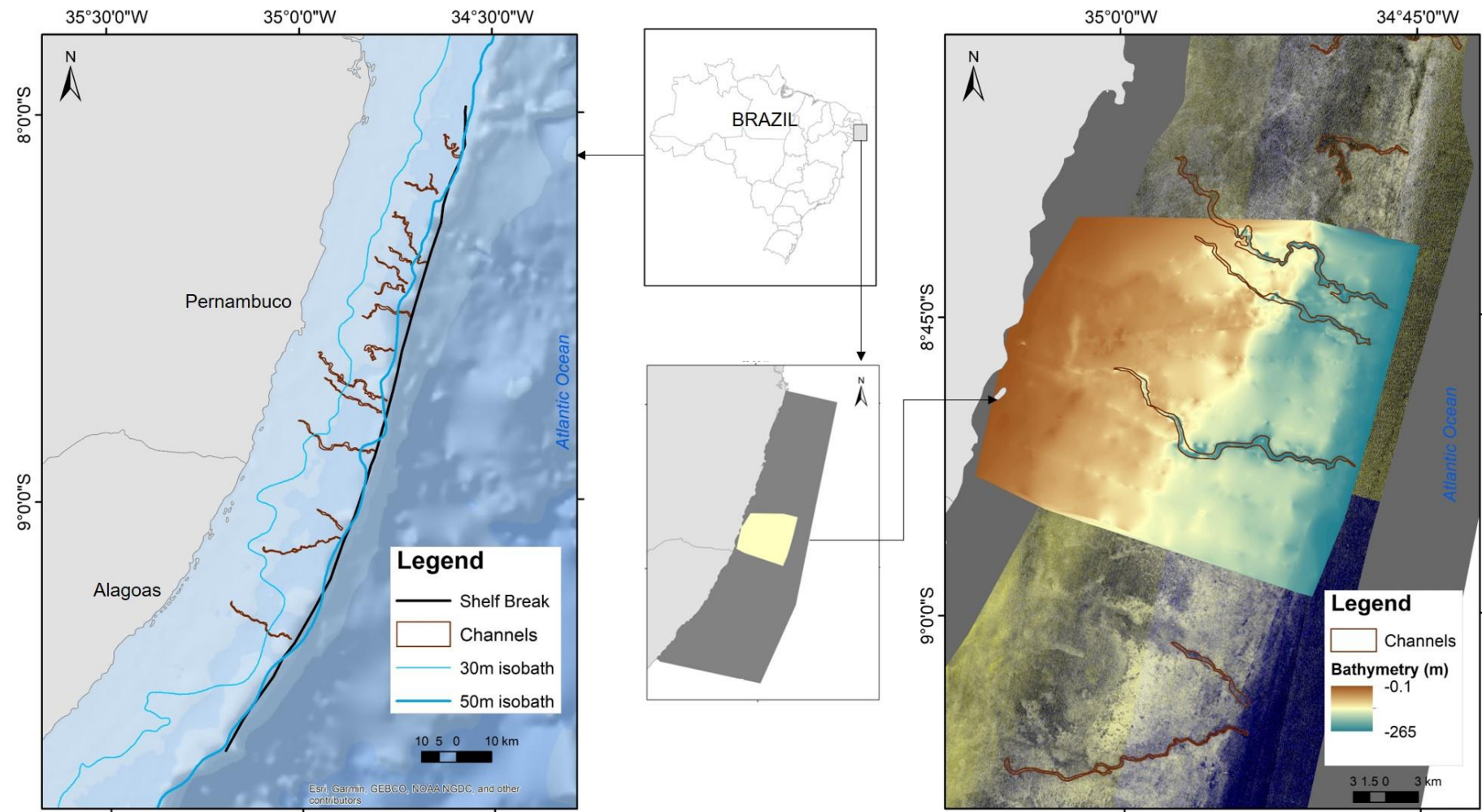


Figure 7 On the left, a map of the study area with all predicted bottom features (channels in brown and shelf break in black), with with 30 and 50-meter isobaths. On the right, a close-up of the area with the bathymetric raster built with available field data and the channels detected in this study (brown polygons)

4.5 Discussion

Our results showed the possibility of using satellite imagery as a tool to map underwater features in areas deeper than previously expected. In the last two decades, six submerged channels and valleys have been described in the study area using bathymetric data derived from field surveys with single and multi-beam echo sounders (Michelli *et al.*, 2001; Camargo *et al.*, 2015; Fontes *et al.*, 2018) and LIDAR (Valle, 2018). Using satellite imagery, fourteen channels could be detected during the present study, including their shelf break incision. (Green and Edwards, 2000; Nazeer *et al.*, 2014). We observed that atmospheric correction improved the possibility of detecting bottom features in depths greater than 30 meters. In the original unprocessed images, the limits between the shallow continental shelf and deep water remained undetected, and the entire marine region (with exception to the coastal zone) appeared homogeneous. Additionally, upon further observations and subsequent image analyses (*i.e.* compositing bands RGB 321 and using histogram equalize as stretch type), it was possible to observe the first indications that some channel-like features could also be mapped. Although satellite images are seldom used to map in-water features deeper than 30 meters, the application of atmospheric correction algorithms have been used in general in several studies to improve the accuracy and enhance the mapping potential of final products (*e.g.* Su *et al.*, 2013; Eugenio *et al.*, 2017).

The sunglint removal algorithm (Hedley *et al.*, 2005), applied subsequently to land and cloud masking, provided the most visually significant differences between pre and post processing imagery. Sunglint is known to affect proper visualization of sea bottom features to the point where they can be completely outshined by glint effects (Hochberg *et al.*, 2003; Deidda and Sanna, 2012). In our study area, removing the apparent roughness on seawater surface caused by sunglint was paramount in the benthic features identification processes for both scenes. Considering the depth range in the area, it was not surprising that out of Landsat-8's four visible bands, the red band (0.64 – 0.69 μ m) provided no useful information, since its penetration in the water column is confined to the first few meters (Fisher *et al.*, 2016). Furthermore, applying masks to land, cloud and construction areas, enabled an optimal histograms' usage and handling. This proved to be essential to a more detailed visualization of the bottom indentations and to define the limits between shallow and deep water.

Further image processing, specifically water column correction (Green and Edwards, 2000) and noise filtering were used to enhance the features already displayed after sunglint removal. By doing so, we were able to vectorize the channel-like structures and shallow/deep water boundaries, and thus, compare our results with ground data for the area. Knowing that

the presence of paleochannels and valleys has been described for the Northeast Continental Shelf (Martins and Coutinho, 1981; Knoppers *et al.*, 1999; Vital *et al.*, 2010; Vital, 2014; Camargo *et al.*, 2014;), it is reasonable to infer that the channel-like morphology we were able to see in the images are indeed, paleochannels. To confirm the depth differences between the features and the surrounding areas, we used bathymetry data provided by different sources (*i.e.* Michelli *et al.*, 2001; Camargo *et al.*, 2015; CMAR II and PELD-TAMS Projects). The analysis of these data with the vectorized channels and the Brazilian Nautical Chart (DHN, 2017) corroborate this hypothesis, since the features exhibit depths of more than 70 meters and are located mainly between the 30- and 50-meters isobaths (Figure 7).

Paleochannels have been mapped using remote sensing in land areas through indirect and direct interpretations of these ancient rivers' characteristic spectral signature (Wang *et al.*, 2012). Yet, the application of satellite imagery to detect these features on continental shelves seascapes have not been fully explored, mainly due to depth and turbidity in target areas. Considering the depth range in the external continental shelf, we believe that we were able to map the valleys due to the signal discontinuity in these deep regions, and not to a different spectral signature itself. In fact, this was also made possible due to the extremely low sediment fluxes that are typical in the Northeast Continental Shelf, a direct consequence of the low availability and transport of coastal sedimentation (Vital *et al.*, 2010; Vervoot and Annen, 2006; Camargo *et al.*, 2015). Hence, they remain reasonable “preserved” in shape and form, and can be detected in bathymetric surveys and now, in satellite imagery.

These areas are part of the NE Brazilian Ecologically or Biologically Significant Marine Areas (EBSA). The presence of paleochannels add to the complexity of the environments within the area and may act as a fish “corridor”, linking species along the shelf-edge zone in South America with those in the southwestern Atlantic and Caribbean (CDB, 2014; Druel, 2012; Bax *et al.*, 2014).

Seascape ecology is a new field that has as one of its main constraints difficulties for mapping submerged features, particularly in deeper areas. The presence of positive topography (*i.e.* beachrocks and reefs) and heterogeneous substratum has been indicated for the study area (Fontes *et al.*, 2019; Camargo *et al.*, 2015). This also highlights the possibility of further using Landsat imagery to detect mesophotic reef habitats and focus field surveys. As the region harbours several Marine Protected Areas, the present result may help on future marine spatial planning activities in the area.

4.6 Acknowledgments

The authors thank the Center for Research and Conservation of Marine Biodiversity of the Northeast (CEPENE) of the Chico Mendes Brazilian Institute of Biodiversity (ICMBIO) and Projeto Recifes Costeiros, Fundação Toyota do Brasil, Fundação SOS Mata Atlântica for supporting the field work. This research is a contribution of the Long-Term Ecological Research Program (PELD-CNPq 441632/2016-5 ILTER-Brazil -Tamandaré site 18), and Ciências do Mar II, AUXPE 1979/2014. This study was financed in part by the Coordenação de Aperfeiçoamento de Pessoal de Nível Superior – Brasil (CAPES) – Finance Code 001.

References

- Assis, H. M. B. D., Lopes, H., Gomes, R. B., Salviano, K. D. S., Valle, M. M., Oliveira, P. R. A., & Moura, L. P. (2016). Carta textural e geomorfológica da plataforma rasa de Alagoas - setor Porto Calvo. Recife, PE: CPRM, 1 mapa, color.
- Bax, N. J., Cleary, J., Donnelly, B., Dunn, D. C., Dunstan, P. K., Fuller, M., & Halpin, P. N. (2016). Results of efforts by the Convention on Biological Diversity to describe ecologically or biologically significant marine areas. *Conservation Biology*, 30(3), 571-581.
- Cainelli, C., & Mohriak, W. U. (1999). Some remarks on the evolution of sedimentary basins along the Eastern Brazilian continental margin. *Episodes-Newsmagazine of the International Union of Geological Sciences*, 22(3), 206-216.
- Camargo, J. M. R. D., Araújo, T. C. M. D., Maida, M., & Ushizima, T. M. (2007). Morfologia da plataforma continental interna adjacente ao município de Tamandaré, sul de Pernambuco-Brasil. *Revista brasileira de Geofísica*, 25, 79-89.
- Camargo, J. M. R., Araújo, T. C. M., Ferreira, B. P., & Maida, M. (2015). Topographic features related to recent sea level history in a sediment-starved tropical shelf: Linking the past, present and future. *Regional Studies in Marine Science*, 2, 203-211.
- Conti, L. A., Furtado, V. V. (2009). Topographic registers of paleo-valleys on the Southeastern Brazilian continental shelf. *Braz. J. Oceanogr.* 57, 113–121. <https://doi.org/10.1590/S1679-87592009000200004>
- De Keukelaere, L., Sterckx, S., Adriaensen, S., Knaeps, E., Reusen, I., Giardino, C., ... & Vaiciute, D. (2018). Atmospheric correction of Landsat-8/OLI and Sentinel-2/MSI data using iCOR algorithm: Validation for coastal and inland waters. *European Journal of Remote Sensing*, 51(1), 525-542.
- Deidda, M., & Sanna, G. (2012). Pre-processing of high resolution satellite images for sea bottom classification. *Italian Journal of Remote Sensing/Rivista Italiana di Telerilevamento*, 44(1).

Diretoria de Hidrografia e Navegação (DHN). (2017). “*Carta Náutica 01 – Costa e Ilhas ao Largo*”, em *GeoTiff*. Available online at: <http://www.dhn.mar.mil.br>

Druel, E. (2012). Ecologically or Biologically Significant Marine Areas (EBSAs): the identification process under the Convention on Biological Diversity (CBD) and possible ways forward (No. 17/12). *IDDRI Working Paper*.

Emílsson, I. (1961). The shelf and coastal waters off southern Brazil. *Bol. Inst. Ocean.* 11, 101–112. <https://doi.org/10.1590/S0373-55241961000100004>

Eugenio, F., Marcello, J., Martin, J., Rodríguez-Esparragón, D. (2017). Benthic Habitat Mapping Using Multispectral High-Resolution Imagery: Evaluation of Shallow Water atmospheric Correction Techniques. *Sensors* 17, 2639.

Eugenio, F.; Marcello, J., and Martin, J. (2015). High-resolution maps of bathymetry and benthic habitats in shallow-water environments using multispectral remote sensing imagery. *IEEE Transactions on Geoscience and Remote Sensing*, 53(7), 3539–3549.

Ferreira, B. P., & Maida, M. (2006). *Monitoramento dos recifes de coral do Brasil*. MMA, Secretaria de Biodiversidade e Florestas.

Ferreira, B. P., Maida, M., Castro, C. B., Pires, D. O., Damico, T. M., Prates, A. P., & Marx, D. (2006). The status of coral reefs in Brazil. In *Proc. 10th Int. Coral Reef Symp* (Vol. 1, pp. 1011-1015).

Fisher, A., Flood, N., & Danaher, T. (2016). Comparing Landsat water index methods for automated water classification in eastern Australia. *Remote Sensing of Environment*, 175, 167-182.

Fontes, V. C.; Gomes, M.P.; Vital, H.; Ferreira, B.P.; Maida, M. (2019). Reefs distribution and inter-reef sedimentation on Tamandaré continental shelf, NE-Brazil. In (book) “Seafloor Geomorphology as Benthic Habitat: GeoHab Atlas of Seafloor Geomorphic Features and Benthic Habitats”, Second Edition. Publisher: *Elsevier Science (in press)*

Frédou, T., Ferreira, B. P., & Letourneur, Y. (2006). A univariate and multivariate study of reef fisheries off northeastern Brazil. *ICES Journal of Marine Science*, 63(5), 883-896.

Fritz, C., Dörnhöfer, K., Schneider, T., Geist, J., Oppelt, N. (2017). Mapping Submerged Aquatic Vegetation Using RapidEye Satellite Data: The Example of Lake Kummerow (Germany). *Water* 9, 510. <https://doi.org/10.3390/w9070510>

Gao, J. (2009). Bathymetric mapping by means of remote sensing: Methods, accuracy and limitations. *Progress in Physical Geography: Earth and Environment*, 33(1), 103–116. doi:10.1177/0309133309105657

Gomes, M. P., Vital, H., Eichler, P. P., & Gupta, B. K. S. (2015). The investigation of a mixed carbonate-siliciclastic shelf, NE Brazil: side-scan sonar imagery, underwater photography, and surface-sediment data. *Italian Journal of Geosciences*, 134(1), 9-22.

Gomes, M.P., Vital, H., Stattegger, K., Schwarzer, K. (2016). Bedrock control on the Assu Incised Valley morphology and sedimentation in the Brazilian Equatorial Shelf. *Int. J. Sediment Res.* 31, 181–193. <https://doi.org/10.1016/j.ijsrc.2015.04.002>

Green, E.P., Edwards, A.J. (2000). Remote sensing handbook for tropical coastal management, Coastal management sourcebooks. *Unesco Pub*, Paris.

H. Su, Hongxing L., Q. Wu. (2015). Prediction of Water Depth From Multispectral Satellite Imagery—The Regression Kriging Alternative. *IEEE Geosci. Remote Sens. Lett.* 12, 2511–2515. <https://doi.org/10.1109/LGRS.2015.2489678>

Harris, M. S., Sautter, L.R., Johnson, K.L., Luciano, K.E., Sedberry, G.R., Wright, E.E., Siuda, A.N.S. (2013). Continental shelf landscapes of the southeastern United States since the last interglacial. *Geomorphology* 203, 6–24. <https://doi.org/10.1016/j.geomorph.2013.02.014>

Harris, P. T., Baker, E. K. (2012). Why Map Benthic Habitats?, in: *Seafloor Geomorphology as Benthic Habitat*. *Elsevier Publisher*, pp. 3–22. <https://doi.org/10.1016/B978-0-12-385140-6.00001-3>

Hedley, J. D., Harborne, A. R., & Mumby, P. J. (2005). Simple and robust removal of sun glint for mapping shallow-water benthos. *International Journal of Remote Sensing*, 26(10), 2107-2112.

Hochberg, E. J., Andréfouët, S., & Tyler, M. R. (2003). Sea surface correction of high spatial resolution Ikonos images to improve bottom mapping in near-shore environments. *IEEE transactions on geoscience and remote sensing*, 41(7), 1724-1729.

Knoppers, B., Ekau, W., & Figueiredo, A. G. (1999). The coast and shelf of east and northeast Brazil and material transport. *Geo-Marine Letters*, 19(3), 171-178. <https://doi.org/10.1007/s003670050106>

Leão, Z. M., Kikuchi, R. K., & Testa, V. (2003). Corals and coral reefs of Brazil. In *Latin American coral reefs* (pp. 9-52). Elsevier Science.

Mahiques, M. M. D., Sousa, S. H. D. M., Furtado, V. V., Tessler, M. G., Toledo, F. A. D. L., Burone, L., ... & Alves, D. P. V. (2010). The Southern Brazilian shelf: general characteristics, quaternary evolution and sediment distribution. *Brazilian Journal of Oceanography*, 58(SPE2), 25-34.

Maida, M., & Ferreira, B. P. (1997). Coral reefs of Brazil: an overview. In *Proceedings of the 8th international coral reef symposium* (Vol. 1, No. 263, p. 74). Smithsonian Tropical Research Institute Panamá.

Manessa, M. D. M., Haidar, M., Budhiman, S., Winarso, G., Kanno, A., Sagawa, T., Sekine, M. (2016). Evaluating the performance of Lyzenga's water column correction in case-1 coral reef water using a simulated Woldview-2 imagery. *IOP Conf. Ser. Earth Environ. Sci.* 47, 012018. <https://doi.org/10.1088/1755-1315/47/1/012018>

Martins, L. R., & Coutinho, P. N. (1981). The Brazilian continental margin. *Earth-Science Reviews*, 17(1-2), 87-107.

Michelli, M., Araújo, T., Maida, M., Vital, H. (2001). Indicatives of ancient conditions of sea level stability on the southern Pernambuco continental shelf. *Pesqui. Em Geociências* 28, 25. <https://doi.org/10.22456/1807-9806.20266>

- Nazeer, M., Nichol, J.E., Yung, Y.-K. (2014). Evaluation of atmospheric correction models and Landsat surface reflectance product in an urban coastal environment. *Int. J. Remote Sens.* 35, 6271–6291. <https://doi.org/10.1080/01431161.2014.951742>
- Ojeda, H. A. O. (1982). Structural framework, stratigraphy, and evolution of Brazilian marginal basins. *AAPG Bulletin*, 66(6), 732-749.
- Olavo, G., Costa, P. A., Martins, A. S., & Ferreira, B. P. (2011). Shelf-edge reefs as priority areas for conservation of reef fish diversity in the tropical Atlantic. *Aquatic conservation: marine and freshwater ecosystems*, 21(2), 199-209.
- Ponte, F. C., & Asmus, H. E. (1978). Geological framework of the Brazilian continental margin. *Geologische Rundschau*, 67(1), 201-235.
- Richter, R., & Schlöpfer, D. (2013). Atmospheric/Topographic Correction for Satellite Imagery (ATCOR-2/3 User Guide, Version 8.3. 1, February 2014). *ReSe Applications Schlöpfer, Langeggweg*, 3.
- Silveira, C.B.L.; Strenzel, G.M.; Maida, M., Araújo T.C.M.; Ferreira, B.P. 2019. Multi Resolution Satellite-Derived Bathymetry in Shallow Coral Reefs: Improving linear algorithms with geographical analysis (JCOASTRES-D-19-00029). *Journal of Coastal Research (in press)*
- Su, H.; Liu, H.; Wang, L.; Filippi, A.M.; Heyman, W.D., and Beck, R.A. (2013). Geographically adaptive inversion model for improving bathymetric retrieval from satellite multispectral imagery. *IEEE Transactions on Geoscience and Remote Sensing*, 52(1), 465–476. doi:10.1109/TGRS.2013.2241772
- Testa, V., & Bosence, D. W. (1999). Physical and biological controls on the formation of carbonate and siliciclastic bedforms on the north-east Brazilian shelf. *Sedimentology*, 46(2), 279-301.
- Valle, M. M. (2018). Caracterização das feições sedimentares da plataforma de Alagoas, com base em levantamento aerobatimétrico LIDAR (Master's Thesis). Universidade Federal de Pernambuco.
- Vervoort, R. W., & Annen, Y. L. (2006). Palaeochannels in Northern New South Wales: Inversion of electromagnetic induction data to infer hydrologically relevant stratigraphy. *Soil Research*, 44(1), 35-45. <https://doi.org/10.1071/SR05037>
- Vital, H. (2014). The north and northeast Brazilian tropical shelves. *Geological Society, London, Memoirs*, 41(1), 35-46.
- Vital, H., Gomes, M. P., Tabosa, W. F., Frazão, E. P., Santos, C. L. A., Júnior, P., & Saraiva, J. (2010). Characterization of the Brazilian continental shelf adjacent to Rio Grande do Norte State, NE Brazil. *Brazilian Journal of Oceanography*, 58(SPE1), 43-54. <https://doi.org/10.1590/S1679-87592010000500005>
- Wang, X., Guo, Z., Wu, L., Zhu, C., & He, H. (2012). Extraction of palaeochannel information from remote sensing imagery in the east of Chaohu Lake, China. *Frontiers of Earth Science*, 6(1), 75-82. <https://doi.org/10.1590/S1679-87592010000500005>

Wu, J., Wang, D., & Bauer, M. E. (2005). Image-based atmospheric correction of QuickBird imagery of Minnesota cropland. *Remote Sensing of Environment*, 99(3), 315-325.

5 CONCLUSÃO

Os resultados alcançados nesta Tese demonstram de forma prática a utilização de técnicas de sensoriamento remoto em ambientes recifais e de plataforma. A área de estudo, localizada em grande parte na APA Costa dos Corais, é de extrema importância socioeconômica e ambiental, e não obstante, possui uma demanda de dados diretos acerca de sua topografia e biodiversidade.

Os modelos batimétricos desenvolvidos no primeiro manuscrito desta Tese foram utilizados para a derivação de métricas de topografia que por sua vez, são tidas como *proxies* de biodiversidade. Foram assim, o primeiro passo para um monitoramento remoto em alta resolução da zona costeira de Tamandaré. Adicionalmente, a batimetria da área era uma lacuna a ser preenchida, posto que a área de estudo, um local de intenso uso, incluindo de transporte marítimo, contava apenas com a carta náutica oficial da Marinha do Brasil datada de 1962. As técnicas que precisaram ser empregadas para o desenvolvimento destes modelos refletem a condição heterogênea da área, com uma alta complexidade de substratos comum a recifes de coral.

O mapeamento dos habitats bentônicos de Tamandaré, desenvolvido no decorrer do segundo manuscrito aqui apresentado, forneceu dados importantes acerca da biodiversidade encontrada na área. Foi também utilizado para o cálculo de métricas ecológicas, como a diversidade de habitats por área. Esta espacialização da distribuição de ecossistemas na zona costeira possibilita a inferência de áreas prioritárias para manejo e proteção, além da análise das medidas de manejo presentes.

Os resultados obtidos com a modelagem preditiva de *Millepora alcicornis* podem impulsionar o uso de ferramentas como o MaxEnt para outras espécies. Estes modelos são extremamente úteis para a seleção de áreas prioritárias, principalmente considerando a variedade de impactos já sofridos pelos recifes costeiros. Neste trabalho, foi possível avaliar de forma qualitativa e quantitativa como cada variável topográfica, regional e ecológica atuou na distribuição de *Millepora alcicornis*. Foram também substanciais para verificar diretamente a importância da Zona de Proteção da Vida Marinha (“área-fechada”) presente na região de estudo. Ademais, o extenso trabalho de campo realizado na região deixa uma gama de possibilidades de estudos futuros, complementares e contínuos a este.

O terceiro manuscrito apresentou a utilização de duas imagens de satélite Landsat-8 para o mapeamento e verificação de feições de fundo a mais de 50 metros de profundidade.

Esta representa a primeira descrição de paleocanais da área de uma forma unificada, sendo capaz de otimizar futuros esforços de campo e pesquisas na área. A descrição minuciosa da metodologia aplicada para a obtenção do grau de detalhe que obtivemos, possibilita a replicação deste resultado em outras regiões da plataforma Nordeste. É possível que o sensoriamento remoto esteja sendo subutilizado como ferramenta de detecção de feições submarinas em toda a costa e recomendamos que esta tentativa seja realizada em outras regiões da costa.

Em suma, os resultados alcançados nesta tese podem auxiliar o Planejamento Espacial Marinho da APA Costa dos Corais. Um planejamento com base ecossistêmica depende de dados diretos da região, inferidos em escalas condizentes com a ecologia, complexidade topográfica e dimensões da área, como os obtidos nos estudos aqui apresentados. Com estes resultados, foi possível fornecer um mapeamento específico da zona costeira e plataforma adjacente.

REFERÊNCIAS

- ADAM, T. C.; BURKEPILE, D. E.; RUTTENBERG, B. I.; PADDACK, M. J. Herbivory and the resilience of Caribbean coral reefs: knowledge gaps and implications for management. **Marine ecology progress series**, vol. 520, p. 1-20. 2015.
- AGARDY, T.; DI SCIARA, G. N.; CHRISTIE, P. Mind the gap: addressing the shortcomings of marine protected areas through large scale marine spatial planning. **Marine policy**, vol. 35, n. 2, p. 226-232. 2011.
- ALMANY, G. R.; CONNOLLY, S. R.; HEATH, D. D.; HOGAN, J. D.; JONES, G. P.; MCCOOK, L. J.; WILLIAMSON, D. H. Connectivity, biodiversity conservation and the design of marine reserve networks for coral reefs. **Coral reefs**, vol. 28, n. 2, p. 339-351. 2009.
- ANDRÉFOUËT, S.; KRAMER, P.; TORRES-PULLIZA, D.; JOYCE, K. E.; HOCHBERG, E. J.; GARZA-PÉREZ, R.; ZUBIA, M. Multi-site evaluation of IKONOS data for classification of tropical coral reef environments. **Remote sensing of environment**, vol. 88, n. 1-2, p. 128-143. 2003.
- BAK, R. P. M.; GERARD N.; MEESTERS, E. H. Coral reef crisis in deep and shallow reefs: 30 years of constancy and change in reefs of Curacao and Bonaire. **Coral reefs**, vol. 24, n. 3, p. 475-479. 2005.
- BELLWOOD, D. R.; HUGHES T. P.; FOLKE, C.; NYSTRÖM, M. Confronting the coral reef crisis. **Nature**, vol. 429, n. 6994, p. 827-833. 2004.
- BENFIELD, S. L.; GUZMAN, H. M.; MAIR, J. M.; YOUNG, J. A. T. Mapping the distribution of coral reefs and associated sublittoral habitats in Pacific Panama: a comparison of optical satellite sensors and classification methodologies. **International journal of remote sensing**, vol. 28, n. 22, p. 5047-5070. 2007.
- BRAGA, C. Z. F.; GHERARDI, D. F. M. Mapeamento de recifes costeiros utilizando imagens orbitais. In: SIMPÓSIO BRASILEIRO DE SENSORIAMENTO REMOTO (SBRS), 10.; 2001, Foz do Iguaçu. **Anais [...]**. São José dos Campos: INPE, 2001. p. 759-767.
- BRUCKNER, A.W. Priorities for effective management of coral diseases. **NOAA tech. memo N.M.F.S. O.P.R.**, p. 1-54. 2002.
- BURKE, L.; REYTAR, K.; SPALDING, M. & PERRY, A. **Reefs at risk revisited**. Washington, D.C.: World Resources Institute, 2011.
- DE LACERDA, L. D.; KREMER, H. H.; KJERFVE, B.; SALOMONS, W.; CROSSLAND, J. I. M.; CROSSLAND, C.J. **South American basins: LOICZ global change assessment and synthesis of river catchment-coastal sea interaction and human dimensions**. Netherlands.: Netherlands Institute for Sea Research. 2002.
- EUGENIO, F.; MARCELLO, J.; MARTIN, J.; RODRÍGUEZ-ESPARRAGÓN, D. Benthic habitat mapping using multispectral high-resolution imagery: evaluation of shallow water atmospheric correction techniques. **Sensors**, vol. 17, n. 11, p. 2639-2662. 2017.
- FERREIRA, B. P.; MAIDA, M. **Monitoramento dos recifes de coral do Brasil: situação atual e perspectivas**. Brasília: MMA – Ministério do Meio Ambiente, 2004. 116 p.

- GAINES, S. D.; WHITE, C.; CARR, M. H.; PALUMBI, S. R. Designing marine reserve networks for both conservation and fisheries management. **Proceedings of the national academy of sciences**, vol. 107, n. 43, p. 18286-18293. 2010.
- GAO, J. 2009. Bathymetric mapping by means of remote sensing: methods, accuracy and limitations. *Progress in physical geography: earth and environment*, vol. 33, n. 1, p. 103–116. 2009.
- GREEN, E.; MUMBY, P. J.; EDWARDS, A. J.; CLARK, C. D. **Remote sensing handbook for tropical coastal management**. Paris: Unesco Publishing, 2000.
- HAMILTON, S. L.; CASELLE, J. E.; MALONE, D. P.; CARR, M. H. Incorporating biogeography into evaluations of the Channel Islands marine reserve network. **Proceedings of the national academy of sciences**, vol. 107, n. 43, p. 18272-18277. 2010.
- HEDLEY, J.; ROELFSEMA, C.; CHOLLETT, I.; HARBORNE, A.; HERON, S.; WEEKS, S.; TICZON, V. (2016). Remote sensing of coral reefs for monitoring and management: a review. **Remote sensing**, vol. 8, n. 2, p. 118-158. 2016.
- HODGSON, G.; LIEBLER, J. **The global coral reef crisis: trends and solutions**. Reef Check, Institute of the Environment, University of California. Los Angeles, California. 2002.
- ICMBIO – Plano de Manejo da Área de Proteção Ambiental Costa dos Corais. Brasília, 2012.
- JAMESON, S. C.; TUPPER, M. H.; RIDLEY, J. M. The three screen doors: can marine “protected” areas be effective? **Marine pollution bulletin**, vol. 44, n. 11, p. 1177-1183. 2002.
- KERR, J. T.; OSTROVSKY M. From space to species: ecological applications for remote sensing. **Trends in ecology and evolution**, vol. 18, p. 299– 305. 2003.
- LICEAGA-CORREA, M.A.; EUAN-AVILA, J. I. Assessment of coral reef bathymetric mapping using visible Landsat thematic mapper data. **International journal of remote sensing**, vol. 23, n. 1, p. 3–14. 2002.
- MARQUES, M.; DA COSTA, M. F.; MAYORGA, M. I. D. O.; PINHEIRO, P. R. Water environments: anthropogenic pressures and ecosystem changes in the Atlantic drainage basins of Brazil. **AMBIO: A journal of the human environment**, vol. 33, n. 1, p. 68-77. 2004.
- MCCOOK, L. J.; ALMANY, G. R.; BERUMEN, M. L.; DAY, J. C.; GREEN, A. L.; JONES, G. P.; THORROLD, S. R. Management under uncertainty: guide-lines for incorporating connectivity into the protection of coral reefs. **Coral reefs**, vol. 28, n. 2, p. 353-366. 2009.
- MMA – Ministério do Meio Ambiente. **Avaliação e ações prioritárias para a conservação da biodiversidade das zonas costeira e marinha**. Brasília: Fundação Bio-RIO, SECTAM, IDEMA, SNE, 2002.
- MUMBY, P. J.; GREEN, E. P.; EDWARDS, A. J.; CLARK, C. D. The cost-effectiveness of remote sensing for tropical coastal resources assessment and management. **Journal of environmental management**, vol. 55, n. 3, p. 157–66. 1999.
- PASCAL, N.; ALLENBACH, M.; BRATHWAITE, A.; BURKE, L.; LE PORT, G.; CLUA, E. Economic valuation of coral reef ecosystem service of coastal protection: A pragmatic approach. **Ecosystem services**, vol. 21, p. 72-80. 2016.

- PHILIPSON P.; LINDELL T. Can coral reefs be monitored from space? **Ambio**, vol. 32, p.586–593. 2003.
- PITTMAN, S. J.; BROWN, K. A. Multi-scale approach for predicting fish species distributions across coral reef seascapes. **PloS one**, vol. 6, ed. 5. 2011.
- RAITSOS, D. E.; BREWIN, R. J.; ZHAN, P.; DREANO, D.; PRADHAN, Y.; NANNINGA, G. B.; HOTEIT, I. Sensing coral reef connectivity pathways from space. **Scientific reports**, vol. 7, n. 1, p. 9338. 2017.
- ROBERTS, C. M. Marine biodiversity hotspots and conservation priorities for tropical reefs. **Science**, vol. 295, n. 5558, p. 1280–84. 2002.
- ROBERTS, C. M.; MCCLEAN, C. J.; VERON, J. E.; HAWKINS, J. P.; ALLEN, G. R.; MCALLISTER, D. E.; VYNNE, C. Marine biodiversity hotspots and conservation priorities for tropical reefs. **Science**, vol. 295, n. 5558, p. 1280-1284. 2002.
- SCHLÜTER, A.; VANCE, C.; FERSE, S. Coral reefs and the slow emergence of institutional structures for a global land-and sea-based collective dilemma. **Marine policy**, p. 103505. 2019.
- SELGRATH, J. C.; ROELFSEMA, C.; GERGEL, S. E.; VINCENT, A. C. Mapping for coral reef conservation: comparing the value of participatory and remote sensing approaches. **Ecosphere**, vol. 7, n. 5, p. 01325. 2016.
- SMITH, G. B. The 1971 red tide and its impact on certain reef communities in the mid-eastern Gulf of Mexico, *Environmental Letters*, 9: 141– 152. 1975.
- SPALDING, M.; BURKE, L.; WOOD, S. A.; ASHPOLE, J.; HUTCHISON, J.; ZU ERMGASSEN, P. Mapping the global value and distribution of coral reef tourism. **Marine policy**, vol. 82, p. 104-113. 2017.
- WILKINSON, C.; SALVAT, B. Coastal resource degradation in the tropics: does the tragedy of the commons apply for coral reefs, mangrove forests and seagrass beds. **Marine pollution bulletin**, vol. 64, n. 6, p. 1096-1105. 2012.